Cosmological Predictions of Scalar-Tensor theories in Teleparallel Gravity

Zinovia Oikonomopoulou

Supervised by Prof. Jackson Levi Said

Co-supervised by Prof. Kristian Zarb Adami

Institute of Space Science and Astronomy

Faculty of Science

University of Malta

May, 2024

A dissertation submitted in partial fulfilment of the requirements for the degree of PhD in Your Degree.

L-Università ta' Malta

WWW.UM.EDU.MT

First edition, December 30, 2024

List of Publications

- Dialektopoulos, K.F., Said, J.L. Oikonomopoulou, Z. Classification of teleparallel Horndeski cosmology via Noether symmetries. Eur. Phys. J. C 82, 259 (2022). https://doi.org/10.1140/epjc/s10052-022-10201-7.
  My contribution to this document was calculating the Lagrangian and the system of 62 equations. I derived the cases and verified the results of K.F. Dialektopoulos. I also contributed to the writing of this project.

- Konstantinos F. Dialektopoulos, Jackson Levi Said, Zinovia Oikonomopoulou, New insights from GW170817 in the dynamical system analysis of Einstein Gauss–Bonnet gravity, Physics of the Dark Universe, Volume 42, 2023, 101350, ISSN 2212-6864. https://doi.org/10.1016/j.dark.2023.101350.
  I performed all the calculations presented in this document and contributed to the writing of the project.

- Ahmedov, B., Dialektopoulos, K.F., Levi Said, J., Nosirov, A., Oikonomopoulou, Z., Yunusov, O. (2023). Cosmological perturbations in the teleparallel analogue of Horndeski gravity. Journal of Cosmology and Astroparticle Physics, 2023. https://api.semanticscholar.org/CorpusID:259243717
  I calculated the second-order action of the tensor modes and the expressions of the $\alpha_i(t)$ functions. I derived the results for scalar and vector perturbations and verified the calculations of A.Nosirov and O.Yunusov. I also contributed to the writing of the project.

- B.Ahmedov, K.F.Dialektopoulos, J.L.Said, A.Nosirov, O.Yunusov, Z.Oikonomopoulou. Stable bouncing solution in Teleparallel Horndeski gravity: violations of the no-go theorem. https://doi.org/10.48550/arXiv.2311.11977-under review.
  In this project, I performed the calculations for the construction and the behaviour

of the three toy models and verified the results of A.Nosirov and O.Yunusov. I also contributed to the writing of the project.

L-Università ta' Malta

Declaration by Postgraduate Students

(a) Authenticity of Dissertation

I hereby declare that I am the legitimate author of this Dissertation and that it is my original work.
No portion of this work has been submitted in support of an application for another degree or qualification of this or any other university or institution of higher education.
I hold the University of Malta harmless against any third party claims with regard to copyright violation, breach of confidentiality, defamation and any other third party right infringement.

(b) Research Code of Practice and Ethics Review Procedures

I declare that I have abided by the University's Research Ethics Review Procedures.
As a Master's student, as per Regulation 58 of the General Regulations for University Postgraduate Awards, I accept that should my dissertation be awarded a Grade A, it will be made publicly available on the University of Malta Institutional Repository.

Faculty/Institute/Centre/School	Faculty of Science
Degree	PhD in Your Degree
Title	Cosmological Predictions of Scalar-Tensor theories in Teleparallel Gravity
Candidate (Id.)	Zinovia Oikonomopoulou ([redacted])
Signature of Student	[redacted]
Date	December 30, 2024

08.02.2018

La science, la nouvelle noblesse!
C'est la vision de nombres. Nous
allons á l'Esprit. C'est trés certain,
c'est oracle, ce que je dis.
Je comprends, et ne sachant
m'expliquer sans paroles païennes,
je voudrais me taire.

Arthur Rimbaud
Une Saison en Enfer

Dedicated to the two persons who taught me

to face the challenges with grace and wisdom,

my dearest parents.

Acknowledgements

The accomplishment of this study would not have been possible without the contribution and valuable assistance of several individuals in my life. Therefore, I seize this opportunity to communicate my appreciation to each of them separately.

First, I would like to express my deepest gratitude to Prof. Jackson Levi Said who provided me with encouragement and patience over the past three years. Completing this PhD would not have been achievable without his priceless guidance and profound scientific knowledge and experience. I feel extremely fortunate for the opportunity to work closely with such a dedicated supervisor who motivated me to always strive for excellence in my work and consistently reach my full potential. His commitment to my academic progress shaped my research direction and elevated the quality of my studies.

In addition, I am extremely grateful to Dr. K. Dialektopoulos. His extensive knowledge in the field of physics and his insightful comments and recommendations served as a genuine source of inspiration for me.

Gratitude is extended to Abdurakhmon Nosirov and Odil Yunusov, with whom I had the pleasure of collaborating on two scientific projects. Engaging in discussions and sharing ideas enhanced my scientific development.

Last but not least, I thank my beloved family and friends for their unwavering support and belief in me at every stage of this journey. Words cannot express my heartfelt gratitude for they have endured my constant unavailability always with kindness and a sense of humour that made the anxiety and stress vanish in thin air.

I attribute the greatest gratitude to my deceased parents. Without their love, affection and hard work all of their lives I wouldn't have been the person I am today. They are my light in the dark.

Abstract

The cosmological tensions following observational analysis as well as the late-time cosmic accelerated expansion provide a solid motivation for the adequacy of General Relativity as the primary theory for describing gravity. Under that novel viewpoint, scalar-tensor theories are commonly utilized as the typical method for investigating potential deviations from the ΛCDM model. Scalar-tensor theories are among the most extensively examined topics of modified gravity since their dynamical analysis reveals quite interesting behaviour associated with the various eras of cosmic evolution. The capacity of scalar-tensor theories to elucidate different cosmological epochs validates the increasing interest of the scientific community in the Horndeski theory of gravity, which is considered the most general scalar-tensor theory resulting in second-order field equations. The revival of the Horndeski theory in its contemporary form has generated profound research beyond the standard model of cosmology involving the broader framework of scalar-tensor theories. Following the detection of the GW170817 event, the constraints imposed on the terms of the Horndeski Lagrangian served as a starting point for its incorporation into Teleparallel Gravity. This results in the Teleparallel Analogue of Horndeski theory, known as the BDLS theory, which is discussed in the current thesis, followed by the classification of its models using the Noether Symmetry Approach. The investigation of the BDLS cosmological perturbations is also included along with their potential for further research on whether the No-go argument could be circumvented in a healthy manner. Furthermore, the Einstein Gauss-Bonnet model is examined by utilizing a dynamical system approach. This scalar-tensor theory contains a highly diverse phase space due to the inclusion of the fourth-order Gauss-Bonnet invariant combined with the second-order scalar field contribution. The critical points that emerge have the potential to enhance our comprehension of cosmic evolution as they differ noticeably compared to those already present in the literature.

Contents

List of Figures

List of Tables

List of Abbreviations

1

Introduction

Modifying gravity on cosmological scales has gained increasing momentum over the past decade. This has been prompted by the advancements in theoretical frameworks, particularly in higher-dimensional theories, alongside the development of constructing renormalizable gravitational theories. Of equal importance is the significant progress that has been made on the observational front. A critical element in that direction has been the ability to measure the growth of structure at redshifts of $z \simeq 0.8$. These measurements provide a means to evaluate and potentially reject numerous proposals and models related to modified gravity. In addition, a wealth of ongoing research endeavours focus on examining the impact of gravitational modifications on the Cosmic Microwave Background Radiation (CMB) measurements, weak gravitational lensing and various other cosmological probes. After all, and from the theoretical viewpoint, constructing a cosmological model is a crucial part of interpreting the current observational data as well as making predictions for the future.

Still, a consistent cosmological framework requires a relativistic theory of gravitation. Einstein's theory of GR had a pivotal role in the advancement made in the field of cosmology which could be regarded as one of the major achievements in the scientific research of the twentieth century. The theory of GR presents a coherent and exhaustive interpretation of the concepts of space, time, matter and gravity. In contrast to classical mechanics which regards space and time as absolute entities, GR recognizes them as dynamical quantities that are influenced by the presence and motion of matter and energy. This leads to the central concept of GR that, while most forces are represented by fields defined on spacetime, gravity is an intrinsic property of spacetime itself. This distinctive perspective of physics paved the way for further insight and understanding into the nature of the Universe [102], [135].

Einstein's theory revolutionized our comprehension of the Universe by recognizing it, for the first time, as a dynamical system conducive to physical measurements and mathematical modelling [94]. Consequently, cosmology was integrated into a scientific discipline. Further scientific endeavours in the field of cosmic evolution culminated in the development of the widely accepted Standard Big Bang model, which, until recently, encompassed the majority of cosmological observations.

Nevertheless, GR is a classical theory in physics and thus raises the question of whether it could still be a fundamental theory when attempting to describe gravity and spacetime at scales below the Planck length. Furthermore, although GR has well passed all observational tests so far, there are some extra theoretical arguments indicating that we might want to consider a more consistent theory of gravity. Space-time singularities arise as a result of the principles of GR, appearing in the solutions of the gravitational field. Although the presence of the Big Bang singularity has gained significant attention in the fields of theoretical astrophysics and cosmology, there are valid concerns regarding whether this mathematical concept could represent the actual state of the Universe in the past. In addition, the flatness and horizon issues along with the observed late-time accelerated expansion have led to the realization that the standard model of cosmology based on the principles of GR is insufficient for correctly depicting the Universe at extreme regimes [136], [8]. This fact prompts the scientific community to question the exclusivity of GR as the only accurate theory for explaining gravitational interactions.

One of the most intriguing challenges in contemporary cosmology is the Hubble tension, which has gained significant attention and has become a highly debated topic since its appearance almost a decade ago [52]. In simple terms, this tension stems from the discrepancy between the values of the current expansion rate of the Universe determined either indirectly through a model-dependent method utilizing data from the angular scale of standard rulers or directly from the luminosity of standard candles.

The former method primarily involves observational measurements of the sound horizon angular scales concerning the CMB and Baryonic Acoustic Oscillations (BAO). Considering the standard model of cosmology, the ΛCDM model for the Universe, the Planck collaboration has announced the value for the current cosmic expansion rate to be $H_0 = 67.36 \pm 0.54$ km/s/Mpc at 68% confidence level [66].

The second method incorporates the luminosity of the type-Ia supernovae (SNIa), calibrated by Cepheids and it is based on the distance ladder technique. In this particular context, the prominent contributor is the Supernovae H_0 for the Equation of State (SH0ES) collaboration [120]. The SH0ES collaboration has introduced an enhanced measurement of the cosmic expansion rate of $H_0 = 73.29 + \pm 0.90$ km/s/Mpc [104], leading to a tension of 5.6σ in comparison to the result of the Planck collaboration measurements.

Numerous researches have been undertaken aiming to ascertain the origin of the Hubble tension. However, to date, no compelling explanation has been derived [60], [81], [120]. The reevaluations of the Planck measurements and observational data from the Hubble Space Telescope (HST) suggest that the discrepancy in the value of H_0 is probably not connected to systematics such as calibration inaccuracies or photometric biases. As a result, several researchers in the cosmological field assume that the Hubble tension is a strong motivation that triggers the investigation of new physics extending beyond the standard ΛCDM model of cosmology.

Over time, a variety of alternative theoretical models have been developed in an attempt to resolve or even relax the Hubble tension. While several extensions of the ΛCDM model can mitigate this tension, the bulk of existing observational data does not provide significant support for any of them.

Following the aforementioned motivations and facts, multiple alternative theories of gravity have been proposed. These theories aim to develop a semiclassical theoretical framework that can effectively reproduce the achievements of GR. One of the most compelling approaches has resulted in the emergence of modified theories of gravity [68], [80]. According to these theories, gravity may exhibit different behaviours on larger or smaller scales when compared to the thoroughly tested behaviour in the middle range of the spectrum.

In theoretical physics, one of the most widely used methods of modifying gravity is the Brans-Dicke theory [36]. The primary objective in this theory is the modification of Einstein's formulation of GR by integrating Mach's principle into the theory. According to Mach's perspective, the average motion of distant celestial objects determines the local inertial frames. This concept indicates that the gravitational coupling at a specific point in spacetime is defined by the presence of matter in its vicinity. For this reason, it eventually becomes a function of the spacetime coordinates and the notion of inertia as well as the Equivalence Principle must be revised according to this perspective.

Following that reasoning, the Brans-Dicke theory suggested that the inertial masses of the particles should not be considered as fundamental constants but rather as a manifestation of their interaction with some cosmic fluid. However, the absolute scale of elementary particle masses can be determined by measuring gravitational accelerations. This leads to an equivalent conclusion that the gravitational constant must be linked to the average value of a scalar field associated with mass density. This scalar field, denoted as ϕ, is expected to originate from all forms of matter, much like gravity itself. Consequently, one could interpret this theory as an extension of the gravitational field from a purely geometric perspective to one that incorporates both geometric and scalar components.

To advance further, there is no requirement to restrict the gravitational Lagrangian to solely being a linear function of the Ricci scalar minimally coupled to matter. It is possible to construct and investigate more complex forms of the Lagrangian that can include additional interactions and terms. The formulation of the Lagrangian could incorporate higher-order terms of the curvature tensor, such as $R^2, R^{\mu\nu}R_{\mu\nu}, R^{\alpha\beta\mu\nu}R_{\alpha\beta\mu\nu}$ as well as nonminimally coupling terms between a scalar field and the geometry.

The second of these scenarios outlines the framework of scalar-tensor theories, often utilized as the representative method to describe deviations for GR. Scalar-tensor theories are among the most recognized and extensively studied alternatives in the existing literature. The most general form of the Lagrangian for scalar-tensor theories which leads to second-order field equations in four dimensions is the Horndeski theory of gravity [77]. The Horndeski theory has been utilized in various ways to develop cosmological models of inflation and dark energy. The significance of the second-order field equations present in that theory lies in their capacity to prevent higher-order derivatives, which have the potential to cause ghost-like instabilities often encountered in the development of theoretical models.

The formulation of the Horndeski theory in its modern form resulted from the development of Galileon theories. This resurgence has prompted significant research beyond the standard model of cosmology utilizing the broad framework of scalar-tensor theories. Moreover, the Horndeski theory could be regarded as an extension of GR in the sense that provides the proper platform to explore modified gravity theories that might address the limitations of General Relativity and bring novel insights to several cosmological inquiries, such as Brans-Dicke, quintessence and dilaton to mention a few. This fact explains the increased interest in Horndeski's theory which has led to numerous studies and applications of its principles in interpreting cosmological and astrophysical observations beyond GR in recent years [77], [87].

Regarding the first scenario, it includes gravity theories that are higher than second-order in derivatives. These theories exhibit intriguing phenomenology and are frequently proved to be more resilient to instabilities than initially thought.

However, it is crucial for any innovative theory that attempts to explain gravity to adhere to certain requirements in order to gain credibility and be considered valid. To begin with, the candidate theory must be able to reproduce the Newtonian laws in the weak-field and slow-motion limits. Additionally, the new theory must be able to successfully depict the known behaviours and properties of baryonic matter and radiation, while also possessing the capacity to provide a coherent explanation for the development of large-scale structures in the Universe. Finally, the theoretical model that is being suggested needs to effectively forecast and elucidate the cosmological dynamics in a consistent and reliable manner which aligns with the results obtained from observations. This would ensure that the model is able to provide accurate insights into the mechanisms of cosmological evolution.

General Relativity is considered as the fundamental theory capable of meeting the aforementioned requirements. It posits the integration of space and time into a spacetime configuration and interprets gravitational interaction as a modification in the geometry of spacetime. In this context, the notion of gravitational force is absent. Consequently, geometry replaces gravity and the trajectories followed by particles are determined by geodesics rather than force equations as seen in electrodynamics.

Even so GR stands out as a fundamental theory describing interactions, yet without adhering to the gauge model. In order to bridge the gap and develop a gauge theory for gravity an alternative approach is to explore the principles of TG as it can be regarded as a gauge theory for the translation group. The utilization of TG as a framework provides a unique opportunity to study the dynamics of gravity under this new perspective. According to TG, every point in spacetime is associated with a Minkowski tangent space where the translation operates. The gravitational interaction is now described in a manner similar to the Lorentz force equation of electrodynamics with torsion having the role of the force. This fact indicates a change in the way gravitational interactions are understood and interpreted. In comparison to GR where geodesic equations dominate, in TG the focus shifts towards force equations that play a crucial role in determining the trajectories of the particles in spacetime [6], [17].

The reason that gravity can be approached by two equivalent descriptions can be attributed to its unique feature of universality. Gravity, along with the other fundamental interactions in nature can be elucidated within the context of a gauge theory which is Teleparallel gravity theory. Yet, the universality of free fall permits a geometric approach based on the Equivalence Principle, which is GR. From this point of view, when considering the field equations, curvature and torsion serve as complementary methods for defining the gravitational field, therefore the choice between a curved or a torsioned spacetime becomes a matter of convention.

As TG is a gauge theory of the translation group, the primary field now is a connection which is the translational gauge potential with respect to which the variations of the action are calculated. While GR also involves a connection, the Levi-Civita connection, it does not serve as an actual gravitational variable or a gravitational connection in terms of classical fields. The rationale behind this fact is that the Levi-Civita connection represents both gravitational and inertial effects.

At this point, it is noteworthy to mention that numerous researchers of the scientific community propose that torsion might have been a contributing factor in the dynamics during the early stages of the Universe. Following this concept, torsion could also have generated observable impacts today. Indeed, the presence of torsion results in repulsive contributions to the energy-momentum tensor, leading to cosmological models without singularities. In addition, torsion possesses the ability to account for topological effects that could manifest themselves today as intrinsic angular momenta of cosmic structures such as galaxies. Furthermore, the presence of torsion within the energy-momentum tensor could potentially impact the spectrum of cosmological perturbations leading to characteristic lengths of large-scale structures in the Universe. As a result, it could influence the overall spatial distribution of matter and energy and introduce new dynamics into the study of cosmological evolution and structure formation.

The teleparallel approach of gravitation has been a concept known since the early twentieth century. It was initially introduced and employed by Einstein in an unsuccessful endeavour to merge electromagnetism and gravity. However, the formulation of teleparallelism as a gravitational theory was established in the 1950s following the publication of Møller's work.

Currently, Teleparallel Gravity represents a significant amount of gravity theories, especially focusing on advancements in the scalar-tensor sector, where the teleparallel equivalent of the Horneski theory has been gaining recognition in the scientific community because of its much richer phenomenology when compared to the classical Horndeski case. Due to the torsion tensor and its irreducible decomposition, a comprehensive collection of 14 new scalar invariants can now be included in the Lagrangian. As a result of the novel term, G_{tele} which includes the scalar invariants in the Lagrangian, the severely constrained terms of the classical Horndeski theory can now survive the limitations imposed by the Gravitational Wave (GW) propagation speed.

It is important to highlight at this point, that the classical Horndeski theory, which is formulated using curvature and the Levi-Civita connection, is now to be considered as a subcase of the teleparallel Horndeski theory. This fact indicates a multitude of possibilities for theoretical advancements in the study of scalar-tensor theories within the teleparallel framework.

Recent results and measurements in the realms of observational astrophysics and cosmology, particularly in precision cosmology, are significantly shaping the progress of novel theoretical models in the teleparallel framework. Furthermore, as observational cosmology continues its evolution, it is approaching the critical boundary of the region where GR must align effectively with measurements such as the late-time tensions and uncertainties in the physics that govern the early stages of the Universe.

As several important issues have been resolved in the context of TG and there is an increasing demand generated from cosmological observations for novel and viable gravity theories, scientific research is highly motivated to enhance the perspectives and interpretations of TG. The exploration of the teleparallel framework may allow for a further investigation of the fundamental interactions in the cosmos and provide valuable insights into the mechanisms of the Universe. This ongoing process is essential for minimising the distance between theoretical predictions and data obtained through observation and contributing to the advancement of our understanding of the Universe.

Chapter 2 of the present thesis introduces the fundamental principles of TG as a different theoretical framework for describing gravity. The analysis highlights the fact that TG – a gauge theory of translations – associates gravity with torsion rather than curvature which is the prevailing explanation in GR. As a result, TG assumes the presence of a gravitational force instead of relying on geometrization leading to the absence of the concept of geodesics. Subsequent to this, the second chapter elaborates on the formulation of the Teleparallel analogue of Horndeski theory (BDLS) which is the main topic of the thesis. Due to the 14 new scalar invariants resulting from the decomposition of the torsion tensor and its contractions with the scalar field, BDLS theory provides a wide range of phenomenology. Based on this fact, Chapter 2 concludes that the Lagrangian of the BDLS theory could actually endure the GW propagation speed constraint. This conclusion paves the way for exploring the polarization of GW in the BDLS framework, thus serving as a promising foundation for future research.

Chapter 3 incorporates the mathematical concept of dynamical systems to analyze the Einstein Gauss-Bonnet model of modified gravity. The novel approach here is that we focus on how the solutions of the system are affected when the Einstein Gauss-

Bonnet theory is required to be consistent with the GW speed constraint. The requirements of compatibility result in an autonomous dynamical system without the need to make any assumptions about the various periods of cosmic evolution. The analysis of the dynamical system results in a total of seven critical points. These critical points provide a new viewpoint to understand the phenomenology of the Einstein Gauss-Bonnet model. Among them, two critical points do not correspond to the stages of the CDM model and most likely are associated with the early stages of the Universe. Additionally, the third critical point is a stable one, dominated by the potential energy of the scalar field. The important feature of this critical point is that is related to a phase of late-time accelerated expansion of the Universe and could play the role of the attractor of the model. The dynamical system also has two critical points related to scaling solutions where the energy density of the scalar field tracks the one of the background. Nevertheless, when attempting to combine these two scaling solutions with the third critical point, they fail to describe the evolution of the Universe in the Einstein Gauss-Bonnet framework. The characteristics and stability properties of the seven critical points provide a richer perspective on the dynamical behaviour of the Einstein Gauss-Bonnet model, warranting further investigation in future studies.

Motivated by the extensive theoretical landscape of the BDLS theory, Chapter 4 delves into the investigation of the symmetries derived from the Noether symmetry approach applied in BDLS. Since Noether's theorem relates symmetries with conservation laws, this approach improves the accessibility of accurate solutions that may otherwise be difficult to obtain. The investigation starts with the formulation of the point-like Lagrangian of the theory and the next step is the utilization of the Rund-Trautman identity to the point-like Lagrangian. This results in a system of 62 equations for the coefficients of the generator vector and the G_i functions of the BDLS theory. Consequently, a diverse range of cases has emerged. Each of these cases describes a different cosmological model necessitating an in-depth investigation to achieve a detailed understanding of its characteristics. The fourth chapter presents a set of four cases to effectively demonstrate the advantages of the methodology being examined. In each of these four cases, the G_i functions along with the coefficients of the generator vector are presented which are the crucial ingredients for the development of a cosmological model in the BDLS context. The main objective of this study is to illustrate the successful correlation between the functions defining various cosmological models and the application of the Noether symmetry approach. The wide range of classification cases has revealed the multitude of distinct cosmological scenarios, each with its own features. This fact presents intriguing dynamics that warrant additional study and investigation.

Chapter 5 investigates the cosmological perturbations in the BDLS framework on a Friedmann-Lemaître-Robertson-Walker (FLRW) background while assuming a zero spin connection for the tetrad. After formulating the equations of motion for the FLRW background, we decompose the torsion tensor and calculate its contractions with the scalar field for tensor, scalar and vector modes. The next step includes the expansion of the action of perturbations up to the second order. Analyzing the second-order action enables a detailed examination of each type of perturbation. This analysis is crucial for broadening our understanding of how the different types of perturbation impact the dynamical features of BDLS theory. The following stage of the perturbation analysis is to prevent the emergence of instabilities. To accomplish this, we derive the constraint equations by varying the action with respect to the non-dynamical fields for each type of perturbation. In that way we have the final form of the quadratic action for tensor, scalar and vector modes, facilitating the derivation of the stability criteria that guarantee the absence of ghosts and gradient instabilities in the theory. The fifth chapter also provides an in-depth study of the power spectrum related to scalar and tensor perturbations. The study of the power spectrum allows a detailed examination of the inflationary models in the context of BDLS and also enables the calculation of the tensor-to-scalar ratio related to the slow roll parameters. In addition, this chapter discusses the use of the α-parametrization in the perturbation analysis. Through the four time-dependent $\alpha_i(t)$ functions the perturbation results can be presented in an easy and accessible manner that can be readily comprehended within the academic community.

Chapter 6 of the thesis investigates the possibility of having healthy non-singular cosmological models in the BDLS framework thereby circumventing the *No-go* theorem. The classical Horndeski theory enables the generation of bouncing solutions, however, these solutions are plagued with pathologies in the tensor sector. Because of the novel Lagrangian contribution, G_{tele}, in the BDLS theory it is possible to develop healthy non-singular models and this new possibility would have a significant positive impact on the BDLS framework. Nonetheless, the probability of accomplishing this aim remains uncertain and also the BDLS evading solutions may be relevant only to certain scenarios. The sixth chapter demonstrates three BDLS toy models that offer a way to evade the *No-go* theorem while meeting the GW propagation speed constraint. In these three models, the cosmological perturbation results of Chapter 5 were incorporated. In addition, the first two models use a power law bouncing scale factor while for the third model, we use a scale factor which is an exponential function of the cosmic time. In all these toy models the G_{tele} term is a simple function of the torsion scalar along with the scalar invariants of the BDLS theory and the expressions of G_4 and G_5 are not trivial ones. The evasion of the *No-go* theorem with these three BDLS toy models presents a perfect starting point for exploring the research even more.

2

The Teleparallel analogue of Horndeski theory

This chapter first provides an overview of the fundamental concepts and principles of the Teleparallel Gravity theory and then discusses the development of the analogue of Horndeski's theory within the teleparallel context. Additionally, it examines the necessary conditions and constraints that the emerging theory must fulfil to establish its validity.

2.1 | Teleparallel Gravity

Gravitation distinguishes itself among the four fundamental interactions inherent in Nature. Its origin lies in energy-momentum and it assumes a unique description in GR where gravitational phenomena coalesce with inertia. The other three recognized interactions – electromagnetic, weak and strong forces – are defined by renormalised quantum field theories – the Standard Model – and exhibit remarkable agreement with experimental results. However, gravitation is the only interaction which deviates from conforming to the gauge context and efforts of quantize GR are so far unsuccessful. [113], [105]. In addition and despite achieving notable success, the ΛCDM model based on the principles of GR, faces numerous weaknesses that could be exploited. The investigation for determining the origin of the late-time accelerated expansion of the Universe along with the Hubble tension, presents two considerable challenges in the field of contemporary cosmology. The previously outlined issues define a compelling case for the scientific community to explore alternative methods and tactics in creating an acceptable cosmological scheme.

Teleparallel Gravity (TG), a gauge theory of translations, is one such approach, which involves transforming curvature-based theories of gravity to torsion-based ones. In TG, we replace the Levi-Civita connection with the teleparallel, torsion-full connection which complies with the metricity condition [6]. This change in the geometric framework leads to the conclusion that the Ricci scalar $\mathring{R}$ (over-circles denote quantities calculated with the Levi-Civita connection) is dynamically equivalent to the torsion scalar T up to a boundary term B. The presence of this fact guarantees that GR is equivalent to a Teleparallel Equivalent of General Relativity (TEGR) [17], [91].

Although equivalent, there is a clear distinction between the two theories in terms of their conceptual framework. GR employs the notion of curvature to geometrize the gravitational interactions; geometry replaces the concept of gravity and the trajectories are defined through geodesics rather than force equations. On the other hand, TG assigns gravity to torsion not by utilizing geometrization, but through the action of a force. Consequently, TG does not involve geodesic equations, instead it employs force equations similar to the Lorentz force equations of electrodynamics.

In TG, similar to any other theory of gravity, the gravitational interactions are elucidated using the concept of the tangent space, which is a Minkowski space conventionally prescribed as n_{AB}. In this context and for each point within the four-dimensional spacetime, we can establish four vector fields e^A, that collectively constitute an orthonormal basis in the tangent space. These frame fields operate as the general linear bases on the differentiable manifold of spacetime. The complete assemblage of such frames, with the essential prerequisites for constructing a differentiable manifold, forms the bundle of linear frames. At each point of spacetime, a frame field establishes a basis for the vectors residing within the tangent space. The components of these fields, namely ${e^A}_\mu$, correspond to the tetrad fields which comprise a non-degenerate matrix and they relate Minkowski tangent space to the spacetime manifold,

$$g_{\mu\nu} = {e^A}_\mu \, {e^B}_\nu \, \eta_{AB} \quad \text{and} \quad \eta_{AB} \; = \; {E_A}^\mu \, {E_B}^\nu \, g_{\mu\nu} \tag{2.1}$$

where ${E_A}^\mu$ is the inverse tetrad field. Here, Greek indices pertain to the coordinates of spacetime while Latin indices signify the Minkowski space.

The frame components, ${e^A}_\mu$, meet the following orthogonality conditions :

$${e^A}_\mu \, {E_B}^\mu = \delta^A_B \quad \text{and} \quad {e^A}_\mu \, {E_A}^\nu = \delta^\nu_\mu \,, \tag{2.2}$$

It is worth mentioning that the tetrad fields along with their bundles are integral components of spacetime; they are inherently present once the spacetime is defined as a differentiable manifold. In addition, the bundle of linear frames exhibits the key property of soldering, facilitating the link between the tangent space tensors (internal tensors) with the space-time tensors (external tensors). As an example, consider the Lorentz vector u^B and the corresponding spacetime vector u^μ. The relation between them, on account of the soldering property, is defined as

$$u^\mu \; = \; {E_B}^\mu \; u^B \tag{2.3}$$

To ensure the covariant property of objects under general coordinate and gauge transformations, it is essential to introduce a connection leading to derivatives with well-defined tensorial behaviour under point-dependent transformations. Considering the linear group $GL(4,\mathbb{R})$ of transformations and particularly the Lorentz group $SO(3,1)$ the related connection is the Lorentz connection, $\omega\mu$, defined on the bundle of linear frames. The existence of the property of soldering in that bundle leads to the presence of torsion for every connection.

A Lorentz connection, also known as the spin connection, assumes values in the Lie algebra of the Lorentz group,

$$\omega_\mu = \frac{1}{2}\omega^{AB}{}_\mu \, S^{AB}, \tag{2.4}$$

where S_{AB} is a representation of the Lorentz generators, antisymmetric in the algebraic indices, a property that the spin connection inherits. Through the spin connection, ω_μ, one is able to define the Fock-Ivanenko covariant derivative,

$$\mathcal{D}_\mu = \partial_\mu - \frac{i}{2}\,\omega^{AB}{}_\mu \, S_{AB} \tag{2.5}$$

While the Fock-Ivanenko derivative can encompass all kinds of fields, both tensorial and spinorial, the covariant derivative, ∇_μ, is limited to tensorial fields only. As a result, when describing the correlation between spinor fields and gravitation, it is mandatory to employ the Fock-Ivanenko derivative [132].

When considering the relevant general linear and spacetime-indexed connection to each spin connection under the soldering process, it becomes necessary to acknowledge its non-tensorial character. Consequently, this leads to the emergence of a non-homogeneous term and yields the following result [5]:

$$\Gamma^\lambda{}_{\nu\mu} = E_A{}^\lambda \, \partial_\mu \, e^A{}_\nu + E_A{}^\lambda \, \omega^A{}_{B\mu} \, e^B{}_\nu = E_A{}^\lambda \, \mathcal{D}_\mu \, e^A{}_\nu, \tag{2.6}$$

which encapsulates the fact that the total covariant derivative of the tetrad with connection terms for both internal and external indices vanishes,

$$\partial_\mu \, e^A{}_\nu + \omega^A{}_{B\mu} \, e^B{}_\nu - \Gamma^\lambda{}_{\mu\nu} \, e^A{}_\lambda = 0 \tag{2.7}$$

It should be emphasized that the tetrad and the spin connection describing the geometry are not uniquely defined by the metric and affine connection. Under a local Lorentz transformation, $\Lambda^A{}_B(x)$, of the tetrad alone, the connection coefficients of Eq.(2.6) are not invariant, unless the transformation is global, $\partial_\mu \Lambda^A{}_B = 0$. To ensure that the connection is invariant when subjected to local Lorentz transformations, it is necessary to transform the spin connection as well, which undergoes the rule:

$$\omega'^{A}{}_{B\mu} = \Lambda^{A}{}_{C}(x)\,\omega^{C}{}_{D\mu}\,\Lambda_{B}{}^{D}(x) + \Lambda^{A}{}_{C}(x)\,\partial_{\mu}\Lambda_{B}{}^{C}(x) \tag{2.8}$$

Consequently, the tetrad and spin connection constructing a specific metric-affine geometry, are uniquely determined up to a local Lorentz transformation. This Lorentz gauge freedom becomes significant when incorporating a flat, metric-compatible spin connection. In this scenario, it is always feasible, at least locally, to select a gauge in which the spin connection vanishes identically, $\omega^{A}{}_{B\mu} = 0$. This particular gauge is referred to as the Weitzenböck gauge [72], [138].

In the TG context, the substitution of the Levi-Civita connection with the teleparallel connection leads to a significant change. One result of this procedure is that the Riemann tensor of the theory will become zero. Essentially, by altering the underlying connection, the geometrical structure is transformed, causing the Riemann tensor to lose its previous non-zero values of GR. However, the presence of the torsion tensor is guaranteed and is the antisymmetric part of the affine connection coefficients

$$T^{A}{}_{\mu\nu} := 2\,\Gamma^{A}{}_{[\nu\mu]} \tag{2.9}$$

Under the Lorentz group, the torsion tensor is capable of being decomposed into three distinct components which are irreducible by nature. These components include the axial part, the vector part and the purely tensorial part as follows [11]:

$$a_{\mu} := \frac{1}{6}\,\epsilon_{\mu\nu\lambda\rho}\,T^{\nu\lambda\rho}\,, \tag{2.10}$$

$$v_{\mu} := T^{\lambda}{}_{\lambda\mu}\,, \tag{2.11}$$

$$t_{\lambda\mu\nu} := \frac{1}{2}\left(T_{\lambda\mu\nu} + T_{\mu\lambda\nu}\right) + \frac{1}{6}\left(g_{\nu\lambda}\,v_{\mu} + g_{\nu\mu}\,v_{\lambda}\right) - \frac{1}{3}\,g_{\lambda\mu}\,v_{\nu}\,, \tag{2.12}$$

where $\epsilon_{\mu\nu\lambda\rho}$ is the totally antisymmetric Levi-Civita tensor density in four dimensions.

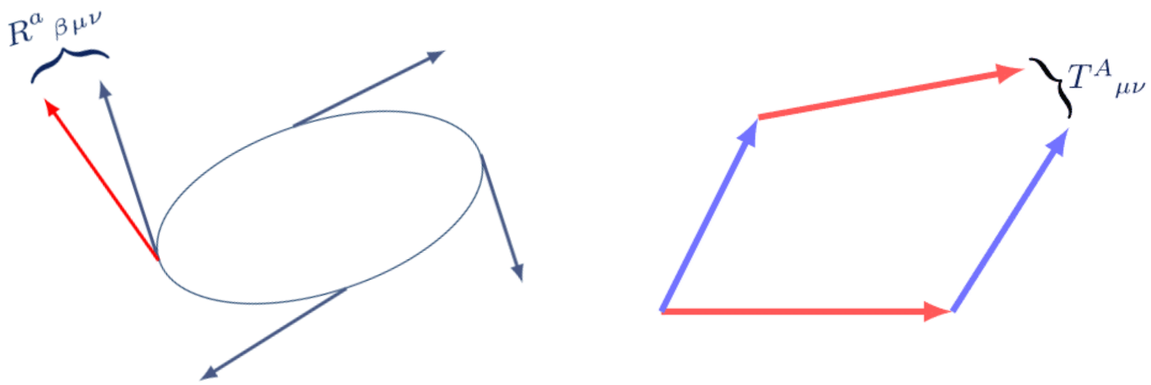

Figure 2.1: Geometric representation of the concepts of curvature and torsion. The image on the left demonstrates how curvature causes a vector to change when it is parallel transported along a closed curve. In the presence of torsion, the process of parallel transport does not exhibit symmetry when the transported vector and the direction of the transport are exchanged, as illustrated in the image on the right [17], [28].

The previously stated process of decomposing the torsion tensor has a critical role in facilitating the formation of the scalar invariants :

$$T_{\text{ax}} := a_{\mu}\, a^{\mu} = -\frac{1}{18}\left(T_{\lambda\mu\nu}T^{\lambda\mu\nu} - 2\,T_{\lambda\mu\nu}T^{\mu\lambda\nu}\right)\,, \tag{2.13}$$

$$T_{\text{vec}} := v_{\mu}\, v^{\mu} = T^{\lambda}{}_{\lambda\mu}\, T_{\rho}{}^{\rho\mu}\,, \tag{2.14}$$

$$T_{\text{ten}} := t_{\lambda\mu\nu}\, t^{\lambda\mu\nu} = \frac{1}{2}\left(T_{\lambda\mu\nu}T^{\lambda\mu\nu} + T_{\lambda\mu\nu}T^{\mu\lambda\nu}\right) - \frac{1}{2}T^{\lambda}{}_{\lambda\mu}T_{\rho}{}^{\rho\mu} \tag{2.15}$$

These three scalars are considered to be the most comprehensive torsion invariants, showcasing their utmost generality. Being quadratic in the torsion tensor, these scalars could be merged to yield the following formula of the torsion scalar :

$$T := \frac{3}{2}\,T_{\text{ax}} + \frac{2}{3}\,T_{\text{ten}} - \frac{2}{3}\,T_{\text{vec}} \tag{2.16}$$

Apart from the torsion tensor, TG theory enables the establishment of tensors with comparable importance. The contortion tensor serves as an exemplification of such a case. It is defined as the difference between the Levi-Civita connection $\mathring{\Gamma}^{\sigma}_{\mu\nu}$ and the teleparallel connection $\Gamma^{\sigma}_{\mu\nu}$ [6]

$$K^{\sigma}{}_{\mu\nu} := \Gamma^{\sigma}{}_{\mu\nu} - \mathring{\Gamma}^{\sigma}{}_{\mu\nu} = \frac{1}{2}\left(T_{\mu}{}^{\sigma}{}_{\nu} + T_{\nu}{}^{\sigma}{}_{\mu} - T^{\sigma}{}_{\mu\nu}\right), \tag{2.17}$$

and thus it is possible to establish a relation between TG and theories of gravity based on curvature and the Levi-Civita connection.

Likewise, the incorporation of the superpotential tensor as a Hamiltonian boundary term related to the gravitational energy-momentum pseudotensor, defined as

$$S_A{}^{\mu\nu} := K^{\mu\nu}{}_A - E_A{}^{\nu}\, T^{A\mu}{}_A + E_A{}^{\mu}\, T^{A\nu}{}_A \tag{2.18}$$

An interesting property of the torsion scalar is that it can be expressed as [11, 17]

$$T := S_A{}^{\mu\nu}\, T^{A}{}_{\mu\nu}, \tag{2.19}$$

which is a combination of the superpotential and torsion tensor.

The torsion scalar which is obtained using the teleparallel connection is ultimately equivalent to the Ricci scalar as computed in GR up to a divergence term B [17, 6, 10]

$$\mathring{R} = -T + \frac{2}{e}\partial_{\mu}\left(e\, T^{\lambda}{}_{\lambda}{}^{\mu}\right) = -T + B, \tag{2.20}$$

where $\mathring{R}$ refers to the Ricci scalar calculated using the Levi-Civita connection and the determinant of the tetrad field, e, is given by $e = det(e^{A}{}_{\mu}) = \sqrt{-g}$.

The meaning of Eq.(2.20) implies that the field equations obtained from a Lagrangian including the torsion scalar would be identical to those derived from the Einstein-Hilbert action of GR. The presence of the term B establishes a dynamical equivalence between these two theories, leading to the formulation of the TEGR.

Therefore, the action in the context of TEGR is as follows [17]:

$$\mathcal{S}_{TEGR} = -\frac{1}{2\kappa^2}\int d^4x\, e\, T + \int d^4x\, e\, \mathcal{L}_m \tag{2.21}$$

where $\kappa^2 = 8\pi G$ and $\mathcal{L}_m$ is the Lagrangian for the matter fields.

Because of their dynamic equivalence, the field equations derived from the variation of Eq.(2.21) concerning the tetrad and spin connection allow for all the same solutions as in GR. In the case of TEGR and as the tetrad and spin connection assume the role of fundamental variables, they possess independent degrees of freedom (DoF) and thus could in principle be determined by additional equations. However, the spin connection in TEGR is related to DoF that are connected to the Lorentz group and do not affect the number of dynamical equations. As a consequence, the field equations for the spin connection are identically satisfied.

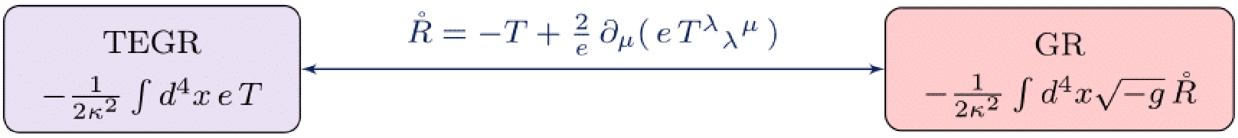

Figure 2.2: The dynamical equivalence between the two theoretical frameworks of TG and GR. The arrow connecting the two frames in the image corresponds to Eq.(2.20) which represents the relationship between the Ricci scalar of GR and the torsion scalar of TG [17].

2.2 | Horndeski theory in General Relativity

Lovelock's theorem asserts that the field equations of GR are the sole second-order Euler-Lagrange equations derived from a local gravitational action involving only the second derivative of the four-dimensional spacetime metric [49], [96], [97]. In light of the rationales presented earlier and to advance GR, it is important to relax the assumptions of Lovelock's theorem. For instance, to consider other fields rather than the metric tensor or to accept higher than second-order derivatives of the metric. Furthermore, to employ dimensionality other than four or even relinquish the demand for divergence-free field equations. However, the easiest method to loosen Lovelock's assumptions is to introduce an additional DoF, specifically a scalar field alongside the metric.

The Horndeski theory is the most general scalar-tensor theory which has been extensively employed due to its ability to generate second-order field equations in four dimensions. This theory includes a single scalar field as a new DoF, with the computation of the Lagrangian relying on the Levi-Civita connection of GR [77], [87].

In four dimensions the Lagrangian of Horndeski theory that produces field equations of second order for both the scalar field ϕ and the metric $g_{\mu\nu}$ is [56]

$$\mathcal{L} = \sum_{i=2}^{5} \mathring{\mathcal{L}}_i \tag{2.22}$$

with,

$$\mathring{\mathcal{L}}_2 = G_2(\phi, X) \tag{2.23}$$

$$\mathring{\mathcal{L}}_3 = -G_3\,(\phi, X)\,\mathring{\Box}\phi \tag{2.24}$$

$$\mathring{\mathcal{L}}_4 = G_4(\phi, X)\mathring{R} + G_{4X}(\phi, X)\,[\,(\mathring{\Box}\phi)^2 - \mathring{\nabla}_\mu\mathring{\nabla}_\nu\phi\,\mathring{\nabla}^\mu\mathring{\nabla}^\nu\phi\,] \tag{2.25}$$

$$\mathring{\mathcal{L}}_5 = G_5(\phi, X)\,\mathring{G}_{\mu\nu}\mathring{\nabla}^\mu\mathring{\nabla}^\nu\phi - \frac{1}{6}\,G_{5X}(\phi, X)\,[\,(\mathring{\Box}\phi)^3 + 2\,\mathring{\nabla}_\nu\mathring{\nabla}_\mu\phi\,\mathring{\nabla}^\nu\mathring{\nabla}^\lambda\phi\,\mathring{\nabla}_\lambda\mathring{\nabla}^\mu\phi - 3\,\mathring{\Box}\phi\,\mathring{\nabla}_\mu\mathring{\nabla}_\nu\phi\,\mathring{\nabla}^\mu\mathring{\nabla}^\nu\phi\,] \tag{2.26}$$

The over-circles denote calculations using the Levi-Civita connection of GR. The terms G_2, G_3, G_4 and G_5 are functions that depend on the scalar field and the kinetic term X and can vary arbitrarily. When calculating the kinetic term, the Levi-Civita connection covariant derivative of ϕ is utilized, $X = -\frac{1}{2}\mathring{\nabla}_\mu\phi\,\mathring{\nabla}^\mu\phi$. In addition, the d'Alembertian operator can be expressed as $\mathring{\Box} = \mathring{\nabla}_\mu\mathring{\nabla}^\mu$. By strategically choosing the functions outlined in Eqs (2.23)-(2.26), we are able to reproduce any second-order scalar-tensor theory. For instance, with the special choice of $G_4 = M_{Pl}^2/2$ we can formulate the Einstein-Hilbert action, while for the $G_4 = f(\phi)R$, a nonminimal coupling can be achieved. In addition, the G_2 term is used in building k-essence models. The G_3 term has been studied within the framework of kinetic gravity braiding. This is a novel aspect of modifying gravity where the scalar equation of motion involves the second derivative of the metric and vice versa [57].

Regarding the existence of the Ricci scalar, $\mathring{R}$, and the Einstein tensor $\mathring{G}_{\mu\nu}$ in the previous formulation, it is important to address a specific observation. When gravity is introduced into the theory, the process of covariantization occurs by promoting $\eta_{\mu\nu}$ to $g_{\mu\nu}$ and ∂_μ to $\mathring{\nabla}_\mu$. Nonetheless, this approach produces field equations with higher derivatives which could potentially lead to instabilities. To mitigate this concern, the inclusion of terms dependent on curvature becomes necessary. This inclusion justifies the presence of $\mathring{R}$ and $\mathring{G}_{\mu\nu}$ as counter terms, thereby ensuring that the derived field equations are genuinely of second order.

2.3 | Horndeski theory in Teleparallel Gravity

The theory of Horndeski distinguishes itself as the most comprehensive four-dimensional scalar-tensor theory of gravity. Its foundation lies in contracting the metric tensor with a scalar field, leading to the emergence of field equations of second order.

The dependence of Horndeski's gravity on the Levi-Civita connection should not be regarded as an unquestionable postulate of the theory. Therefore, it could be replaced by a connection originating from an alternative theory linked to a distinct geometry, and, on a broader scale, a dissimilar perspective of the nature of gravity. Based on that argument, substituting the Levi-Civita connection with the torsion-full connection of TG is a logical progression towards creating the teleparallel analogue of the Horndeski theory. However, advancing this theory within the TG framework involves more than just changing connections. In this approach, several requirements must be taken into account to ensure the validity of the new theory [13], [17].

Firstly, it is necessary to ensure that the field equations do not exceed the second-order in the derivatives of the tetrad fields to prevent the occurrence of ghost-like instabilities. Another important aspect is the requirement for a covariantization technique for the scalar field ϕ from the tangent space to general manifolds. As indicated by the contortion relation presented in Eq.(2.17), both TG and GR exhibit equivalent coupling procedures. Taking this into consideration, the covariantization method in TG is

$$\partial_\mu \rightarrow \mathring{\mathcal{D}}_\mu \equiv \mathring{\nabla}_\mu \tag{2.27}$$

where $\mathring{\mathcal{D}}$ is the Levi-Civita covariant derivative calculated with the tetrads. The outcome matches the one calculated in GR, guaranteeing that in the TG theory, the Horndeski gravity will retain the same contributions as described in Eqs.(2.23)-(2.26). However, the switch of the connection will inevitably incorporate extra terms in the ultimate expression of the Lagrangian in the teleparallel context.

To determine those additional terms, it is necessary to take into account the contractions of the irreducible components of the torsion tensor, denoted in Eqs.(2.10)-(2.12), together with a scalar field ϕ. Under the analysis presented in [13], the linear contractions of the irreducible parts result in the following family of scalars :

$$I_1 = t^{\mu\nu\sigma}\,\phi_{;\mu}\,\phi_{;\nu}\;\phi_{;\sigma} \tag{2.28}$$

$$I_2 = v^\mu \phi_{;\mu} \tag{2.29}$$

$$I_3 = a^\mu\,\phi_{;\mu} \tag{2.30}$$

Each of these scalar quantities must remain invariant when subjected to parity transformations. Consequently, I_3 cannot be included in the set as it violates parity. Furthermore, due to the antisymmetry of the torsion tensor in its last two indices, I_1 vanishes leaving only I_2 as the surviving scalar of the set.

Following the same reasoning for the quadratic contractions of the torsion tensor, it is worth noting that the theorem of Lovelock explicitly prohibits the inclusion of any additional term in the general relativistic version of Horndeski's theory. Conversely, in the TG scenario, an infinite array of terms can be constructed, contributing to the formulation of second-order field equations. Yet, the attributing of physical meaning to these higher-order terms is severely doubtful. Therefore, the scalar invariants have been constrained to encompass no more than quadratic contractions of the torsion tensor.

As a result, the additional terms in the Lagrangian should initially include T_{ax}, T_{vec} and T_{ten} of Eqs.(2.13)-(2.15). Following that, the entire family of quadratic contractions of the torsion tensor with the scalar field can be established. By retaining solely those scalars that remain invariant under parity transformations, the resulting outcome can be summarized in the following manner :

$$J_1 = a^\mu \, a^\nu \, \phi_{;\mu} \, \phi_{;\nu} \, , \tag{2.31}$$

$$J_2 = v^\mu \, v^\nu \, \phi_{;\mu} \, \phi_{;\nu} \tag{2.32}$$

$$J_3 = v_\sigma \, t^{\sigma\mu\nu} \, \phi_{;\mu} \, \phi_{;\nu} \, , \tag{2.33}$$

$$J_4 = v_\mu \, t^{\sigma\mu\nu} \, \phi_{;\sigma} \, \phi_{;\nu} \tag{2.34}$$

$$J_5 = t^{\sigma\mu\nu} \, t_\sigma{}^\alpha{}_\nu \, \phi_{;\mu} \, \phi_{;\alpha} \, , \tag{2.35}$$

$$J_6 = t^{\sigma\mu\nu} \, t_\sigma{}^{\alpha\beta} \, \phi_{;\mu} \, \phi_{;\nu} \, \phi_{;\alpha} \, \phi_{;\beta} \, , \tag{2.36}$$

$$J_7 = t^{\sigma\mu\nu} \, t^{\alpha\beta}{}_\sigma \, \phi_{;\mu} \, \phi_{;\nu} \, \phi_{;\alpha} \, \phi_{;\beta} \tag{2.37}$$

$$J_8 = t^{\sigma\mu\nu} \, t_{\sigma\mu}{}^\alpha \, \phi_{;\nu} \, \phi_{;\alpha} \, , \tag{2.38}$$

$$J_9 = t^{\sigma\mu\nu} \, t^{\alpha\beta\rho} \, \phi_{;\sigma} \, \phi_{;\mu} \, \phi_{;\nu} \, \phi_{;\alpha} \, \phi_{;\beta} \, \phi_{;\rho} \tag{2.39}$$

$$J_{10} = \epsilon^\mu{}_{\nu\sigma\rho} \, a^\nu \, t^{\alpha\rho\sigma} \, \phi_{;\mu} \, \phi_{;\alpha} \, , \tag{2.40}$$

In the above collection, J_9 vanishes because of the antisymmetry property of the torsion tensor in its last two indices. Furthermore, $J_2 = I_2^2, J_3 = J_4$ and $J_7 = -2J_6$ due to $t_{\sigma\mu\nu} + t_{\mu\mu\sigma} + t_{\nu\sigma\mu} = 0$ and thus only seven scalars remain that contain quadratic contractions of the torsion tensor and scalar field derivatives.

Following the above analysis, it is evident that a new component needs to be incorporated to accommodate the newly constructed scalar invariants of the theory. The upcoming presentation will demonstrate each contribution of the Lagrangian and its modifications made in the TG context.

The first Lagrangian term shares an identical structure as the one observed in the classical Horndeski theory of GR, and is

$$\mathcal{L}_2 \;=\; G_2(\phi, X), \tag{2.41}$$

where the calculation of the kinetic term X was relied upon the use of tetrads, $X := -\frac{1}{2}\mathring{\mathcal{D}}_\mu\phi\,\mathring{\mathcal{D}}^\mu\phi = -\frac{1}{2}\partial_\mu\phi\,\partial^\mu\phi$.

After implementing the coupling recipe provided in TG, the next Lagrangian term possesses a comparable structure as well, leading to

$$\mathcal{L}_3 \;=\; -G_3\,(\phi, X)\,\Box\,\phi. \tag{2.42}$$

The d'Alembertian operator maintains its Levi-Civita formulation resulting from the coupling procedure, evaluated via the tetrad fields, $\Box := \mathring{\mathcal{D}}_\mu\,\mathring{\mathcal{D}}^\mu = \mathring{\nabla}_\mu\,\mathring{\nabla}^\mu$.

In line with the reasoning stated above regarding the coupling recipe, the next term of the Lagrangian will conform to Eq.(2.20), thereby yielding the following :

$$\mathcal{L}_4 \;=\; G_4(\phi, X)(-T + B) \;+\; G_{4X}(\phi, X)\,[\,(\Box\phi)^2 - \nabla_\mu\nabla_\nu\phi\,\nabla^\mu\nabla^\nu\phi\,] \tag{2.43}$$

When considering the final contribution to the Lagrangian, it becomes necessary to substitute the Einstein tensor with its teleparallel equivalent, denoted as $\mathcal{G}_{\mu\nu}$, which ultimately yields the following result :

$$\begin{aligned}\mathcal{L}_5 = G_5(\phi, X)\,\mathcal{G}_{\mu\nu}\nabla^\mu\nabla^\nu\phi - \frac{1}{6}\,G_{5X}(\phi, X)\,[\,(\Box\phi)^3 + 2\,\nabla_\nu\nabla_\mu\phi\,\nabla^\nu\nabla^\lambda\phi\,\nabla_\lambda\nabla^\mu\phi \\ - 3\,\Box\phi\,\nabla_\mu\nabla_\nu\phi\,\nabla^\mu\nabla^\nu\phi\,]\end{aligned} \tag{2.44}$$

Upon examining the definitions of $\mathcal{L}_4$ and $\mathcal{L}_5$ terms, it becomes evident that the coupling prescription when merged with the equivalence of torsion and Ricci scalars yields identical counter terms to those observed in the classical Horndeski scenario. Nevertheless, the correlation between each term of the classical Horndeski Lagrangian fails to encompass the entirety of the concept at hand. Incorporating a novel Lagrangian term is imperative to encapsulate the complete array of contractions, leading to second-order field equations. Uniquely manifested in TG theory, this new term, referred to as $\mathcal{L}_{tele}$, is

$$\mathcal{L}_{tele} := G_{tele}\left(\phi, X, T, T_{ax}, T_{vec}, I_2, J_1, J_3, J_5, J_6, J_8, J_{10}\right)\,, \tag{2.45}$$

Therefore, the Lagrangian associated with the BDLS theory [13], can be expressed as

$$\mathcal{L}_{BDLS} = \sum_{i=2}^{5} \mathcal{L}_i + \mathcal{L}_{tele}\,, \tag{2.46}$$

The theory being discussed here is the most general theory involving a scalar field, leading to second-order field equations concerning the derivatives for both the tetrad and the scalar field. It is evident that to restore the classical Horndeski theory and its subclasses, the newly introduced term, $\mathcal{L}_{tele}$ must be set equal to zero. In particular, when the teleparallel Lagrangian term is zero and with the conditions of $G_4 = 1, G_5 = 0$, one could derive the kinetic braiding theory of gravity [58]. Continuing along the same vein, under the conditions of $G_3 = G_5 = 0$ and $G_4 = \tilde{G}_4(\phi)$, the generalized Brans-Dicke theory can be formulated [116] while for $\tilde{G}_4(\phi) = 1$ we could also derive the quintessence modified theory [8] as special case of the classical Horndeski theory.

When the $\mathcal{L}_{tele}$ term is not zero, the BDLS theory could lead to the most important of the modified teleparallel theories studied in the literature by taking certain combinations for the Lagrangian terms. In the case of $G_2 = G_3 = G_4 = G_5 = 0$ and $G_{tele} = c_1 T_{ax} + c_2 T_{ten} + c_3 T_{vec}$, then one could derive the theory known as New General Relativity (NGR) [75]. For $c_1 = 3/2, c_2 = 2/3$ and $c_3 = -2/3$, the NGR Lagrangian reduces to that of the TEGR. In addition, when $G_{tele} = f(T)$, where $f(T)$ is an arbitrary function of the torsion scalar T, we can formulate the $f(T)$ theory of teleparallel gravity which can lead to an interpretation of the late-time acceleration of the Universe while including the description of radiation and matter dominated eras [41].

Another avenue in the BDLS context is to set $G_3 = 0, G_5 = 0, G_4 = \tilde{G}_4(\phi)$ while the G_{tele} is a function of the torsion scalar and the boundary term B [10]. The $f(T, B)$

modified theory is a generalization of TEGR. When the function f is independent of the boundary term, it leads to the $f(T)$ theory. Additionally, if the combination of $-T+B$ appears in the argument of the function we can recover the standard $f(\mathring{R})$ theory of modified gravity.

The inclusion of the novel Lagrangian term, $\mathcal{L}_{tele}$, enables BDLS theory to offer an explanation for the accelerated expansion of the late Universe without necessitating the presence of the cosmological constant. In addition, BDLS has the potential to describe different evolutionary eras in cosmic history and approach the inflationary process.

Moreover, the $\mathcal{L}_{tele}$ term enables the generation of numerous novel teleparallel theories. It would be beneficial to conduct a comprehensive analysis of these newly formulated theories, focusing on both cosmological and astrophysical aspects. In the same line of thought, exploring the constraints arising from large-scale structures could lead to the enhancement of physically viable choices for the BDLS Lagrangian.

In summary, BDLS theory encompasses the conventional Horndeski gravity but it also has the capacity to advance it further by simply modifying the underlying geometrical framework.

2.4 | BDLS Theory after GW170817

Recent gravitational wave observations by the LIGO Collaboration with an upper limit of $|c_g/c-1| \gtrsim 10^{-5}$ have placed stringent constraints on Horndeski gravity. This section discusses the analysis of gravitational wave propagation within the context of the Teleparallel analogue of Horndeski gravity. It is demonstrated that within this framework is feasible to construct a broader Horndeski gravity model without eliminating the highly constrained terms $G_4(\phi,X)$ and $G_5(\phi,X)$.

2.4.1 | The Gravitational Wave Propagation Equation

As outlined by the principles of GR, compact concentrations of energy, such as neutron stars and black holes, are expected to significantly distort spacetime. Any alteration in the shape of these energy concentrations is predicted to generate a dynamically evolving deformation that propagates at the speed of light. This phenomenon of propagating distortion is defined as a gravitational wave (GW) [131]. The distortions can be elucidated through tensor perturbations of the metric. Tensor perturbations are characterized by the functions h_+ and $h_\times$ presumed to be both small and operating as the dual components of a traceless, divergenless and symmetric tensor $\mathcal{H}_{ij}$ [63].

To acquire the GW propagation equation, it is advisable to begin by examining a cosmological background that is spatially flat, $ds^2 = -dt^2 + a^2(t)(dx^2 + dy^2 + dz^2)$. The metric perturbations about this background can then be defined as $g_{\mu\nu} \to g_{\mu\nu} + \delta g_{\mu\nu}$, with the constraint that the magnitude of $\delta g_{\mu\nu}$ is very small, i.e. $|\delta g_{\mu\nu}| << 1$.

The tensor perturbations of the metric, at first-order perturbation level, can be described as $\delta g_{\mu\nu} = a^2\, \delta^i_\mu\, \delta^j_\nu\, h_{ij}$, with i, j to account for the spatial indices. Within this context, the general form of the propagation equation in a zero-curvature cosmological background, [121], [17], assumes the following form :

$$\ddot{h}_{ij} + (\,3 + \alpha_M\,)H\,\dot{h}_{ij} - (\,1 + \alpha_T\,)\,\frac{k^2}{a^2}\,h_{ij} = 0, \tag{2.47}$$

where $H = \dot{a}/a$ is the Hubble parameter, $\alpha_M = \frac{1}{H M_*^2}\frac{dM_*^2}{dt}$ is the Planck mass running rate which describes the rate of evolution of the effective Planck mass. This term contributes to both tensor and scalar perturbations and its time evolution in the Jordan frame leads to the appearance of anisotropic stress. The function $\alpha_T = c_T^2 - 1$ is the excess speed tensor. It is related to the propagation speed of GW and signifies any deviation of the propagation speed from the speed of light. [71], [26].

The collective findings of GW170817 and its electromagnetic counterpart impose stringent constraints on the upper limit of a_T with deviations of a maximum of one part in 10^{15} [3]. These constraints are contradictory to the most attractive versions of the standard Horndeski theory due to the significant disparities between their propagation speed and the speed of light. Quartic and quintic Galileon models, de-Sitter Horndeski and the Fab Four have been extensively studied as they offer compelling scenarios that encompass well-behaved inflationary stages and diverse phenomenology during the cosmological history. In light of this circumstance, several theories have emerged that transcend the conventional Horndeski. Conversely, the present investigation endeavours to ascertain the extent to which the BDLS theory can uphold the original spirit of the Horndeski theory of gravity.

Considering that the variables in Eq.(2.47) rely on the model being used, it becomes essential to utilize the tetrad perturbation approach when operating within the BDLS framework. In theories built upon tetrads the perturbation of the background tetrad, denoted as $e^A{}_\mu$, without the inclusion of the spin connection, is expressed as

$$e^A{}_\mu \rightarrow e^A{}_\mu + \delta\, e^A{}_\mu . \tag{2.48}$$

The diagonal tetrad $e^A{}_\mu$ in the given context is defined as $e^A{}_\mu = diag(1, a(t), a(t), a(t))$, where $a(t)$ is the scale factor of the Universe. It is important to note that this tetrad corresponds to a spatially flat FLRW cosmology. In this setting, the tetrad perturbation related to the tensor modes is

$$\delta e^K{}_\mu = \frac{1}{2}\, \delta^i_\mu\, \delta^{Kj}\, h_{ij}, \tag{2.49}$$

By replacing the above quantities into the field equations, which are obtained from the Euler-Lagrange equations for the background variables and h_{ij}, the resultant formula can be contrasted to Eq.(2.47). Although it requires considerable effort, this technique has the potential to explore the characteristics of GW propagation in any modified theory of gravity. The excess speed tensor can be expressed as [17], [14], [26], [71]

$$a_T = \frac{2\,X}{M_*^2}\left(2\,G_{4,X} - 2\,G_{5,\phi} - G_{5,X}\,(\ddot{\phi} - \dot{\phi}\,H) - 2\,G_{tele,J_8} - \frac{1}{2}\,G_{tele,J_5}\right) \tag{2.50}$$

and the effective Planck mass is defined as

$$M_*^2 = 2(G_4 - 2X\,G_{4,X} + X\,G_{5,\phi} - \dot{\phi}XHG_{5,X} + 2XG_{tele,J_8} + \frac{1}{2}XG_{tele,J_5} - G_{tele,T}) \quad (2.51)$$

There are only three scalars that survive in this setting and contribute to the formulation of G_{tele}, which are $T = 6H^2/N^2$, $T_{vec} = -9H^2/N^2$ and $I_2 = 3H\dot{\phi}/N^2$.

From the expression provided in Eq.(2.50), it becomes clear that the inclusion of the G_{tele} term has the potential to reintroduce cosmological models that were previously excluded due to the constraint of the GW propagation speed. By setting $a_T = 0$, which corresponds to the propagation speed being equal to the speed of light, this revival becomes achievable. Consequently, this new constraint effectively transforms every standard Horndeski model into a collection of solutions, thereby, broadening the range of possibilities in the current framework.

By using Eq.(2.50), both the standard Horndeski models and potential new ones can be restricted in terms of GW propagation speed, when solving for the G_{tele} contribution.

2.4.2 | Reviving Horndeski after GW170817

The GW170817 event – the first detection of GWs from the inspiral of a binary neutron star – was observed by the two Advanced LIGO detectors and the Advanced VIRGO detector. This event was followed by the detection of GRB170817A, a gamma-ray burst observed by the Fermi Gamma-Ray Burst Monitor and INTEGRAL. The observation of a GW and its electromagnetic counterpart confirm the beginning of a new era in discoveries using multimessenger observations [3]. The detection of the GW170817 event imposes a significant limitation on the GW propagation speed when compared to the speed of light [2], as indicated by

$$-3\cdot 10^{-15} \lesssim c_g - 1 \lesssim 7\cdot 10^{-16}, \quad \text{in } c = 1 \text{ units} \quad (2.52)$$

where this constraint corresponds to $a_T = 0$ in Eq.(2.50).

In the conventional Horndeski gravitational framework, where G_{tele} equals zero, the aforementioned condition has the potential to eliminate numerous cosmological models. To be precise, according to Eq.(2.50), the subsequent conclusion holds :

$$a_T = 0 \Rightarrow G_4(\phi, X) = G_4(\phi) \text{ and } G_5(\phi, X) = \text{const.} \tag{2.53}$$

If G_{tele} is not equal to zero, the application of the same constraint on the propagation speed of GW is necessary for the validity of BDLS theory. To examine further, it is essential to equate the a_T term in Eq.(2.50) to zero. As elucidated by the authors in [14] when the constraint $a_T = 0$ holds in the BDLS framework, the outcome is

$$G_5 = G_5(\phi) \tag{2.54}$$

$$G_{tele} = G_{tele}(\phi, X, T, T_{vec}, T_{ax}, I_2, J_1, J_3, J_6, J_8 - 4J_5, J_{10}), \tag{2.55}$$

with the G_4 term to depend on both the scalar field ϕ and the kinetic term X.

As a result, the ultimate form of the BDLS Lagrangian which satisfies the condition of GWs travelling at the speed of light, becomes

$$\begin{aligned}\mathcal{L} =& G_2(\phi, X) + G_3(\phi, X)\Box\phi + G_4(\phi, X)(-T + B) + \\ & G_{4,X}(\phi, X)\left[(\Box\phi)^2 - \phi_{;\mu\nu}\phi^{;\mu\nu} + 4J_5\right] + G_5(\phi, X)\mathcal{G}_{\mu\nu}\phi^{;\mu\nu} - 4J_5\, G_{5,\phi} + \\ & G_{tele}(\phi, X, T, T_{vec}, T_{ax}, I_2, J_1, J_3, J_6, J_8 - 4J_5, J_{10})\end{aligned} \tag{2.56}$$

The inclusion of the functions $G_4(\phi, X)$ and $G_5(\phi)$ in the Lagrangian stated above reveals a notable development, as these functions were previously omitted from the standard Horndeski theory. It is crucial, at this point, to observe the newly introduced terms that are proportional to J_5. This correction has been incorporated to guarantee that $a_T = 0$. Consequently, numerous significant models could potentially meet the constraint of GWs without necessitating any modification of the functions G_4 and G_5.

The detection of GW indicates a new era in modern astrophysics and cosmology due to the fact that the underlying gravitational theory defines not only the features of

GW such as the propagation speed and polarization but also the characteristics of the background on which they propagate. As a result, by analyzing the properties of the GWs we can impose constraints on the range of gravitational theories and also establish a method to distinguish them.

In particular, the investigation of GW polarization is a crucial evaluation of gravity that has not been thoroughly studied yet compared to other properties of GWs like their propagation speed. In [16] the authors examined the properties of the DoF related to the BDLS theory within a Minkowski background and they concluded to a maximum of seven propagating DoF. Since the propagating DoF can be expressed as polarization modes of the GWs, the authors in [16] have concluded that BDLS theory includes an additional breathing mode in the polarization for the massless sector in comparison to the classical Horndeski gravity [78]. This fact leads to a maximum of four polarization modes in the BDLS theory. While the existence of vectorial propagating DoF are predicted, BDLS presents only the combination of scalar and tensor polarizations for the massless sector and scalar models of the massive sector. Additionally, by analyzing the GW signal from the merging of compact binaries consisting of neutron stars and black holes we can obtain the measurement of the luminosity distance without the need for the cosmic distance ladder. By identifying the accompanying electromagnetic signal, one is able to establish the luminosity distance – redshift relation. Hence, from the combination of GW and electromagnetic observational data we can investigate the constraint ability on the cosmological parameters of the BDLS theory [40], [139].

2.5 | Conclusion

Even though Teleparallel Gravity is equivalent to General Relativity, it is important to understand that it represents a different theoretical framework. In General Relativity, gravitational interactions are interpreted through the concept of curvature. This means that geometry replaces the notion of gravitational force, therefore the trajectories are defined by geodesics and not by force equations. On the other hand, Teleparallel Gravity attributes gravity to torsion rather than curvature, even though without geometrization. This theory assumes the existence of a gravitational force, which results in the absence of geodesics and the presence of force equations that bear resemblance to the Lorentz equations in the field of electrodynamics.

The justification for gravity to possess two equivalent explanations is based on its characteristic property of universality. Similar to the fundamental interactions, gravity can also be approached as a gauge theory and this is exactly the Teleparallel Gravity. Moreover, the universality of free fall enables the formulation of the second approach, resulting from the Equivalence Principle, which is General Relativity. Since gravity is a universal interaction, it permits a geometrical analysis, thereby allowing for the existence of the two distinct explanations. According to this, curvature and torsion serve as alternative representations of the same gravitational field.

Horndeski gravity distinguishes itself as the most comprehensive scalar-tensor theory. It incorporates a single scalar field and results in second-order field equations. This theory holds a profound significance in the realm of modified gravity, although it has encountered significant challenges and limitations in light of the GW170817 event. By recognizing its importance, the current chapter discusses the development of the teleparallel equivalent of Horndeski gravity, known as the BDLS theory, by establishing specific assumptions and designating torsion as the mediator of gravity. The BDLS theory offers a vastly enhanced phenomenology due to the incorporation of a collection of 14 novel scalar invariants derived from the decomposition of the torsion tensor and its contractions with the scalar field. According to this fact, the conventional Horndeski theory could potentially endure in the context of BDLS theory through the Lagrangian as described in Eq.(2.45). It is important to highlight at this point the fact that the standard Horndeski using the Levi-Civita connection is now a subset of the broader BDLS theory when the condition $\mathcal{L}_{tele} = 0$ holds.

Due to the fact that the classical Horndeski theory was severely constrained by the propagation speed of GW, it is reasonable to explore the propagation of tensor modes within the context of BDLS theory. To achieve this objective, a feasible option is to utilize the flat FLRW metric and its associated tetrad with zero spin connection.

The crucial outcome of introducing cosmological perturbations is the form of the excess speed tensor, which is indicated in Eq.(2.50). As stipulated by that equation, the presence of a correction term is implicated in both $\mathcal{L}_4$ and $\mathcal{L}_5$, guaranteeing the viability of various models when subjected to the constraint of $a_T = 0$ in the BDLS scenario.

It is important to acknowledge the corrections made to the coefficients of the terms G_4 and G_5, as indicated in Eq.(2.56). This is significant because it ensures that the Lagrangian of the BDLS theory is consistent with the currently observed speed of GWs. Importantly, these corrections are made without eliminating the coupling functions, thus preserving the fundamental principles of the Horndeski theory. This fact leads to new perspectives for investigating the polarization of GW within the framework of BDLS, making it an ideal starting point for future research endeavours.

In recent years, TG has focused on utilizing its description of gravitational interactions to address the Hubble tension and also to explain the late-time behaviour of the Universe by employing contemporary observational data. Following that, conducting consistency tests using current cosmological data would enable the evaluation of the validity of the BDLS theory. Certain data sets are influenced by the dynamical behaviour of the Universe, while others by the large-scale growth. Nevertheless, it is important for these distinct observational sets to align with each other to approach and explain the cosmological tensions within a valid theory of gravity.

In order to conduct cosmological examinations on the free parameters defined in the BDLS context, numerical solutions can be employed over the theoretical parameters and extract the cosmological parameters applicable to this theoretical framework.

Considering the CMB dataset, the CMB shift parameter may be used which is associated with the expansion history of the cosmological background from decoupling to the present time. Then, one could estimate the ratio of the position of the first acoustic peak between the BDLS theory and the ΛCDM model. As a result, the CMB shift parameter can be used to place constraints on the BDLS theory since the CMB acoustic peaks are related to the geometry of the model being examined.

Before the recombination era, baryons exhibited a tight coupling with photons leading to the imprinting of sound wave oscillations on baryon perturbations and also on the temperature anisotropies of the CMB radiation. The detection of these density waves in the early Universe provides another independent way to constrain the cosmological parameters of the BDLS theory and could resolve the remaining degeneracies within the CMB data.

GWs generated from the merging of binary black holes and neutron stars are considered to be an important observational tool for evaluating cosmological theories. The GWs produced by a binary system carry significant information regarding the luminosity of the system, thereby indicating its luminosity distance which can be compared to the theoretical values predicted from BDLS theory.

In conclusion, it might be possible that future research focusing on investigating large-scale constraints could justify the reintroduction of Horndeski's theory in the teleparallel framework. Such a prospect would enhance the development of viable cosmological models in the BDLS context, thereby yielding more effective results describing the evolutionary history of the Universe.

3

New insights from GW170817 in the dynamical system analysis of Einstein Gauss-Bonnet gravity

The chapter discusses the theoretical context of the Einstein Gauss-Bonnet theory of gravity by employing a dynamical system analysis. The crucial requirement for the theory to be compatible with the GW170817 event has a major impact on the autonomous feature of the dynamical system and the properties of each critical point associated with the different eras of cosmic evolution.

3.1 | Nonminimally Coupled Gauss-Bonnet Cosmology

Over the last decades, there has been a revival of interest in theories that suggest alternatives or modifications to Einstein's four-dimensional theory of gravity [68], [49], [80]. These theories vary in origin in addition to motivation. Several among them have their foundations in multidimensional perspectives whereby gravity can propagate in more than four dimensions. Various models also exist founded upon scalar-tensor couplings that lead to detectable effects in cosmology or even violate the Equivalence Principle.

Among the vast number of these theories, one model exists which displays that gravity could be modified by incorporating quadratic order terms of the curvature tensor in the Lagrangian. This particular form of gravity modification corresponds to the n-dimensional spacetime Lagrangian formulation of Lovelock's theorem [49]. Within this context, there is a unique quadratic combination of the curvature tensor, defined as Gauss-Bonnet (GB) term, considered to be a topological invariant in four-dimensional spacetime. The inclusion of the GB term in the conventional Einstein-Hilbert action, does not affect the differential order of the resulting equations of motion [69], [89].

Even though the GB term corresponds to a total divergence in four dimensions, it can significantly influence the behaviour of a system provided that it is coupled to a dynamically evolving scalar field. Scalar fields play a significant role in contemporary cosmology. They appear as dilaton or moduli fields in the gravitational sector or as part of the matter sector, such as the Higgs field. The inclusion of scalar fields broadens the spectrum of qualitative dynamics within homogeneous and isotropic FLRW models beyond what conventional perfect fluid models can explain. Once such coupling occurs, the Einstein Gauss-Bonnet (EGB) model emerges as a scalar-tensor theory of the Horndeski group and the main subject of the current chapter. The accelerated solutions that this model or its modifications might generate [50], [89], along with its implication on large-scale structure, have inspired scientific interest in pursuing further research on the topic [108], [112].

The EGB model, similar to all the theories that aim to elucidate gravity, must possess the ability to accurately capture nearly every evolutionary phase of the Universe while also providing insights and clarification of the observed dynamical behaviour. The initial stage in determining whether the EGB model could accomplish such a task involves the implementation of the action of the model, which is a combination of the Einstein-Hilbert action of GR and the GB term, outlined below

$$S = \int d^4x \sqrt{-g} \left(\frac{R}{2} - \frac{\omega}{2} g^{\mu\nu} \partial_\mu\phi \, \partial_\nu\phi - V(\phi) - f(\phi)\, \mathcal{G} \right) + S_{\text{matter}} \,, \tag{3.1}$$

where

$$\mathcal{G} = R^2 - 4R_{\alpha\beta}\, R^{\alpha\beta} + R_{\alpha\beta\gamma\delta}\, R^{\alpha\beta\gamma\delta}\,,$$

is the Gauss-Bonnet (GB) term, a topological invariant in four dimensions spacetime. We assume ω to be a constant, with allowed values $\omega = \pm 1$. However, in the present study, we focus only on the canonical scalar case, $\omega = 1$, to avoid any potential presence of phantom cases during the study. The action clearly indicates that the scalar field is non-minimally coupled to the GB term through an arbitrary function $f(\phi)$. Each of the matter fields of the model is collectively indicated by the action S_{matter}, and $V(\phi)$ is the potential of the scalar field ϕ.

At this point, a suitable choice for the remainder of this study is to employ a spatially flat FLRW spacetime – the spacetime in the comoving frame – with line element,

$$ds^2 = -N^2\, dt^2 + a^2(t) \sum_{i=1}^{i=3} (\, dx^i\,)^2\,, \tag{3.2}$$

where $a(t)$ is the scale factor, dx^i describes the Cartesian coordinates of the spatial part of the metric, and N represents the lapse function or dilation factor, a real-valued function used to quantify the rate at which time elapses for an observer in a different reference frame. Typically, this function is determined through the application of the Lorentz transformation, a set of equations that detail the alteration of spacetime measurements across different reference frames. Due to its high degree of symmetry based on isotropy and homogeneity of the Universe, FLRW metric is recognized to belong to the general class of spherically symmetric spacetimes. For consistency with the cosmological principle, the lapse function is set to be a coordinate-time dependent function, $N = N(t)$ determining the relation between proper and coordinate time. This choice facilitates the transition between various time parameterizations i.e. a change in the frame of reference. In this particular setting, the scalar field of the theory is a function of only the cosmic time since it inherits all the symmetries of spacetime.

In that ansatz, the Ricci scalar and the GB term would lead to the following :

$$R = \frac{6}{N^2}\left(2H^2 + \dot{H} - \frac{\dot{N}}{N}H\right), \quad \text{and} \quad \mathcal{G} = \frac{24H^2}{N^4}\left(\dot{H} + H^2 - \frac{\dot{N}}{N}H\right) \tag{3.3}$$

At the present stage, we introduced the Hubble parameter, identified as $H = \dot{a}/a$, with over-dots indicating the derivatives of the scale factor with respect to cosmic time.

Assuming the self-interaction potential to have an exponential dependence upon the scalar field is a quite popular choice in the field of cosmology and the reason is that the scale-invariant form makes the exponential potential particularly simple to study analytically. The cosmological role of exponential potentials has been studied thoroughly, mostly as an effective way of leading to a phase of early inflation or as a means to build quintessence models [8]. In addition, as it was pointed out in [53], if the potential driving inflation is too steep, then the energy density of the scalar field with exponential potential does not simply dissipate, but it converges towards an attractor solution of the system. This solution mimics the equation of state (EoS) of a barotropic fluid and remains a constant proportion of the total energy density. The exponential potential form is frequently found in higher-dimensional theories of gravity and it possesses a solid theoretical basis in the context of string theory or Kaluza-Klein type of models [53], [84], [99], [20], [106], [76].

Accordingly, the expression of the potential as a decreasing function of the scalar field is provided by

$$V(\phi) = V_0 e^{-\lambda\phi}, \tag{3.4}$$

where λ and V_0 are both real and positive constants. Additionally, λ is dimensionless and characterizing the slope of the potential.

In terms of the coupling function, $f(\phi)$, it has been demonstrated in the literature that both linear and exponential forms could result in scalarization, indicating that black holes with non-trivial scalar hair exist. Consequently, the choice for the coupling function might be stated as follows :

$$f(\phi) = \frac{e^{k\phi}}{k}, \tag{3.5}$$

where k is a real and positive constant.

After the replacement of each of these terms into Eq.(3.1), the gravitational part of the model yields the following Lagrangian density :

$$\mathcal{L} = -a^3 N\, V(\phi) + \frac{3a\dot{a}^2}{N} + \frac{a^3\dot{\phi}^2}{2N} + \frac{3}{N}\left(\ddot{a} - \frac{\dot{a}\dot{N}}{N}\right)\left(a^2 - \frac{8f(\phi)\dot{a}^2}{N^2}\right). \tag{3.6}$$

By performing integration by parts, the final form of the Lagrangian density reads

$$\mathcal{L} = -a^3 N V(\phi) - \frac{3a\dot{a}^2}{N} + \frac{8\dot{a}^3\dot{f}}{N^3} + \frac{a^3\dot{\phi}^2}{2N}. \tag{3.7}$$

As for the part of the action in Eq.(3.1) associated with the matter content of the Universe, the corresponding action is determined by

$$S_{\text{matter}} = \int d^4x\sqrt{-g}\mathcal{L}_{\text{matter}} \tag{3.8}$$

Under the assumption that the Universe consists of a perfect fluid characterized by an isotropic pressure, its energy-momentum tensor produced by the variation of the preceding action is defined by

$$T_{\mu\nu} = -\frac{2}{\sqrt{-g}}\frac{\delta\mathcal{L}_{\text{matter}}}{\delta g^{\mu\nu}} = (\rho + p)u_\mu u_\nu + p g_{\mu\nu}, \tag{3.9}$$

where $u^\mu u_\mu = -1$ is the four-velocity and $\rho = \rho_m + \rho_r$ is the energy density of non-relativistic matter and radiation. In addition, the related pressure is $P = P_r = \rho_r/3$.

The Euler-Lagrange equations for the scale factor, the lapse function and the scalar field lead to the following three equations of the model :

$$16H\left(H^2+\dot{H}\right)\dot{f}(\phi)-2\dot{H}+V(\phi)-\frac{\dot{\phi}^2}{2}+H^2\left(8\ddot{f}(\phi)-3\right)=p\,, \tag{3.10}$$

$$3H^2-V(\phi)-24H^3\dot{f}(\phi)-\frac{1}{2}\dot{\phi}^2=\rho\,, \tag{3.11}$$

$$\ddot{\phi}+3H\dot{\phi}+V'(\phi)+24H^2f'(\phi)\left(H^2+\dot{H}\right)=0 \tag{3.12}$$

The $\dot{}$ symbolizes derivatives with respect to cosmic time t and $'$ derivatives with respect to the argument. In particular, the variation of the action with respect to the lapse function $N(t)$, leads to the constraint equation of the model, Eq.(3.11). In the case where the lapse function is fixed before the variation procedure, the constraint equation simply does not exist. In the preceding analysis, and without any loss of generality, we are free to employ the lapse gauge, $N=1$.

3.2 | Dynamical System Analysis

A dynamical system is commonly referred to as an ensemble of components which advances over a period of time. The basic objective of studying a dynamical system is to determine whether or not a perturbation near a critical point increases or decays with time. According to this concept, a dynamical system is composed of an abstract phase space the coordinates of which indicate the state of the system at any moment in time along with a set of differential equations which capture the imminent future of the state variables provided their current values [38]. The dynamical system approach provides enriched insight into the development of the cosmological models, however, it faces the flaw of using highly idealised assumptions concerning the actual mechanisms describing the evolution of the Universe [39], [51], [1].

The state of a physical system at any given moment in time is expressed as a specific element x of the state space X, which could be either finite or infinite in dimensions.

It follows that the evolution of the system is outlined by autonomous differential equations related to time derivatives, expressed implicitly as

$$\frac{dx}{dt} = f(x),\ x \in X, \tag{3.13}$$

where the map $f : X \to X$. When X is finite-dimensional state space, Eq.(3.13) describes an autonomous system of ordinary differential equations. In the case that X is a function of space, the map f consists of spatial derivatives resulting in an autonomous system of partial differential equations. It becomes evident that even though dynamical systems offer an excellent method for investigating model evolution, a single general framework to analyze their behaviour is highly unlikely to occur. Consequently, to accurately describe the features of a dynamical system a wide range of techniques may be used to the evolution rule governing it [82], [129], [4].

Numerous cosmological models are defined by a system of nonlinear differential equations. However, considering that this system oftentimes proves hard to solve, the dynamical systems method is one of the most effective ways to analyze cosmological behaviour by focusing on key variables and parameters to simulate cosmological scenarios with accuracy [12], [70]. In particular, the qualitative examination of a spatially homogeneous model where its dynamics are determined by an autonomous system of ordinary differential equations. Inhomogeneous cosmological models might be investigated as well, yet they present a challenging task due to their evolution equations which are now partial differential equations. These equations lead to infinite-dimensional state space, thereby making the investigation considerably more complicated in that case. As a result, examining these models requires a more rigorous and intricate approach compared to the homogeneous cosmological models.

The initial step in investigating the EGB model using the dynamical system approach involves considering the constraint equation, Eq.(3.11), and then identifying the phase space variables that are crucial for the analysis [48], [8]

$$x_1 = \frac{\dot{\phi}}{\sqrt{6}H}, \; x_2 = \frac{\sqrt{V}}{\sqrt{3}H}, \; x_3 = H^2 \frac{\partial f(\phi)}{\partial \phi}, \; x_4 = \frac{\sqrt{\rho_r}}{\sqrt{3}H}, \; x_5 = \frac{\sqrt{\rho_m}}{\sqrt{3}H}\,. \tag{3.14}$$

Both the first variables are linked to the kinetic term and potential energy of the scalar field that appears in the theory. The coupling between the GB invariant and the scalar field is expressed by the third variable, x_3, while the variables x_4 and x_5 are related to matter fields [8]. It is worth mentioning that while the solutions of the dynamical system can be depicted as trajectories on the phase space determined by the previously stated variables, its evolution is independent of the variables used to describe it.

Considering a flat FLRW spacetime, we can use the dynamical variables to define the dimensionless density parameters. In a similar vein, we can express the scalar field equation of state along with the effective equation of state of the EGB model as

$$\Omega_\phi = x_1^2 + x_2^2, \; \Omega_{GB} = 8\sqrt{6}\,x_1\,x_3, \; \Omega_r = x_4^2, \; \Omega_m = x_5^2\,, \tag{3.15}$$

$$w_\phi = \frac{x_1^2 - x_2^2}{x_1^2 + x_2^2}, \; w_{eff} = -1 - \frac{2}{3}\frac{\dot{H}}{H^2} \tag{3.16}$$

The constraint equation, Eq.(3.10), can be expressed now in the following manner :

$$x_1^2 + x_2^2 + 8\sqrt{6}\,x_1\,x_3 + x_4^2 + x_5^2 = 1 \tag{3.17}$$

After defining the variables, the next step is developing a series of equations that demonstrate how these variables evolve over time. Through these equations, we can gain a deeper understanding of how the state variables impact the overall system dynamics. In order to ensure that the EGB model remains valid, a logarithmic time variable is introduced. The logarithmic time variable, the number of e-foldings, is critical in ensuring the ongoing applicability of the EGB model and is described as

$$N = \int_{t_i}^{t_f} H(t)\,dt\,. \tag{3.18}$$

The evolution equations of the variables with respect to the number of e-foldings are

$$\frac{dx_1}{dN} = x_1' = -3x_1 + \sqrt{\frac{3}{2}}\,\lambda\,x_2^2 - 4\sqrt{6}\,x_3 - (4\sqrt{6}\,x_3 + x_1)\,\frac{\dot{H}}{H^2} \tag{3.19}$$

$$\frac{dx_2}{dN} = x_2' = -\sqrt{\frac{3}{2}}\,\lambda x_1 x_2 - x_2\,\frac{\dot{H}}{H^2} \tag{3.20}$$

$$\frac{dx_3}{dN} = x_3' = k\sqrt{6}\,x_1\,x_3 + 2\,x_3\,\frac{\dot{H}}{H^2} \tag{3.21}$$

$$\frac{dx_4}{dN} = x_4' = -2\,x_4 - x_4\,\frac{\dot{H}}{H^2} \tag{3.22}$$

$$\frac{dx_5}{dN} = x_5' = -\frac{3}{2}\,x_5 - x_5\,\frac{\dot{H}}{H^2}\,, \tag{3.23}$$

The system described by the Eqs.(3.19)-(3.23) includes one pending issue associated with defining the fraction $\dot{H}/H^2$, which might interfere with the dynamics of the EGB model. This fraction has been regarded as a constant in several publications [48]; however, the present research aims at broadening the methodology and analysing any potential consequences or impacts of its evaluation.

To calculate the aforementioned fraction, and therefore, obtain an autonomous dynamical system, the analyses of [110] and [111] will be applied, where it has been proven that the EGB model might be compatible to the GW170817 event. The latter is feasible considering that within the context of EGB, the gravitational wave speed is

$$c_T^2 = 1 - \frac{Q_f}{2Q_t}\,, \tag{3.24}$$

where $Q_f = 8\left(\ddot{f} - H\dot{f}\right)$ and $Q_t = 1 - 4H\dot{f}$.

It follows that, since $c_T^2 = 1$ in accordance with the GW170817 event, then $Q_f|_{z=0} = 0$ leading to $k = H_0$ according to Eq.(3.5).

Taking the time derivative of Eq.(3.10) and replacing the derivative of the potential from Eq.(3.12) while accounting for the contribution of all the matter fields, yields

$$-2\dot{H} - \dot{\phi}^2 + 8H^2\left(\ddot{f} - H\dot{f}\right) + 16H\dot{H}\dot{f} - \rho_m - \frac{4\rho_r}{3} = 0\,. \tag{3.25}$$

After solving Eq.(3.25) for $\dot{H}/H^2$, we acquire the following formula :

$$\frac{\dot{H}}{H^2} = \frac{6\,x_1^2 + 4\,x_4^2 + 3\,x_5^2}{16\,\sqrt{6}\,x_1\,x_3 - 2}, \tag{3.26}$$

By substituting this result in Eqs (3.19)-(3.23) we derived the final version of the autonomous dynamical system, which is

$$x_1' = -3x_1 + \sqrt{\frac{3}{2}}\,\lambda\,x_2^2 - 4\,\sqrt{6}\,x_3 - (4\,\sqrt{6}\,x_3 + x_1)\left(\frac{6\,x_1^2 + 4\,x_4^2 + 3\,x_5^2}{16\,\sqrt{6}\,x_1\,x_3 - 2}\right) \tag{3.27}$$

$$x_2' = -\sqrt{\frac{3}{2}}\,\lambda\,x_1 x_2 - x_2\left(\frac{6\,x_1^2 + 4\,x_4^2 + 3\,x_5^2}{16\,\sqrt{6}\,x_1\,x_3 - 2}\right) \tag{3.28}$$

$$x_3' = k\,\sqrt{6}\,x_1\,x_3 + 2\,x_3\left(\frac{6\,x_1^2 + 4\,x_4^2 + 3\,x_5^2}{16\,\sqrt{6}\,x_1\,x_3 - 2}\right) \tag{3.29}$$

$$x_4' = -2\,x_4 - x_4\left(\frac{6\,x_1^2 + 4\,x_4^2 + 3\,x_5^2}{16\,\sqrt{6}\,x_1\,x_3 - 2}\right) \tag{3.30}$$

$$x_5' = -\frac{3}{2}\,x_5 - x_5\left(\frac{6\,x_1^2 + 4\,x_4^2 + 3\,x_5^2}{16\,\sqrt{6}\,x_1\,x_3 - 2}\right) \tag{3.31}$$

It is evident now, that by employing the GW speed constraint, we can determine the formula of the fraction $\dot{H}/H^2$ as a function of the variables of the EGB model, leading to an autonomous dynamical system. Therefore, instead of making any assumptions regarding the various evolutionary eras of the Universe, the subsequent paragraphs demonstrate that these eras along with the value of that fraction can be obtained by analyzing the characteristic features of each critical point of the dynamical system. This approach allows for a more accurate understanding of the evolutionary processes and their significance in cosmic history.

The constants k and λ are assumed to be arbitrary in the remainder of the research. As it will be noticed in the following analysis, the fraction $\dot{H}/H^2$ has a constant value at each critical point of the system. This means that according to Eqs (3.27)-(3.31), whenever we focus on a critical point, the matter fields of the model do not interact with the scalar field or with the GB invariant. Therefore, Eqs (3.30)-(3.31) evolve independently.

The critical points of the dynamical system are then computed to evaluate their distinct characteristics and behaviour. The physical properties of these critical points are outlined in Table (3.1) while Table (3.2) demonstrates the details of hyperbolicity and stability conditions associated with them. The system contains a total of seven critical points and the features of each one of them will be thoroughly discussed in the subsequent section along with their connection to various eras of cosmic evolution.

Point	$\{x_1, x_2, x_3, x_4, x_5\}$	Existence	Ω_ϕ	Ω_{GB}	Ω_m	Ω_r	$\dot{H}/H^2$	w_ϕ	w_{eff}
A	$\{0, 0, 0, 0, 1\}$	Always	0	0	1	0	$-3/2$	–	0
B	$\{0, 0, 0, 1, 0\}$	Always	0	0	0	1	-2	–	$1/3$
C	$\{0, 1, \lambda/8, 0, 0\}$	Always	1	0	0	0	0	-1	-1
D	$\{1, 0, 0, 0, 0\}$	Always	1	0	0	0	-3	1	1
E	$\{\frac{2\sqrt{2/3}}{\lambda}, \frac{2}{\sqrt{3}\lambda}, 0, \frac{\sqrt{\lambda^2-4}}{\lambda}, 0\}$	$\lambda^2 > 4$	$4/\lambda^2$	0	0	$\frac{\lambda^2-4}{\lambda^2}$	-2	$1/3$	$1/3$
F	$\{\frac{\sqrt{3/2}}{\lambda}, \frac{\sqrt{3/2}}{\lambda}, 0, 0, \frac{\sqrt{\lambda^2-3}}{\lambda}\}$	$\lambda^2 > 3$	$3/\lambda^2$	0	$\frac{\lambda^2-3}{\lambda^2}$	0	$-3/2$	0	0
G	$\{\frac{\lambda}{\sqrt{6}}, \frac{\sqrt{6-\lambda^2}}{\sqrt{6}}, 0, 0, 0\}$	$\lambda^2 < 6$	1	0	0	0	$-\lambda^2/2$	$-1+\frac{\lambda^2}{3}$	$-1+\frac{\lambda^2}{3}$

Table 3.1. The conditions for the existence along with the physical properties of the seven critical points. It is important to note the range of the λ parameter for the critical points E, F and G as this parameter can have a significant impact on the existence of a critical point and the overall behaviour of the dynamical system.

Point	Eigenvalues	Hyperbolicity	Stability
A	$\{-3, 3, -3/2, 3/2, -1/2\}$	Hyperbolic	Saddle
B	$\{-4, 4, 2, -1, 1/2\}$	Hyperbolic	Saddle
C	$\{-2, -3/2, 0, \frac{1}{2}\left(-3 \pm \sqrt{3}\sqrt{3-4k\lambda-4\lambda^2}\right)\}$	Non-hyperbolic	Stable
D	$\{6, 3/2, 1, -6+\mathrm{k}\sqrt{6}, \frac{1}{2}\left(6-\sqrt{6}\lambda\right)\}$	λ or k$=\sqrt{6}$, Non-hyperbolic $\lambda<\sqrt{6}$, k$>\sqrt{6}$, Hyperbolic $\lambda<\sqrt{6}$, k$<\sqrt{6}$, Hyperbolic $\lambda>\sqrt{6}$, k$\lessgtr\sqrt{6}$, Hyperbolic	Unstable Repeller Saddle Saddle
E	$\{1/2, 4, \frac{4\left(\mathrm{k}\lambda-\lambda^2\right)}{\lambda^2}, \pm\frac{-\lambda^2+\sqrt{-\lambda^2(-64+15\lambda^2)}}{2\lambda^2}\}$	$\lambda=$ k, Non-hyperbolic $\lambda\lessgtr$ k, Hyperbolic	Unstable Saddle
F	$\{-1/2, 3, \frac{3\left(\mathrm{k}\lambda-\lambda^2\right)}{\lambda^2}, \pm\frac{3(-\lambda^2+\sqrt{-\lambda^2(-24+7\lambda^2)})}{4\lambda^2}\}$	$\lambda=$ k, Non-hyperbolic $\lambda\lessgtr$ k, Hyperbolic	Unstable Saddle
G	$\{\lambda^2, \mathrm{k}\lambda-\lambda^2, \frac{1}{2}(-6+\lambda^2), \frac{1}{2}(-4+\lambda^2), \frac{1}{2}(-3+\lambda^2)\}$	$\lambda=$ k, Non-hyperbolic $\lambda\lessgtr$ k, Hyperbolic	Unstable Saddle

Table 3.2. The stability properties of the seven critical points. Notice that $k = H_0$, for the speed of the gravitational waves to be equal to the speed of light and thus, even though mathematically the above analysis is correct, physically not all the points are viable.

- **Point A.** The first critical point in this investigation refers to a matter-dominated Universe. Based on Table (3.1), $\Omega_m = 1$ and the critical point exists for every value of the parameter λ. Moreover, the effective EoS matches with the matter EoS, $w_{eff} = w_m = 0$, along with zero energy density for the scalar field. Therefore, point A cannot exhibit late-time cosmic acceleration for any physically accepted value of w_{eff}. In the context of Table (3.2), point A is a saddle and hyperbolic critical point characterized by a 3D local stable manifold where the trajectories approach the critical point moving tangentially along the slower direction, that is the line spanned by the eigenvector corresponding to $-1/2$ eigenvalue. In the same vein, point A is characterized by a 2D local unstable manifold, while the term local indicates that these two manifolds with boundaries reside only in the vicinity of the critical point.

- **Point B.** The second critical point is related to a radiation-dominated Universe. In this specific situation, $\Omega_r = 1$ and the critical point is present for all the values of the free parameter λ. In addition, the effective EoS coincides with the radiation EoS, $w_{eff} = w_r = 1/3$ while the energy density of the scalar field is once again equal to zero. Point B cannot account for cosmic acceleration either irrespective of the physically accepted values of w_{eff}. As indicated in Table (3.2), point B is a saddle hyperbolic critical point that has a 2D local stable manifold where the trajectories approach it moving tangentially on the line extended by the eigenvector related to -1 eigenvalue, and a 3D local unstable manifold. Likewise, the term local refers to manifolds defined in the proximity of point B.

- **Point C.** Table (3.1) illustrates that the third critical point is dominated by the potential energy of the scalar field, which behaves identically to the cosmological constant. Given that $w_{eff} = w_\phi = -1$, the Universe exhibits acceleration, yet matter and radiation are suppressed by the scalar field energy density which dominates point C. As the coupling to the GB invariant does not vanish in this case, point C could potentially be linked with the early or late-time acceleration phase of the Universe. From Table (3.2) we recognize point C as a non-hyperbolic critical point featuring one centre manifold and a 4D stable manifold, therefore linear stability theory fails to foresee its behaviour over time. By ignoring both radiation and matter and assuming $3 - 4k\lambda - 4\lambda^2 > 0$, the remainder of the equations can be studied by applying center manifold theory. Following that method, the dimensions of the system are reduced to one. The resulting one-dimensional system is studied by introducing a new variable, $s(t)$, obeying the differential equation $s'(t) = s(t)^3(-12k/\lambda(k+\lambda)^2)$. In this system point C is regarded as a stable critical point. Given that the Hubble rate is constant in the vicinity of this critical point, the expansion continues to accelerate. As a result, the third critical point operates as the attractor of the dynamical system.

- **Point D.** The fourth critical point reveals a Universe dominated by the kinetic energy of the scalar field. Table (3.1) indicates that $\Omega_\phi = 1$ and the critical point can be present over all values of the parameters k and λ. Since $w_{eff} = w_\phi = 1$, point D cannot enable acceleration. In addition, $\rho_\phi \sim a^{-6}$, meaning that in this case, the energy density of the scalar field decreases considerably faster compared to the background density. Table (3.2) states that depending on the values of k and λ being greater or smaller than $\sqrt{6}$, point D is an unstable or saddle critical point. Analyzing each one of this information, we conclude that critical points with steep potentials, like point D, are not linked to any of the phases of the CDM model or even the late-time accelerated expansion. Such solutions, however, are presumably connected to the early cosmological states of evolution.

- **Point E.** The fifth critical point differs from the previous cases since it refers to a scaling solution. According to Table (3.1), the fraction $\Omega_\phi/\Omega_r = 4/\lambda^2 - 4$ is a non-zero constant, indicating that exists a period where both radiation and the scalar field could impact the cosmic evolution. Whenever this point exists, i.e. $\lambda^2 > 4$, the effective EoS aligns with the radiation EoS, $w_{eff} = w_r = 1/3$ and $w_\phi = w_r$, hence point E exhibits no acceleration and the Universe expands as if it is radiation-dominated. Over the evolution period, the existence of the scalar field might have remained hidden on cosmological scales. Table (3.2) demonstrates that the stability behaviour is determined by the relation between k and λ. Still, point E is not a stable critical point in any case, therefore exiting the scaling regime does not require an extra mechanism such as in the case of quintessence models.

- **Point F.** This critical point illustrates one more scaling solution of the system. To be precise, point F is a matter scaling solution where the effective EoS coincides with matter EoS, $w_{eff} = w_m = 0$, $w_\phi = w_m$ and the fraction $\Omega_\phi/\Omega_m = 3/\lambda^2 - 3$ is a non-zero constant. If this point exists, $\lambda^2 > 3$, the Universe develops as though it is dominated by matter preventing point F from exhibiting acceleration. Table (3.2) indicates that the stability features depend on the relation between k and λ. Point F, just like point E, is not a stable critical point either.

- **Point G.** From Table (3.1) it is obvious that the last critical point occurs whenever $\lambda^2 < 6$. Since $w_{eff} = w_\phi = 1 + \lambda^2/3$, point G is a scalar field-dominated critical point. In order to enable acceleration, the condition $w_{eff} < -1/3$ must hold, resulting in the additional relation $\lambda^2 < 2$ for the parameter λ. It is worth noting that in the region of $\lambda \to 0$, the EoS of the cosmological constant is recovered, pointing to the stable accelerated point C of the current study. Far from this limit and as long as $\lambda^2 < 2$, Table (3.2) indicates that point G is not considered a stable accelerated point of the system. The relation between the parameters k and λ determines whether point G is a non-hyperbolic or hyperbolic critical point, which nonetheless is unstable and cannot account for the attractor of the system. One potential interpretation of point G is that it may represent an early accelerated phase of cosmic evolution. Point G could indicate the inflationary period of the Universe, since for $\lambda^2 < 2$, we have $\phi^2 << V(\phi)$. This indicates that the potential is shallow enough and thus creates the necessary conditions for an inflation period to take place in the early stages of cosmic evolution.

Studying the stability properties of the critical points aims to provide a profound understanding of the cosmological evolution described by the EGB model, benefiting interested readers and researchers. According to the results of the critical points analysis and provided that $3 - 4k\lambda - 4\lambda^2 > 0$, it has been proved that point C is the only viable candidate for serving as a stable accelerated attractor of the model. Taking this fact under consideration, either point B or the scaling solution described by point E could result in a radiation-dominated era. However, the presence of point E is only valid under the condition $\lambda^2 > 4$. Yet, this condition directly contradicts the assumption $3 - 4k\lambda - 4\lambda^2 > 0$ of point C. As a result, it can be inferred that the radiation-dominated era is most likely associated with point B.

The examination of the critical points indicates two potential scenarios regarding the defining characteristics of a cosmological period dominated by matter. These scenarios are represented either by the critical point A or by following the scaling solution as described by point F. However, the existence of point F is based on the condition $\lambda^2 > 3$, contradicting the initial assumption made regarding point C. As a result, it can be observed that point A emerges as the only valid critical point associated with a matter-dominated era.

3.3 | Visualization of Phase Portraits

A phase portrait is a geometric representation of the trajectories of a dynamical system in its phase space. It depicts the evolution of an ensemble of trajectories with respect to the nature of the critical points. In the field of cosmology, phase portraits are ideal tools to observe the overall behaviour of every evolutionary era of the Universe – each corresponding to a critical point – and the transition between different epochs. In this context, employing proper diagrams to visualize the nature of the critical points of the analysis facilitates comprehending their distinctive relation to a certain cosmological period described by the variables of the system. The following paragraphs display the phase portraits related to each critical point, discuss the significant steps for their derivation and address whether they are consistent with Sec. (3.2).

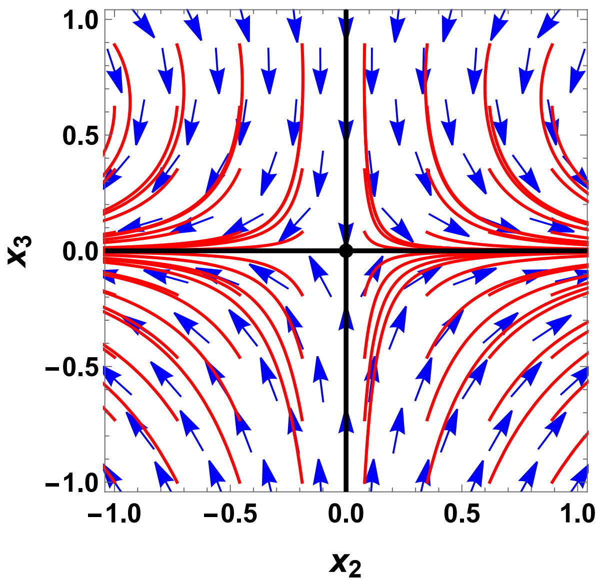

Fig. 3.1. 2D phase portrait of point A.

Given the results of the previous section, point A is a matter-dominated critical point that exists regardless of the values assigned to the parameters k and λ. Since $w_{eff} = w_m = 0$, it is evident that point A cannot be related to cosmic acceleration.

Considering that $x_1 = 4\sqrt{6}\,x_3/3 + \sqrt{3}\,x_2^2/3\,\sqrt{2}$ on this critical point, two equations for the variables x_2, x_3 eventually emerge, namely, $x_2' = 3\,x_2/2 - x_2^3/4 - 2x_2\,x_3$ and $x_3' = -3\,x_3 + x_2^2\,x_3/4 + 2\,x_3^2$. Figure (3.1) illustrates the two-dimensional phase portrait of point A for k= 1/4 and $\lambda = 1/2$. Blue arrows reveal the vector field whereas red lines are numerical solutions representing some of the trajectories in the vicinity of point A. In this phase portrait, the critical point is defined by the black dot in the centre of the diagram. As stated in Tables (3.1), (3.2), point A is hyperbolic with eigenvalues $-3, 3, -3/2$ and $-1/2$, hence, it is a saddle critical point. Figure (3.1) reveals the saddle character of point A, in accordance with the Tables (3.1), (3.2) of the previous section.

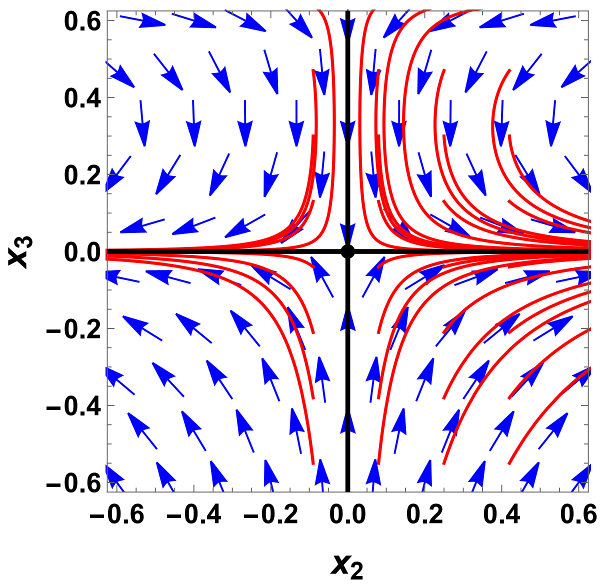

Fig. 3.2. 2D phase portrait of point B.

The second critical point describes a Universe that is dominated by radiation. Similar to point A, the characteristic features of point B do not permit an accelerated solution since $w_{eff} = w_r = 1/3$. On that critical point, $x_1 = 4\sqrt{6}\,x_3/3 + \sqrt{3}\,x_2^2/2$ and that leads to two equations for the variables x_2, x_3 which are $x_2' = 2\,x_2/2 - 3\,x_2^3/8 - 6x_2\,x_3$ and $x_3' = -4\,x_3 + 3x_2^2\,x_3/8 + 6\,x_3^2$ for k= 1/4 and $\lambda = 1/2$. The phase portrait of point B in two dimensions is illustrated in Figure (3.2) for the choice of k= $1/4$ and $\lambda = 1/2$. The vector field is denoted by the blue arrows, while the red lines represent several trajectories in the surroundings of B. Once again the critical point is defined by the black dot in the centre of the phase portrait. Based on Tables (3.1) and (3.2), point B is hyperbolic whose eigenvalues are $-4, 4, 2, -1$ and $1/2$ implying a saddle critical point. Figure (3.2) reveals its saddle nature and confirms the results of the previous section.

The third critical point is dominated by the potential energy of the scalar field. As stated in Table (3.1) $w_{eff} = w_{\phi} = -1$, thus point C could be associated with a period of accelerated expansion. Based on its eigenvalues, point C is non-hyperbolic, therefore linear stability theory cannot forecast its behaviour. The phase space of the new variables X, Y and Z are obtained by a shift to the origin according to $X = x_1, Y = x_2 - 1, Z = x3 - \lambda/8$ for k= $\lambda = 1/2$. Through center manifold theory and ignoring matter and radiation, the dimensions of the system are reduced to one. The equation $s'(t) = s(t)^3 \left(-12k/\lambda(k+\lambda)^2\right)$ describes the behaviour of the new variable $s(t)$.

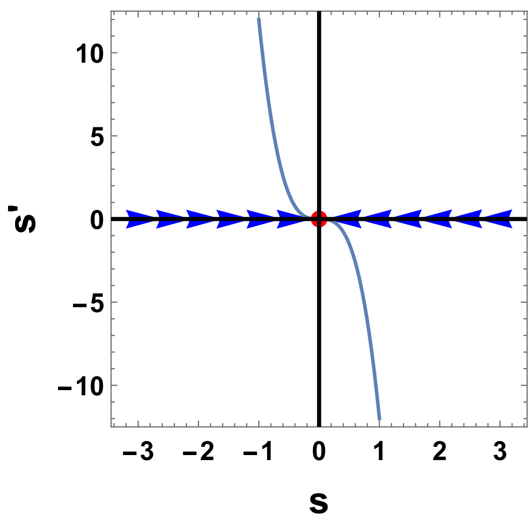

Fig. 3.3. 2D phase portrait of point C.

Figure (3.3) demonstrates the one-dimensional phase portrait, where the grey line indicates the trajectory for $k = \lambda = 1/2$ and the blue arrows denote the vector field. The red dot in the centre of the graph defines point C, a stable critical point which operates as the attractor of the model in terms of the phase portrait.

The next critical point of the analysis, point D, refers to a Universe dominated by the kinetic energy of the scalar field. Since $w_{eff} = w\phi = 1$, it is not possible for point D to sustain an accelerated solution. Following the information outlined in Table (3.2), the critical point D is determined to be either unstable or featuring a saddle behaviour depending on the values of k and λ in relation to $\sqrt{6}$.
Yet, this critical point is present regardless of the values assigned to these parameters. Figure (3.4) displays the three-dimensional vector plot of x_1, x_2 and x_3 for k= 3 and $\lambda = 1$. Blue arrows represent again the vector field in the vicinity of point D while the red dot signifies its coordinates at $x_1 = 1, x_2 = 0$ and $x_3 = 0$. According to Table (3.2) we conclude that for this specific choice of the parameters, point D is hyperbolic and acts as a repeller of the system.

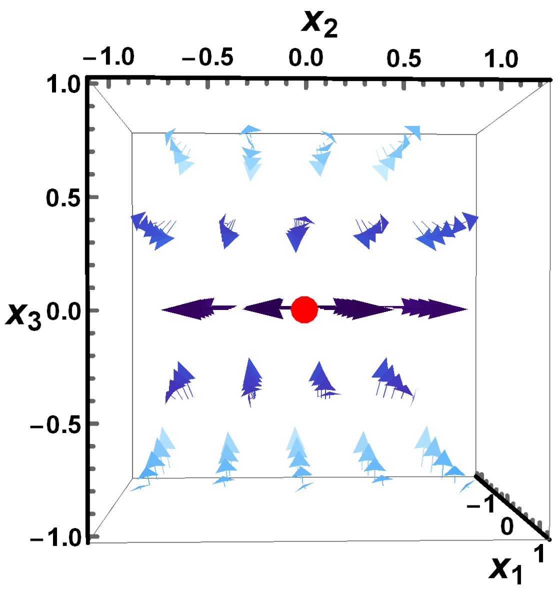

Fig. 3.4. 3D phase portrait of point D.

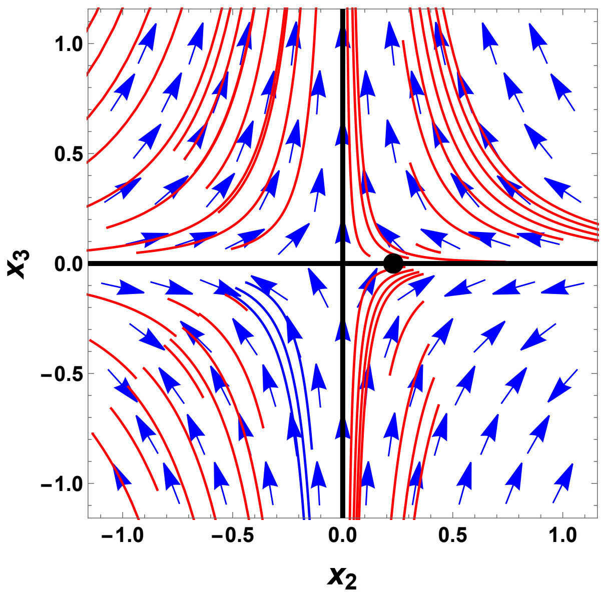

Fig. 3.5. 2D phase portrait of point E.

The fifth critical point occurs for $\lambda^2 > 4$ which indicates a radiation scaling solution, where the ratio $\Omega_\phi/\Omega_r = 4/\lambda^2 - 4$ is a non-zero constant. According to the data in Table (3.1), $w_{eff} = w_r = 1/3$ and $w_\phi = w_r$ which indicates that point E cannot be considered as an accelerated solution of the system. Since $x_1 = 4\sqrt{6}\,x_3 + 5\sqrt{3/2}\,x_2^2$ on that critical point, the remaining variables x_2, x_3 behave as $x_2' = 2\,x_2 - 75\,x_2^3/2 - 60\,x_2\,x_3$ and $x_3' = -4\,x_3 + 75\,x_2^2\,x_3 + 120\,x_3^2$ for the choice of $k = \lambda = 5$.
Figure (3.5) displays the phase portrait of point E considering the variables x_2 and x_3. Once again, the blue arrows of the phase portrait represent the vector field. On the other hand, the red lines correspond to numerical solutions illustrating several trajectories that can be observed in the vicinity of point E. This critical point is defined by the black dot with coordinates $x_2 \simeq 0.23$ and $x_3 = 0$. Furthermore, based on the information presented in Tables (3.1) and (3.2) it can be concluded that point E, for that particular choice of the parameters, is classified as an unstable and non-hyperbolic critical point.

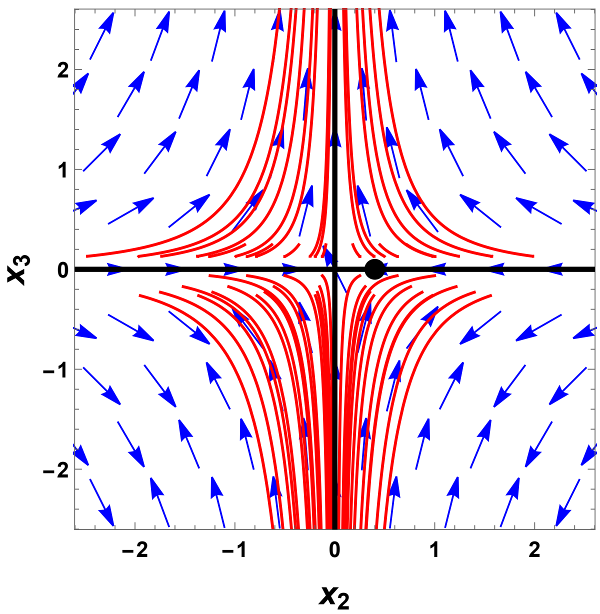

Fig. 3.6. 2D phase portrait of point F.

Point F exists when $\lambda^2 > 2$ as a matter-scaling solution with $\Omega_\phi/\Omega_m = 3/\lambda^2 - 3$ a non-zero constant. In this case, $w_{eff} = w_m = 0$ meaning that point F could not be related to an accelerated phase of the Universe. As $x_1 = 4\sqrt{2}\,x_3/\sqrt{3} + 5\sqrt{6}\,x_2^2$, the differential equations for the state variables x_2, x_3 are $x_2' = 3\,x_2/2 - 9\,x_2^3 - 12\,x_2\,x_3$ and $x_3' = -3\,x_3 + 18\,x_2^2\,x_3 + 24\,x_3^2$ for $k = 4$ and $\lambda = 3$. Figure (3.6) shows the two-dimensional phase portrait for $k = 4$ and $\lambda = 3$. The critical point is marked by the black dot at $x_2 \simeq 0.4$ and $x_3 = 0$. For that specific choice of parameters, point F exists and behaves as a saddle and hyperbolic critical point.

The final critical point is present only when $\lambda^2 < 6$ and indicates a Universe dominated by the scalar field. Given that $w_{eff} = w_\phi = -1 + \lambda^2/3$, for point G to represent an accelerated solution, it is necessary that $\lambda^2 < 2$. Since, $x_1 = -4\sqrt{6}\,x_3/5 + \sqrt{6}\,x_2^2/5$ on the critical point G, the behaviour of the variables is described by the equations $x_2' = x_2/2 - 3\,x_2^3/5 + 12\,x_2\,x_3/5$ and $x_3' = -x_3 + 12\,x_2^2\,x_3/5 - 48\,x_3^2/5$ for $k = 2$, $\lambda = 1$. Figure (3.7) displays the two-dimensional phase portrait of G. As $\lambda^2 = 1 < 2$, this last critical point could be associated with an accelerated phase of the model under study.

Similar to the previous graphs, blue arrows describe the vector field and red lines are for the trajectories near G, marked by the black dot with coordinates $x_2 \simeq 0.91, x_3 = 0$. According to Table (3.2) point G is a hyperbolic, accelerated and saddle critical point for that choice of the parameters k and λ.

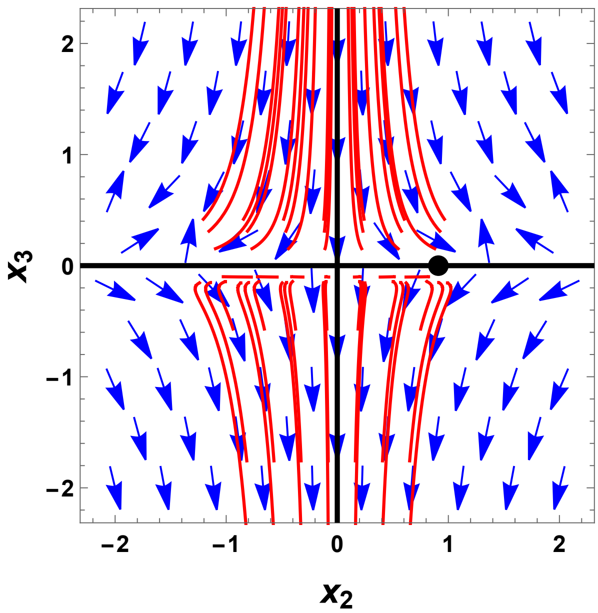

Fig. 3.7. 2D phase portrait of point G.

To complete the visualization process, Figure (3.8) illustrates the evolution of the density parameters for matter, and radiation as well as for the scalar field of the model along with the effective EoS. In addition, the evolution of the deceleration parameter over time is also displayed. The initial conditions are chosen to be $x_1 = 10^{-10}, x_2 = 2.8 \cdot 10^{-8}, x_3 = 9 \cdot 10^{-9}$ and $x_4 = 0.975$ for $\lambda = 1/2$ and $k = 1/4$. According to the analysis of Sec.(3.2), for this choice of parameters the model does not exhibit any scaling solutions. Initially, the scalar field is nearly frozen and Ω_ϕ begins to grow after the radiation-matter equality and deep in the matter-dominated era. Close to the present epoch Ω_ϕ continues to increase up to $\Omega_\phi \to 1$ and the effective EoS resembles the behaviour of the cosmological constant in the standard cosmological model. In these two plots, one can recognize the physical transitions of the Universe from being dominated by radiation to a period where matter became dominant ultimately leading to a stable phase characterized as a dark energy-dominated era where $w_{eff} \to -1$. Following the first plot, the deceleration parameter of the second plot characterizes the expansion rate of the Universe. This plot indicates that the deceleration parameter has changed from positive to negative around the present epoch featuring a viable cosmological model which aligns with the observed physical process of the Universe.

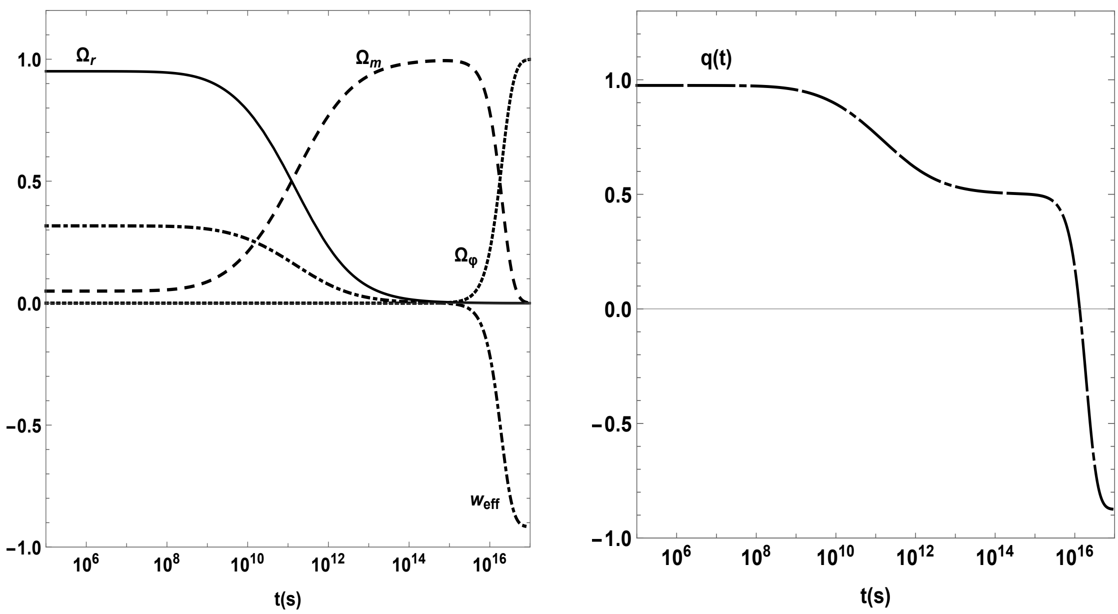

Fig. 3.8. The evolution of Ω_m, Ω_r, Ω_ϕ and the effective equation of state w_{eff} in the left panel, together with the deceleration parameter in the right panel versus time in seconds. The values of the parameters are $\lambda = 1/2$ and $k = 1/4$ while the initial conditions are chosen to be $x_1 = 10^{-10}, x_2 = 2.8 \cdot 10^{-8}, x_3 = 9 \cdot 10^{-9}, x_4 = 0.975$. According to the analysis of the critical points, for this choice of λ and k, point C could give rise to an accelerated phase of the system where $\Omega_\phi = 1$ and $w_{eff} = -1$. The scaling solutions are absent for this choice of parameters.

3.4 | 3-dimensional plots of the critical points

In this section, the 3D vector plots could provide a more precise illustration of the underlying physics that influences the behaviour of the critical points. Through these plots, the visual inspection of the flow properties in the vicinity of each critical point could further emphasize the results conveyed in 2D phase portraits aligning with the information provided in Tables (3.1) and (3.2). Each one of the 3D plots is followed by a brief discussion according to the analysis of Sec.(3.2) and Sec.(3.3).

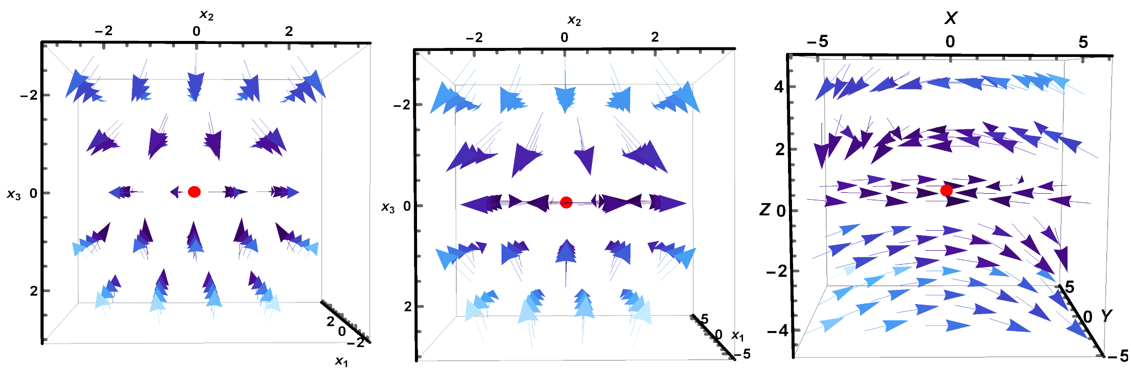

Fig. 3.9. 3D vector plots of points A, B and C.

The plot on the left side of Figure (3.9) demonstrates the three-dimensional phase space of x_1, x_2 and x_3 for $k = 1/4$ and $\lambda = 1/2$ for the first critical point. The blue arrows define the vector field while the red dot in the centre identifies point A. The vector field in this graph could not emphasize more the behaviour of A as a saddle critical point of the system. The central plot describes the three-dimensional phase space for point B for $k = 1/4$ and $\lambda = 1/2$. Once again blue arrows denote the vector field and point B is indicated by the red dot in the centre. As was expected, this critical point is a saddle one, linked to a radiation-dominated Universe. The plot on the right describes the phase space of X, Y and Z variables obtained by a shift to the origin of the initial variables according to $X = x_1, Y = x_2 - 1, Z = x_3 - \lambda/8$ for the choice of $k = \lambda = 1/2$ of the third critical point. The red dot in the centre defines point C, while the blue arrows are for the vector field. It is obvious that point C is a stable critical point in full agreement with the previous section.

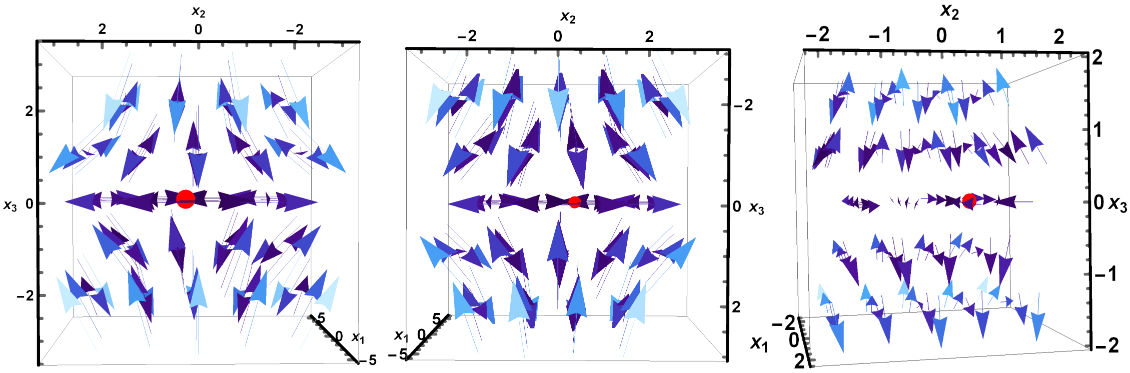

Fig. 3.10. 3D vector plots of points E, F and G.

According to the analysis of Sec.(3.2), point E is considered to be one of the two scaling solutions present in the system. The left plot in Figure (3.10) illustrates the 3D phase space of x_1, x_2 and x_3 for the choice of parameters $k = \lambda = 5$. The critical point is identified by the red dot with coordinates $x_1 \simeq 0.333, x_2 \simeq 0.23$ and $x_3 = 0$. For that specific choice of parameters, point E exists and behaves as an unstable and non-hyperbolic critical point. The plot in the centre of Figure (3.10) showcases the second scaling solution of the system for $k = 4$ and $\lambda = 3$. In that case point F is hyperbolic and saddle critical point defined by the red dot with coordinates $x_1 \simeq 0.4, x_2 \simeq 0.4$ and $x_3 = 0$. Lastly, the plot on the right displays the 3D phase space of point G for $k = 2$ and $\lambda = 1$. This critical point is located at $x_1 \simeq 0.41, x_2 \simeq 0.91$ and $x_3 = 0$. According to the information provided in the Tables (3.1) and (3.2) and for that specific choice of parameters, point G exists and is a saddle critical point of the system.

3.5 | Conclusion

The concept of dynamical systems originated from the pioneering work of Poincaré. Rather than focusing on finding exact solutions to a differential equation, this approach involves the use of topological techniques to analyze the properties of the set of solutions when viewed as trajectories on the phase space. The mathematical advancement of dynamical systems involved the introduction of key concepts like the flow associated with a given differential equation. The objective of using the method of dynamical system is to gain qualitative insights into the behaviour of the cosmological models, encompassing both spatially homogeneous and inhomogeneous scenarios. Ultimately, the aim is to elucidate the permissible range of initial conditions and subsequent evolution that aligns with the current observational data.

Multiple techniques for dynamically analysing and evaluating the EGB model are already present in the scientific literature. Nevertheless, the present analysis follows a different approach and concentrates on the impact on the solutions of the system when the EGB theory complies with the GW speed constraint. As indicated in Sec.(3.2), the requirements of compatibility specified in Eq.(3.24) result in the formulation of Eq.(3.26). Consequently, it has been proved that it is possible to identify the fraction $\dot{H}/H^2$ as an expression of the variables of the dynamical system.

The inclusion of this novel element is crucial for the analysis that followed. It clarifies that the autonomous feature of the dynamical system could be determined from the beginning without the need to formulate any assumptions regarding the value of that fraction throughout the periods of cosmic evolution. Instead, by considering the characteristics and behaviour of every critical point in the analysis, we can successfully determine the periods of cosmic evolution along with the value of that fraction in each case. The investigation that follows identifies seven critical points of the autonomous dynamical system, offering a new perspective which can potentially uncover new insights and enhance the existing phenomenology about the EGB theory. When examining the properties of each critical point, it is important to recognize that two of them might be related to the early periods of the evolution of the Universe. According to the analysis, it is evident that once $\lambda^2 < 2$, point G represents an unstable and accelerated solution of the dynamical system. This behaviour of point G might actually correspond to a relation with the inflationary era of the model. Additionally, the analysis reveals that, at point D, w_ϕ reaches its maximum value, $w_\phi \to 1$, indicating the absence of acceleration. Considering that this critical point is connected to the phase in which the kinetic energy of the scalar field is dominant, it is expected that the field will roll down the potential. As a result, it is unlikely that point D aligns with the evolution stages of the CDM model. These conclusions of the analysis suggest that further research is necessary to investigate thoroughly the properties of the critical points D and G, and their potential relations with the early Universe.

The crucial feature defining the critical point C is that it is dominated by the potential energy of the scalar field which effectively behaves as a cosmological constant. The underlying meaning of this important behaviour is that the Universe is driven towards acceleration. The analysis indicates that point C is identified as a stable critical point of the system. This means that it has the ability to function as the attractor of the dynamical system leading the model towards a phase of accelerated expansion.

Moving forward with the evaluation of the critical points, it was revealed that the system also possesses two scaling solutions. These solutions, namely points E and F, have the characteristic property that the energy density of the scalar field tracks the energy density of the background. These two scaling solutions initially appeared quite promising as they have a significant contribution in the context of modelling dark energy. However, the combination of those two critical points with point C proved to not meet the requirements for constructing a coherent evolutionary history of the Universe within the EGB context. As a result, and intending of accurately describing the eras dominated by matter and radiation, it is necessary to consider points A and B.

The increasing statistical accuracy in galaxy surveys is driving the demand for more precise predictions of the observable quantities that are crucial in shaping our understanding of cosmology and galaxy formation theories. As the field of cosmology evolves and expands, there is a growing emphasis on ensuring that observations can be used effectively to improve our knowledge of the Universe. Survey data from galaxies have successfully constrained certain cosmological parameters to a level similar to the measurements from CMB. Nevertheless, these constraints are based on analyses of nonlinear structures. As a result, these analyses are determined by systematic errors as they often exclude a considerable amount of data to address uncertainties in modelling.

Analytical techniques face severe challenges in dealing with nonlinear structure formation, but there exists a viable alternative route. Driven by the ongoing advancements in numerical methods and computational progress, the forefront of the theoretical research will probably be dominated by numerical simulations [92], [85], [59]. In this context, the estimation of cosmological parameters is usually established by applying methods such as the Monte Carlo Markov chain approach. In present-day analyses, a considerable number of distinct cosmologies must be applied to achieve convergence. Operating an N-body simulation at each one of these iterations is not a feasible endeavour. This means that we need procedures able to generate viable predictions for the parameter space using a limited number of simulations.

Motivated by the interesting phenomenology of the EGB dynamical system analysis, it would be logical to examine whether the EGB model is consistent with observations that provide insights into the expansion history of the Universe and the development of structures. In particular, by using the combined data from CMB, BAO and Supernovae, we may compare and constrain the parameters of the EGB cosmological model employing the Monte Carlo Markov chain method.

Furthermore, the analysis of the background and perturbation evolution can serve as an additional way to constrain the EGB model. This involves examining how the theoretical predictions align with observational data, ultimately narrowing down the permissible range of the parameter values.

Considering the early-time behaviour, it would be advantageous to develop the slow-roll framework of the EGB model and study the possibility of a viable period of inflation. Within this study, we could examine whether the spectral index and the tensor – to – scalar ratio are compatible with the Planck observational data.

4

Classification of Teleparallel Horndeski Cosmology via Noether Symmetries

Incorporating the newly introduced terms in the Lagrangian has enriched the landscape of the theoretical models that can be formulated within the context of the teleparallel analogue of the Horndeski theory. The present chapter serves to introduce and also explore the classification of this extensive range of models which are emerging from the Teleparallel Horndeski. The Noether point symmetries approach provides a unique perspective on that classification as it could elucidate the mathematical properties as well as the symmetries found within these models. Furthermore, this method showcases its ability to differentiate between the various models in the context of second-order teleparallel scalar-tensor theories and accurately determine solutions.

4.1 | The point-like Lagrangian

The Teleleparallel analogue of Horndeski theory, known as the BDLS theory [13], [14], offers an expansive foundation for constructing and developing cosmological models due to the incorporation of the torsion tensor in generating lower-order theories of gravity. Additionally, the BDLS theory is of particular interest since it offers a direct method to circumvent the constraint imposed by the propagation speed of GW [15].

The Noether symmetries approach is widely regarded to be highly beneficial for identifying and investigating these potential models. Utilizing this method allows for the emergence of symmetries that preserve the action and ultimately simplify the equations that govern each system. These symmetries correspond to conserved quantities, resulting in the possibility of finding exact solutions more easily compared to other methods which typically yield limited results. This means that the Noether symmetries approach enables the recognition of key patterns and structures within a system thus shedding light on the principles that guide its dynamics. The concept of incorporating Noether symmetries in the field of cosmology has been a topic of interest for a considerable period of time and has received significant attention in various scholarly studies [45], [124], [31], [44]. It has been suggested in [23] that identifying the Noether point symmetries can serve as a selection criterion in determining the form of the potential energy in dark energy models within the framework of GR. In addition, as reported in [46] the classification of the classical Horndeski models was conducted according to the particular forms of the functions $G_i(\phi, X)$ with the sole criterion being the requirement for the field equations to remain invariant under Noether point symmetries. Therefore, the Noether symmetry approach facilitated a rigorous and systematic process for determining the appropriate forms of the arbitrary functions G_i.

Before examining the implementation of Noether symmetries, the current chapter will commence by formulating the teleparallel Horndeski Lagrangian. The crucial task of this process is to incorporate the newly introduced torsion scalars into Eq.(2.46).

To begin with, we consider the spatially flat FLRW spacetime defined in Eq.(3.2),

$$\mathrm{d}s^2 = -N(t)^2\mathrm{d}t^2 + a(t)^2(\mathrm{d}x^2 + \mathrm{d}y^2 + \mathrm{d}z^2)\,, \tag{4.1}$$

where $N(t)$ corresponds to the lapse function which quantifies the rate at which proper time elapses along a trajectory, and $a(t)$ is the scale factor. This flat spacetime model has a crucial role in contemporary cosmology, providing a fundamental framework for analyzing the large-scale distribution of matter and energy. According to the Cosmological Principle, the Universe is postulated to exhibit homogeneity and isotropy on large scales, leading to the conclusion that the scalar field of the theory is solely dependent on cosmic time, represented by $\phi = \phi(t)$.

At this point, the Weitzenböck gauge, $\omega^{A}{}_{B\mu} = 0$, which is described in Sec.(2.1), can be utilized to derive the metric of Eq.(4.1) by using the specific diagonal tetrad

$$e^{A}{}_{\mu} = \text{diag}\,(\,N(t), a(t), a(t), a(t)\,) \tag{4.2}$$

By implementing the condition $\omega^{A}{}_{B\mu} = 0$, one can effectively relate the spin connection to the metric, resulting in a direct link between the two mathematical structures.

For the flat FLRW spacetime, the torsion tensor only retains its vectorial part,

$$v_{\mu} \;=\; (\,-3H, 0, 0, 0\,), \tag{4.3}$$

with $H = \dot{a}/a$ being the Hubble parameter.

This indicates that the contractions of the torsion tensor in a flat FLRW spacetime, without considering the contribution of the scalar field present in the theory, are solely represented by T_{vec}. As a result, the torsion scalar, which is defined in Eq.(2.16), has the following formula :

$$T_{\text{vec}} \;=\; -\frac{9H^2}{N^2} \;\Rightarrow\; T \;=\; \frac{6H^2}{N^2} \tag{4.4}$$

After analyzing the contractions of the irreducible components of the torsion tensor with the scalar field, as outlined in Eqs (2.28)-(2.30), it becomes evident that only those associated with the vectorial part v_{μ} remain.

As a consequence, the computation of the quadratic contractions of the torsion tensor in a flat FLRW spacetime results in the following expression for the I_2 scalar :

$$I_2 = v^\mu \phi_{;\mu} \Rightarrow I_2 = \frac{3H\dot{\phi}}{N^2} \tag{4.5}$$

In order to enhance the development of Lagrangian formulation, it is necessary to incorporate the derivative operators for the scalar field. This process is crucial as it will elevate the accuracy of the Lagrangian framework allowing for a more comprehensive examination. According to that reasoning, the derivative operators acting on the scalar field $\phi(t)$ of the theory, that need to be included are

$$\mathring{\Box}\phi = -\frac{\ddot{\phi}}{N^2} - \frac{3\dot{a}\,\dot{\phi}}{aN^2} + \frac{\dot{\phi}\,\dot{N}}{N^3}\,, \tag{4.6}$$

$$(\mathring{\nabla}_\mu \mathring{\nabla}_\nu \phi)^2 = \frac{3\dot{a}^2\,\dot{\phi}^2}{a^2N^4} + \frac{1}{N^4}\left(\ddot{\phi} - \frac{\dot{\phi}\,\dot{N}}{N}\right)^2\,, \tag{4.7}$$

$$(\mathring{\nabla}_\mu \mathring{\nabla}_\nu \phi)^3 = -\frac{3\dot{a}^3\,\dot{\phi}^3}{a^3N^6} - \frac{1}{N^6}\left(\ddot{\phi} - \frac{\dot{\phi}\,\dot{N}}{N}\right)^3 \tag{4.8}$$

Moreover, the kinetic term and the Ricci scalar are expressed as

$$X = \frac{\dot{\phi}^2}{2N^2}\,, \quad \mathring{R} = -T + B = \frac{6\ddot{a}}{aN^2} + \frac{6\dot{a}^2}{a^2N^2} - \frac{6\dot{a}\dot{N}}{aN^3}\,. \tag{4.9}$$

At this point in the procedure, it would be beneficial to introduce two Lagrangian multipliers denoted as λ_1 and λ_2 which are associated with the scalars T and I_2 respectively. The application of the Lagrangian multiplier method is focused on deriving solutions that align with holonomic equations defining the potential constraints within the system. This systematic integration of the potential constraints in the process combined with the scalar contributions in the BDLS context, results in the formulation of the Lagrangian which is determined in the following manner :

$$\begin{aligned}\mathcal{L} =& a^3 N \left[G_2(\phi, X) + G_{tele}(\phi, X, T, I_2) + T G_4(\phi, X) - I_2 G_{tele,I2}(\phi, X, T, I2) - T G_{tele,T}(\phi, X, T, I2)\right] \\ &+ \frac{6a\ddot{a}}{N^3}\left[aN^2 G_4(\phi, X) + G_5(\phi)\dot{a}\dot{\phi}\right] + \frac{a\ddot{\phi}}{N^3}\left[a^2N^2 G_3(\phi, X) + 3G_5(\phi)\dot{a}^2 + 6aG_{4,X}(\phi, X)\dot{a}\dot{\phi}\right] \\ &- \frac{a^2\dot{N}}{N^2}\left[6G_4(\phi, X)\dot{a} + aG_3(\phi, X)\dot{\phi}\right] - \frac{3a\dot{a}\dot{N}\dot{\phi}}{N^4}\left[3G_5(\phi, X)\dot{a} + 2aG_{4,X}(\phi, X)\dot{\phi}\right] \\ &+ \frac{3a\dot{a}}{N}\left[aG_3(\phi, X)\dot{\phi} + aG_{tele,I2}(\phi, X, T, I_2)\dot{\phi} + 2G_{tele,T}(\phi, X, T, I_2)\dot{a}\right] \\ &+ \frac{3a\dot{a}^2\dot{\phi}}{N^3}\left[G_5(\phi, X)\dot{a} + 2aG_{4,X}(\phi, X)\dot{\phi}\right] . \end{aligned} \tag{4.10}$$

It is evident that Eq.(4.10) contains terms involving second-order derivatives, which can be eliminated by utilizing the technique of integration by parts. However, it is important to note that there is one particular contribution, namely $a^3\ddot{\phi}\ G_3/N$, which cannot be eliminated during this process. Therefore, in order for the Lagrangian to be considered canonical and depend solely on the first-order derivatives of the variables, a reasonable option would be [46]

$$G_{3XX} = 0 \Rightarrow G_3(\phi, X) = g(\phi)X + h(\phi) . \tag{4.11}$$

This choice may initially seem arbitrary. However, by imposing this limitation it becomes possible to realize various cases of scalar-tensor theories that involve interaction components of the form $\nabla_\mu\phi\nabla^\mu\phi\,\Box\phi$. In addition, it is important to acknowledge that the coincident arrival of GW170817 and its electromagnetic counterpart provides strong limitations on the wide range of scalar-tensor theories and eventually excludes those theories that demonstrate a GW propagation speed which differs from observational data. Even though facing significant limitations, several models belonging to the scalar-tensor theories landscape have the ability to bypass these constraints rendering them potentially valid. Within the Horndeski theory, these encompass kinetic gravity braiding, cubic galileons and Brans-Dicke/$f(R)$ theories as the simplest modifications of gravity. However, distinguishing between the various functional models proves to be a more complex endeavour. Consequently, the choice is to concentrate on the selection models stemming from the aforementioned option described in Eq.(4.11), providing a new spectrum of cosmological scenarios to analyze.

The final form of the point-like BDLS Lagrangian for this setting is expressed as

$$
\begin{aligned}
\mathcal{L} =& a^3 N \left(G_2(\phi, X) + T G_4(\phi, X) - I_2 G_{tele,I2}(\phi, X, T, I_2) - T G_{tele,T}(\phi, X, T, I_2) + G_{tele}(\phi, X, T, I_2)\right) \\
& - \frac{3a\dot{a}^2}{N^3}\Big(\dot{\phi}^2\left(G_5'(\phi) - 2G_{4,X}(\phi, X)\right) + 2N^2\left(2G_4(\phi, X) - G_{tele,T}(\phi, X, T, I_2)\right)\Big) + \\
& + \frac{a^2\dot{a}\dot{\phi}}{N^3}\Big(3N^2\left(G_{tele,I2}(\phi, X, T, I_2) - 2G_{4,\phi}(\phi, X)\right) + g(\phi)\dot{\phi}^2\Big) - \\
& - \frac{a^3\dot{\phi}^4 g'(\phi)}{6N^3} - \frac{a^3\dot{\phi}^2 h'(\phi)}{N}\,,
\end{aligned}
\tag{4.12}
$$

The configuration space of Eq.(4.12) is the minisuperspace $\mathcal{Q} = \{a, \phi, N, T, I_2\}$. The utilization of a minisuperspace description is important in gravitational theories as it aids in gaining deeper insight into the dynamics and enables the interpretation of terms when physical observables are linked to symmetries of the minisuperspace [43], [114]. Furthermore, within the minisuperspace, the gravitational field equations can be simplified, which in turn allows certain DoF to be equivalently described in terms of a scalar field. Besides, by introducing a point-like Lagrangian function, it becomes possible to apply mathematical techniques to accurately derive precise and analytic solutions for the field equations of the theory.

4.2 | Noether Symmetries

According to the Noether theorem, any differentiable symmetry that is present in the action of a physical system is associated with a corresponding conservation law [107]. Consequently, the Noether Symmetry approach is recognized as one of the most systematic and reliable methods to identify conserved quantities. These symmetries can effectively reduce the complexities of a system that involves non-linear partial differentiable equations, enabling the development of new solutions through the usage of conserved quantities [74], [95].

The use of the Noether symmetries approach in the field of cosmological research, is widely acknowledged and has gained considerable attention in the academic literature [124], [140],[31], [45]. The investigation of a cosmological model through this method involves analyzing how the Lagrangian of the model behaves under infinitesimal point transformations that uphold the desired symmetry.

For that purpose, the starting point is to consider a physical system described by the Lagrangian $\mathcal{L}$, which consists of n generalized coordinates q_i with t representing the independent variable. Following that, the infinitesimal transformation applied to the system can be summarized, in a general manner, by the formula below

$$t \Rightarrow t' = t + \epsilon\, \xi(q^i, t) \;\;,\;\; q^i \Rightarrow q^{i'} = q^i + \epsilon\, \eta^i(q^i, t)\,, \tag{4.13}$$

According to the Noether theorem, the transformation which is outlined in Eq.(4.13) is associated with the generator vector $\mathcal{X}$ according to,

$$\mathcal{X} = \xi(q^i, t)\,\frac{\partial}{\partial t} + \eta^i(q^i, t)\,\frac{\partial}{\partial q^i}\,. \tag{4.14}$$

The impact of this infinitesimal transformation upon any differentiable function with $F = F(t, q_i)$ is expressed by the following form :

$$F(t', q_i') = F(t, q_i) + \epsilon\, \mathcal{X}(F(t, q_i)) + O(\epsilon^2) \tag{4.15}$$

In the case that the differentiable function F has also a velocity dependence, i.e. $F(t, q_i, \dot{q}_i)$, then the impact of the transformation is described by

$$F(t', q_i', \dot{q}_i') = F(t, q_i, \dot{q}_i) + \epsilon\, \mathcal{X}^{(1)}(F(t, q_i, \dot{q}_i)) + O(\epsilon^2)\,, \tag{4.16}$$

where

$$\mathcal{X}^{(1)} = \mathcal{X} + (\dot{\eta}^i - \dot{q}^i \dot{\xi}\,)\, \frac{\partial}{\partial \dot{q}^i}\,, \tag{4.17}$$

which is known as the first prolongation of the generator vector.

Similarly, if the function F has a second time-derivative dependence, i.e. $F(t, q_i, \dot{q}_i, \ddot{q}_i)$, then the second prolongation of the generator vector must be applied, which is

$$\mathcal{X}^{(2)} = \mathcal{X}^{(1)} + (\ddot{\eta}^i - \dot{q}^i \ddot{\xi} - 2\ddot{q}^i \dot{\xi}\,)\, \frac{\partial}{\partial \ddot{q}^i}\,. \tag{4.18}$$

When examining a physical system characterized by the Lagrangian $\mathcal{L} = \mathcal{L}(t, q, \dot{q})$, then the action of this system remains invariant under an infinitesimal transformation, up to a total divergence term, as long as the Rund-Trautman identity is satisfied,

$$\mathcal{X}^{(1)}\, \mathcal{L} + \frac{\mathrm{d}\xi}{\mathrm{d}t}\, \mathcal{L} \;=\; \frac{\mathrm{d}f}{\mathrm{d}t}\,, \tag{4.19}$$

where $\mathcal{X}^{(1)}$ is the first prolongation of the generator vector while the function f is regarded as the gauge function expressing the equivalence of the Lagrangian in the action integral up to a total time derivative. In that particular case, the generator vector $\mathcal{X}$ is identified as a Noether symmetry providing insights into the conservation laws that apply to the system described by the Lagrangian $\mathcal{L}$.

Whenever a Noether symmetry exists, the function

$$I(t, q, \dot{q}\,) = f - \mathcal{L}\,\xi - \frac{\partial \mathcal{L}}{\partial \dot{q}^i}\,(\eta^i - \dot{q}^i \xi)\,, \tag{4.20}$$

is known as a Noetherian first integral or conservation law $(\mathrm{d}I/\mathrm{d}t = 0)$ associated with the symmetry expressed by the generator vector.

It is worth noting at this point, that a direct correlation between a Noether symmetry and a first integral is hardly to exist. Once the symmetry has been identified, the determination of the integral requires minimal effort. However, the reverse process is more complex. Given the Lagrangian $\mathcal{L}$ and the integral, the symmetry involves solving a differential equation with the function f as an additional variable originating from boundary terms. Consequently, numerous coefficient functions expressing symmetry could exist associated with a specific first integral.

The utilization of Noether symmetry was introduced in scalar-tensor theories of gravity by De Ritis and collaborators [54] as an effective way to determine the function form of the potential. Through the application of Noether symmetry, it was discovered that the exponential potential was favoured among other formulas leading to inflationary dynamics in the early universe. This fact generated significant interest prompting further investigations into the implementation of Noether symmetry in cosmological scenarios, non-minimal and minimally coupled scalar-tensor theories [22], [55], [123], as well as higher-order and $f(R)$ theories of gravity [125], [124].

The existence of Noether symmetries enables the reduction of complex dynamics and significantly facilitates the calculation of exact solutions. As a result, it was reasonable to be applied in the context of teleparallel gravity as a selection criterion for the cosmological models [23]. For instance, in [24], where Noether symmetries have been employed to assess the viability of $f(T)$ gravity in a background of spatially flat FLRW metric. The objective for the authors was to discover the expressions of $f(T)$

that can incorporate additional Noether symmetries and to solve the field equations for those models aiming to derive analytical solutions for the cosmological functions. In addition, following the rationale of [134], it has been argued that Noether symmetries in a similar background lead to the function form of $f(T) \propto T^n$, however, $n = 3/2$ as it was claimed in [127]. Even more complex Lagrangians incorporating various combinations of topological invariants along with torsion scalar T could be studied using Noether symmetries. In [9] the authors applied this method to investigate the dynamics that emerge from $f(T, B)$ gravity, where B is the boundary term which is defined in Eq.(2.20). In [61] the formalism of $f(T_{\mathcal{G}}, T)$ theory was investigated, where $T_{\mathcal{G}}$ is the torsion analogue of the Gauss-Bonnet topological invariant. The implementation of Noether symmetries has led to specific forms of the function that admit symmetries as well as the reduction of the dynamical system of the theory.

4.3 | BDLS Cosmologies

In Sec. (4.1) it was pointed out that the configuration space of the point-like Lagrangian is represented as $\mathcal{Q} = \{a, \phi, N, T, I_2\}$. When considering the cosmic time t as the independent variable, then the generator vector is described by

$$\mathcal{X} = \xi(t, a, \phi, N, T, I_2)\, \partial_t + \Sigma\eta_{q_i}(t, a, \phi, N, T, I_2)\, \partial q_i\,, \quad q_i = a, \phi, N, T, I_2\,. \tag{4.21}$$

By utilizing the Noether symmetry approach and incorporating the Rund-Trautman identity from Eq.(4.19) to the point-like Lagrangian defined in Eq.(4.12), a total of 62 equations are derived. This system of equations specifically addresses the coefficients of the generator vector $\xi, \eta_a, \eta_\phi, \eta_N, \eta_T$ and η_{I_2} as well as the contribution terms $G_i(\phi, X)$ of the Lagrangian in BDLS theory.

The system of 62 equations combined with the behaviour of the function $g(\phi)$ as described in Eq.(4.11), gives rise to genuine constraints on the unknown functions of the theory alongside the coefficients of the generator vector. The emergence of these constraints is crucial for understanding the underlying principles driving the behaviour of the system. This includes fully considering symmetries and examining each symmetry resulting from the procedure.

The presence of a non-zero coefficient in the generator vector establishes a Noether symmetry. This particular symmetry leads to the development of a wide range of forms for the $G_i(\phi, X)$ functions that could hold significant physical importance and interest.

The immense scope of the teleparallel analogue of the Horndeski theory indicates that the analysis will yield a multitude of potential scenarios, some of which may elaborate lengthy and complex solutions that may not be applicable to the present chapter.

Therefore, the forthcoming discussion shall concentrate only on four particular cases of the scenarios while preserving the complete set of the classification solutions separately [1]. The collection of Tables that encompass each case of the present study can be found in [62]. Each Table provides the detailed results for the coefficients of the generator vector and the $G_i(\phi, X)$ functions.

The thorough presentation of the results in the Tables of [62] allows a deeper understanding of how these coefficients and functions operate in the context of BDLS theory. In addition, it enables the identification of patterns across different cases and thus facilitates a more comprehensive evaluation of the overall study results.

4.3.1 | Four examples of BDLS Cosmologies

This section provides a comprehensive overview of the results regarding the coefficients of the generator vector and the G_i functions of the Lagrangian for the four selected cases of [62].

[1]The full set of Noether symmetry solutions can be found at https://github.com/jacksonsaid/BDLS_Noether_classification.git

Case 1 (2.a.ii.1.a.i.1.b.i.1.b in Table 2a):

Solving the system of the 62 equations leads to the calculation of the coefficients of the generator vector which are

$$\xi(t,a,\phi,N,T,I2) = \tilde{\xi}(t)\,, \tag{4.22}$$

$$\eta_a(t,a,\phi,N,T,I2) = -\frac{1}{3}c_1\,a\,, \tag{4.23}$$

$$\eta_\phi(t,a,\phi,N,T,I2) = \frac{c_1\,g(\phi)}{g'(\phi)}\,, \tag{4.24}$$

$$\eta_N(t,a,\phi,N,T,I2) = N\left(c_1 - \xi(t) - \frac{c_1\,g(\phi)\,g''(\phi)}{g'(\phi)^2}\right)\,, \tag{4.25}$$

$$\eta_T(t,a,\phi,N,T,I2) = 2c_1 T\left(\frac{g(\phi)\,g''(\phi)}{g'(\phi)^2} - 1\right)\,, \tag{4.26}$$

$$\eta_{I_2}(t,a,\phi,N,T,I2) = c_1\Bigg(I_2\left(-\frac{c_1 g(\phi)\,g''(\phi)}{g'(\phi)^2} - 1\right) + \frac{4}{(2c_2+3)\,g(\phi)^3}\Big(g(\phi)\,g'(\phi)\,\tilde{G}_4'(\phi)$$

$$+ \tilde{G}_4(\phi)\left(g(\phi)\,g''(\phi) - 2g'(\phi)^2\right)\Big)\Bigg)\,, \tag{4.27}$$

$$f(t,a,\phi,N,T,I2) = c_7\,, \tag{4.28}$$

For this solution, the BDLS functions are given by

$$G_2(\phi, X) = \frac{g'(\phi)}{2}\left(2c_3 + c_3 X + 2X^2\right) - \tilde{G}_{tele}(\phi, X)\,, \tag{4.29}$$

$$G_3(\phi, X) = c_4 + g(\phi)\,(c_5 + X)\;, \tag{4.30}$$

$$G_4(\phi, X) = \tilde{G}_4(\phi) + \frac{(2c_2+3) X\, g(\phi)^2}{4\, g'(\phi)}\,, \tag{4.31}$$

$$G_5(\phi, X) = c_6 + \int_1^{\phi} \frac{c_2\, g(x)^2}{g'(x)} dx\,, \tag{4.32}$$

$$\begin{aligned} G_{tele}(\phi, X, T, I_2) = & \tilde{G}_{tele}(\phi, X) + \frac{1}{4}\Big(4\tilde{G}_4(\phi)T + 2g(\phi) I_2 (c_3 - 4c_5 + 2X(3 + 2c_2)) + \\ & + 4\bar{G}_{tele}\,(\,\frac{g(\phi)^2\, T}{g'(\phi)^2}\,)\, g'(\phi) + 8 I_2\, \tilde{G}_4'(\phi) + \frac{(2c_2+3)\, g(\phi)^3 I_2\, T}{g'(\phi)^2} + \\ & + \frac{2g(\phi)^2\, X(2c_2 T\, g'(\phi) - (2c_2+3) I_2\, g''(\phi))}{g'(\phi)^2}\Big)\,. \end{aligned} \tag{4.33}$$

The solution outlined above is quite interesting as the G_4 function depends on both the kinetic term and the scalar field, while the G_5 function remains non-zero and is the sole function not relying on X. The non-zero property of G_5 is counterbalanced by the complex structure of the G_{Tele} which encompasses multiple terms to comply with the GW speed constraint. It is important to emphasize that in this particular scenario, along with all the other cases of classification, the denominators cannot become zero due to the specific conditions that govern each case of the study. This fact eliminates the possibility of divergences and ensures the viability of the solutions.

Case 2 (2.a.ii.1.a.ii.2.a.ii in Table 2a):

In this case of solutions, the coefficients of the generator vector are the following :

$$\xi(t,a,\phi,N,T,I2) = \tilde{\xi}(t)\,, \tag{4.34}$$

$$\eta_a(t,a,\phi,N,T,I2) = \frac{3c_1 - a^3\tilde{\eta}_\phi(t,a,\phi,N,I_2)\,g'(\phi)}{3a^2 g(\phi)}\,, \tag{4.35}$$

$$\eta_\phi(t,a,\phi,N,T,I2) = \tilde{\eta}_\phi(t,a,\phi,N,I2)\,, \tag{4.36}$$

$$\begin{aligned}\eta_N(t,a,\phi,N,T,I2) =& N\left(-\frac{3c_1}{a^3 g(\phi)} + \frac{\tilde{\eta}_\phi(t,a,\phi,N,I2)\,g'(\phi)}{g(\phi)} - \tilde{\xi}(t)\right) - \\ & - N\,\frac{\tilde{\eta}_\phi(t,a,\phi,N,I2)\,g''(\phi)}{g'(\phi)}\,,\end{aligned} \tag{4.37}$$

$$\begin{aligned}\eta_T(t,a,\phi,N,T,I2) =& \frac{1}{c_2\,a^3\,N\,g(\phi)^2\,g'(\phi)}\Big(f'(t)\,g'(\phi)^2 + \\ & + a^3\,N\,\tilde{\eta}_\phi(t,a,\phi,N,I2)\Big(-2c_2 T\,g(\phi)\,g'(\phi)^2 + \\ & + 2c_2\,T\,g(\phi)^2\,g''(\phi) - g'\,(\phi)^2\,\tilde{G}'_{Tele}(\phi) + \\ & + g'(\phi)\,g''(\phi)\,\tilde{G}_{Tele}(\phi)\Big)\Big)\,,\end{aligned} \tag{4.38}$$

$$\eta_{I_2}(t,a,\phi,N,T,I2) = \eta_{I_2}(t,a,\phi,N,T,I2)\,, \tag{4.39}$$

$$f(t,a,\phi,N,T,I2) = f(t) \tag{4.40}$$

In this particular case, the functions of the BDLS Lagrangian take the form

$$G_2(\phi, X) = G_2(\phi, X)\,, \tag{4.41}$$

$$G_3(\phi, X) = c_3 + g(\phi)\,(c_4 + X)\,, \tag{4.42}$$

$$G_4(\phi, X) = \frac{c_2\, g(\phi)^2}{g'(\phi)}\,, \tag{4.43}$$

$$G_5(\phi, X) = c_5\,, \tag{4.44}$$

$$\begin{aligned} G_{tele}(\phi, X, T, I_2) = & - G_2(\phi, X) + \tilde{G}_{tele}(\phi) + \frac{4}{3}\, c_2\, I_2\, g(\phi) + 2c_4\, X\, g'(\phi) + \\ & + X^2\, g'(\phi) - \frac{8}{3} c_2\, X\, g'(\phi) - \frac{2c_2\, g(\phi)^2\, I_2\, g''(\phi)}{g'(\phi)^2}\,. \end{aligned} \tag{4.45}$$

When comparing Case 1 and Case 2, it becomes apparent that in the latter the G_5 function remains constant and G_4 is independent of the kinetic term. This difference ultimately allows these terms to meet the GW speed constraint in the classical Horndeski context. However, in the BDLS theory, the inclusion of the correction term gives rise to novel dynamical features that differ from the standard Horndeski theory. Furthermore, it is crucial to recognize that the presence of the G_2 function in the outcome of the G_{Tele} term results in a coupling between the conventional term and the BDLS correction term.

Case 3 (2.b.i2.b.ii.2.b.ii.2 in Table 2b):

Following the same procedure, the coefficients of the Noether vector are

$$\xi(t,a,\phi,N,T,I2) = \tilde{\xi}(t)\,, \tag{4.46}$$

$$\eta_a(t,a,\phi,N,T,I2) = \frac{c_1}{c_2\,a^2}\,, \tag{4.47}$$

$$\eta_\phi(t,a,\phi,N,T,I2) = 0\,, \tag{4.48}$$

$$\eta_N(t,a,\phi,N,T,I2) = -\,N\,\tilde{\xi}(t)\,, \tag{4.49}$$

$$\eta_T(t,a,\phi,N,T,I2) = -\,\frac{3c_1\,(\,2\,\tilde{G}_{tele}(\phi) + T\,G_5'(\phi)\,)}{c_2\,a^3\,G_5'(\phi)}\,, \tag{4.50}$$

$$\eta_{I_2}(t,a,\phi,N,T,I2) = \eta_{I_2}(t,a,\phi,N,T,I2)\,, \tag{4.51}$$

$$f(t,a,\phi,N,T,I2) = c_3\,, \tag{4.52}$$

and the functions of the BDLS model for the third case are given by

$$G_2(\phi,X) = G_2(\phi,X)\,, \tag{4.53}$$

$$G_3(\phi,X) = c_4 + c_5\,X\,, \tag{4.54}$$

$$G_4(\phi,X) = \tilde{G}_4(\phi) + \frac{X}{2}\,G_5'(\phi)\,, \tag{4.55}$$

$$G_5(\phi,X) = G_5(\phi)\,, \tag{4.56}$$

$$G_{tele}(\phi,X,T,I_2) = -\,G_2(\phi,X) + \frac{(\tilde{G}_{tele}(\phi) + T\,G_5'(\phi))\,(2\,\tilde{G}_4(\phi) + X\,G_5'(\phi))}{G_5'(\phi)} + \\ + I_2\left(c_6 + 2\tilde{G}_4'(\phi) + X\,(G_5''(\phi) - c_2)\right)\,. \tag{4.57}$$

In this solution, the G_5 function depends on solely the scalar field while $G4$ relies on both the scalar field and the kinetic term. As a result, the third case depicted above complies once more with the GW constraint of the propagation speed in the BDLS context, however, fails to meet the same requirement in the classical Horndeski theory.

Case 4 (2.b.ii1.a.ii.2.b.i in Table 2b):

In the final case, the coefficients of the generator vector are as follows :

$$\xi(t,a,\phi,N,T,I2) = \tilde{\xi}(t)\,, \tag{4.58}$$

$$\eta_a(t,a,\phi,N,T,I2) = \frac{c_1}{\sqrt{a}}\,, \tag{4.59}$$

$$\eta_\phi(t,a,\phi,N,T,I2) = 0\,, \tag{4.60}$$

$$\eta_N(t,a,\phi,N,T,I2) = -N\,\tilde{\xi}(t)\,, \tag{4.61}$$

$$\eta_T(t,a,\phi,N,T,I2) = -\frac{3\,c_1\,T}{a^{3/2}}\,, \tag{4.62}$$

$$\eta_{I_2}(t,a,\phi,N,T,I2) = -\frac{3c_1\,I_2}{2a^{3/2}}\,, \tag{4.63}$$

$$f(t,a,\phi,N,T,I2) = c_2\,, \tag{4.64}$$

The corresponding functions, in that case, are given by

$$G_2(\phi, X) = \tilde{G}_2(\phi) - \tilde{G}_{tele}(\phi, X)\,, \tag{4.65}$$

$$G_3(\phi, X) = c_3\,, \tag{4.66}$$

$$G_4(\phi, X) = \bar{G}_4'(\phi) + X\tilde{G}_4'(\phi)\,, \tag{4.67}$$

$$G_5(\phi, X) = G_5(\phi)\,, \tag{4.68}$$

$$\begin{aligned} G_{tele}(\phi, X, T, I_2) =& - \tilde{G}_2(\phi) + \tilde{G}_{tele}(\phi, X) + \bar{G}_{tele}(\phi)\, I_2 \sqrt{T} + \hat{G}_{tele}(\phi)\, T - \\ & - \tilde{G}_4(\phi)\, T\, X + 2 I_2 \left(\bar{G}_4'(\phi) + X\, \tilde{G}_4'(\phi)\right) + \frac{3\, X\, T}{2}\, G_5'(\phi)\,. \end{aligned} \tag{4.69}$$

In a manner analogous to the third case, the expression of the functions G_4, G_5 render the viability of the fourth case solely within the BDLS theoretical framework.

The motivation for utilizing the Noether symmetries in the current study is illustrated by the four cases that have been outlined. The presence of additional terms in the Lagrangian within the Teleparallel analogue of Horndeski theory results in an expanded array of cosmological models, some of which are highly intricate by nature. An exploration of the dynamics of these complex cases can be effectively conducted through the application of Noether point symmetries serving as a valuable tool and criterion with the classification as the initial step towards further investigation.

4.4 | Conclusion

The Teleparallel analogue of Horndeski theory, also referred to as the BDLS [13] theory, presents a rich theoretical landscape that has the potential to enhance our understanding of cosmological models. In addition, the propagation speed constraint of the GW can be overcome in the BDLS theoretical framework. This result ensures that the BDLS theory provides an innovative approach for investigating the properties of gravitation and its implications on the cosmological mechanisms governing the evolution of the Universe. Considering that most of the higher-order and curvature-based theories can be transformed into an equivalent of the Horndeski model, BDLS theory offers the opportunity for even higher-order theories of gravity. This fact suggests that there is considerable potential for conducting a thorough investigation of a wide range of gravitational theories in the BDLS context.

Motivated by these reasons, the current chapter investigates the symmetries that emerge from the Noether approach. Noether's theorem focuses on the invariance of the calculus of variations when subjected to an infinitesimal transformation. This transformation is linked to a differential operator, referred to, in this context, as a Noether symmetry. Consequently, this theorem establishes a fundamental connection between symmetries and conservation laws providing insights into the underlying principles governing physical phenomena. When a Noether symmetry is identified, it leads to a simplification of the equations of motion of the system. As a result, this approach enhances the accessibility of precise solutions, which, otherwise, might be elusive.

The initial phase of the research involves the identification of the point-like Lagrangian by utilizing the maximally symmetric configuration of the flat FLRW metric. This process is further facilitated by the incorporation of a tetrad that aligns with the Weitzenböck gauge. Subsequently, the method of integration by parts is implemented to effectively eliminate the second-order derivative terms that are present in the expression of the Lagrangian. Nevertheless, during the course of this procedure, one of the components related to the G_3 term proves resistant to being removed through the integration by parts method. In order to overcome this complication it becomes necessary to implement the mathematical formula outlined in Eq.(4.11) and effectively navigate through the impediment to achieve the desired outcome.

After a rigorous process, the final form of the point-like Lagrangian was derived by removing all the second-order derivative terms. The methodology that guided the rest of the research is outlined in Sec.(4.2), introducing the first-order equation of motion resulting from Noether symmetry. The utilization of the Rund-Trautman identity to the point-like Lagrangian has led to significant advancements in the present research. This has culminated in the establishment of a system of 62 equations that pertain to the coefficients of the generator vector and the contributions G_i of the theory. As a result, a wide array of cases has emerged. Each of these cases corresponds to a distinct cosmological model which requires a thorough examination and detailed analysis to gain a complete understanding of its properties.

The magnitude of these cases is significant and the interested reader could refer to the collections of cases in the Tables of [62]. These Tables contain a detailed list of the solutions accompanied by the specific conditions that characterize each one of them.

Nevertheless, in the present chapter, only a selection of four of these cases is presented to showcase the effectiveness along with the practical benefits of the methodology under consideration. In each of these solutions, the functions within the theory and the coefficients of the generator vector were determined which are the critical components that contribute to the development and structure of a cosmological model in the BDLS context. After all, the primary objective of this extensive investigation is to demonstrate the prosperous relationship between the theoretical functions that characterize each cosmological model and the practical implementation of the Noether symmetry approach.

In conclusion, the extensive range of classification cases has brought to light a plethora of different cosmological models each possessing unique characteristics and properties. This diverse collection of models showcases captivating dynamics that require further thorough investigation within the field of cosmology.

5

Cosmological Perturbations in BDLS theory

The current chapter discusses the cosmological perturbations within the framework of BDLS theory, which serves as the teleparallel analogue of the Horndeski gravity. To thoroughly understand the evolution mechanisms of a cosmological model it is imperative to investigate its behaviour both in the background as well as at the perturbation level. While the curvature-based Horndeski gravity and its teleparallel analogue have been studied in the existing literature [77], [87], [13], [14], [88], [47],[101 [90], a more robust quantitative analysis necessitates a comprehensive understanding of their cosmological perturbations. Therefore, this chapter encompasses the tensor, vector, and scalar components in BDLS theory while presenting the corresponding alpha parametrization that illustrates potential deviations from the ΛCDM model thereby indicating a novel way for the exploration of gravitational theories while, at the same time, aligns with the existing observational context.

5.1 | Background Cosmological Equations

In the realm of gravitational theories, it is commonly accepted that the TEGR theory offers an alternative perspective on gravity by utilizing the torsion tensor rather than curvature. The analysis conducted in Chapter 2 demonstrated that, within this particular framework, it was possible to formulate the teleparallel analogue of Horndeski gravity - the BDLS theory [13]. In the same chapter, the investigation of the structure of the torsion tensor as well as its irreducible decomposition led to the emergence of a new array of scalar invariants characterizing the BDLS theory. Consequently, the severely constrained terms of the classical Horndeski can persist in the current scenario due to the introduction of the novel Lagrangian term, $\mathcal{L}_{tele}$.

Nevertheless, to address the various perplexing aspects of cosmology, it is crucial for any theory to undergo rigorous testing and assessments incorporating a wide range of cosmological data sources. The investigation of cosmological perturbations is a significant step in pursuing this objective. The homogeneous and isotropic FLRW model can effectively describe the average expansion and density distribution of the Universe on large scales. However, on smaller scales, the Cosmological Principle cannot interpret the complex distribution of matter and energy in the observed Universe. Examining the effects of small-scale inhomogeneous and anisotropic perturbations on the overall structure of the cosmos could provide insights into the underlying mechanisms that govern its evolution and behaviour [29], [100], [93], [37].

However, before investigating the cosmological perturbations, it is necessary first to establish the definition of the background and the field equations within the BDLS framework. This part of the study is crucial in order to accurately analyze and interpret the subsequent results related to perturbations. A homogeneous and isotropic FLRW model presents an appropriate option for this aim serving as the background solution with already known and straightforward properties. This particular choice of background enables the analysis and study of the increasing complexity of perturbations systematically. The motivation for this choice of background stems from the idea that selecting a specific set of coordinates in the inhomogeneous universe, which can then be defined by a FLRW model plus perturbations, entails establishing a correlation between spacetime points in the inhomogeneous universe and the homogeneous background. This correlation provides insights into the dynamics of the Universe and the mechanisms shaping its development.

For simplicity, the homogeneous and isotropic FLRW background would include a spatially flat sector as outlined in Eq.(3.2), and is

$$ds^2 = -N(t)^2 dt^2 + a(t)^2(dx^2 + dy^2 + dz^2) \tag{5.1}$$

According to that line element, the corresponding tetrad ansatz can be written in the following diagonal form :

$$e^a{}_\mu = \text{diag}(N(t), a(t), a(t), a(t)) \tag{5.2}$$

This choice of the tetrad is compatible with the Weitzenböck gauge [72], [138] which is defined in Sec.(2.1), and results in a vanishing spin connection.

The field equations that define the behaviour and properties of the flat, homogeneous and isotropic background can then be derived by varying the action obtained from Eq.(2.46) with respect to the dynamical variables of the system. These dynamical variables include the lapse function $N(t)$, the scale factor $a(t)$ and the scalar field $\phi(t)$ present in the theory [14], [13].

By varying the action with respect to the lapse function, the first field equation is

$$\mathcal{E}_{tele} + \sum_{i=2}^{5} \mathcal{E}_i = 0\,. \tag{5.3}$$

The analytical expressions of the $\mathcal{E}_i$ components are

$$\mathcal{E}_{tele} = 6H\dot{\phi}G_{tele,I_2} + 12H^2\, G_{tele,T} + 2X\, G_{tele,X} - G_{tele}\,, \tag{5.4}$$

$$\mathcal{E}_2 = 2X\, G_{2,X} - G_2\,, \tag{5.5}$$

$$\mathcal{E}_3 = 6X\dot{\phi}HG_{3,X} - 2X\, G_{3,\phi}\,, \tag{5.6}$$

$$\mathcal{E}_4 = -6H^2\, G_4 + 24H^2X(G_{4,X} + XG_{4,XX}) - 12HX\dot{\phi}\, G_{4,\phi X} - 6H\dot{\phi}\, G_{4,\phi}\,, \tag{5.7}$$

$$\mathcal{E}_5 = 2H^3\, X\dot{\phi}\,(5G_{5,X} + 2XG_{5,XX}) - 6H^2X\left(3G_{5,\phi} + 2XG_{5,\phi X}\right) \tag{5.8}$$

The term $\mathcal{L}_{tele}$ characterizing the BDLS theory and for the choice of a flat FLRW background, is expressed as

$$\mathcal{L}_{tele} = G_{tele}(\phi, X, T, I_2)\,, \tag{5.9}$$

The Hubble parameter is denoted as $H = \dot{a}/a$. The use of overdots represents derivatives with respect to cosmic time and commas denote partial derivatives with respect to the argument. In this background setting, the torsion scalar is defined as $T = 6H^2$ and $I_2 = 3H\dot{\phi}$ is the only surviving scalar irreducible. In addition, the kinetic term of the scalar field is $X = \frac{1}{2}\dot{\phi}^2$. It is important to note at this point that in the case of $G_{tele} = 0$, Eqs (5.5)-(5.8) become identical with the background equations of the classical Horndeski case as presented in [88].

In a similar way, when considering variations with respect to the scale factor, the second field equation can be derived. This equation is outlined as

$$\mathcal{P}_{tele} + \sum_{i=2}^{5} \mathcal{P}_i = 0\,. \tag{5.10}$$

The $\mathcal{P}_i$ components have the following expressions :

$$\mathcal{P}_{tele} = -3H\dot{\phi}G_{tele,I_2} - 12H^2G_{tele,T} - \frac{d}{dt}\Big(4HG_{tele,T} + \dot{\phi}\,G_{tele,I_2}\Big) + G_{tele}\,, \tag{5.11}$$

$$\mathcal{P}_2 = G_2\,, \tag{5.12}$$

$$\mathcal{P}_3 = -2X\left(G_{3,\phi} + \ddot{\phi}G_{3,X}\right)\,, \tag{5.13}$$

$$\begin{aligned}\mathcal{P}_4 = {} & 2\left(3H^2 + 2\dot{H}\right)G_4 - 12H^2XG_{4,X} - 4H\dot{X}G_{4,X} - 8\dot{H}XG_{4,X} \\ & - 8HX\dot{X}G_{4,XX} + 2\left(\ddot{\phi} + 2H\dot{\phi}\right)G_{4,\phi} + 4XG_{4,\phi\phi} \\ & + 4X\left(\ddot{\phi} - 2H\dot{\phi}\right)G_{4,\phi X}\,,\end{aligned} \tag{5.14}$$

$$\begin{aligned}\mathcal{P}_5 = {} & -2X\left(2H^3\dot{\phi} + 2H\dot{H}\dot{\phi} + 3H^2\ddot{\phi}\right)G_{5,X} - 4H^2X^2\ddot{\phi}G_{5,XX} \\ & + 4HX\left(\dot{X} - HX\right)G_{5,\phi X} + 2\left[2\frac{d}{dt}(HX) + 3H^2X\right]G_{5,\phi} + 4HX\dot{\phi}G_{5,\phi\phi}\end{aligned} \tag{5.15}$$

Finally, varying the action with respect to the scalar field results in the third field equation, the modified Klein-Gordon equation, which is expressed as

$$\frac{1}{a^3}\frac{d}{dt}\left[a^3(J + J_{tele})\right] = P_\phi + P_{tele} \tag{5.16}$$

This last background equation showcases the terms of the standard Horndeski theory denoted as J and P_ϕ, originating from the Lagrangian terms $\mathcal{L}_i$, with $i = 2,3,4,5$. On the other hand, the terms J_{tele} and P_{tele} are solely connected with the BDLS theory.

The J and P_ϕ terms are defined as follows [13], [88] :

$$J = \dot{\phi}\, G_{2,X} + 6HXG_{3,X} - 2\dot{\phi}\, G_{3,\phi} + 6H^2\dot{\phi}\, \left(G_{4,X} + 2XG_{4,XX}\right) - 12HXG_{4,\phi X}$$

$$+ 2H^3X\left(3G_{5,X} + 2XG_{5,XX}\right) - 6H^2\dot{\phi}\, \left(G_{5,\phi} + XG_{5,\phi X}\right) , \tag{5.17}$$

$$P_\phi = G_{2,\phi} - 2X\left(G_{3,\phi\phi} + \ddot{\phi}G_{3,\phi X}\right) + 6\left(2H^2 + \dot{H}\right) G_{4,\phi}$$

$$+ 6H\left(\dot{X} + 2HX\right) G_{4,\phi X} - 6H^2X\, G_{5,\phi\phi} + 2H^3X\dot{\phi}\, G_{5,\phi X} , \tag{5.18}$$

The new terms introduced in the BDLS theory have the expressions :

$$J_{tele} = \dot{\phi}\, G_{tele,X} , \tag{5.19}$$

$$P_{tele} = -9H^2\, G_{tele,I_2} + G_{tele,\phi} - 3\,\frac{d}{dt}\left(HG_{tele,I_2}\right) . \tag{5.20}$$

It is important to highlight, as indicated in Eq.(5.9), that the novel term, G_{tele} is independent of the contributions of T_{ax} and T_{ten}. This outcome stems directly from the choice to designate the background as a maximally symmetric and flat FLRW spacetime, resulting in the nullification of both T_{ax} and T_{ten} in this particular setup. However, when examining perturbations, the factors contributing to the G_{tele} term are expected to be diverse, potentially encompassing a significant array of scalars and irreducibles. This additional information in G_{tele} could pave the way for further investigation of models present in the BDLS framework potentially leading to a deeper understanding of which models align best with observations.

5.2 | Cosmological Perturbations

At present, a wide range of observational methods is used by the scientific community to investigate the large-scale structure of the Universe. Among these methods, the CMB stands out as an observational window that has provided valuable data concerning the early stages of the cosmos. By detecting the anisotropies in the CMB across different angular scales, researchers have gained valuable insights into the state of the Universe at the time of recombination. Additionally, the large-scale galaxy redshift surveys have a crucial role in expanding our knowledge about luminous objects which in turn reveals the distribution of mass in the present time.

Furthermore, investigations on the spectra of quasar absorption lines and also on weak gravitational lensing are opening new aspects of research by providing additional information on the distribution of matter. These analyses are particularly significant as they offer insights into the spreading of matter independent of its ability to emit light, thereby addressing the biasing issue. The exploration of weak gravitational lensing is not only limited to the baryonic form of matter, but it extends to dark matter, providing a promising method to determine its concentration in the Universe with accuracy.

As a result, it is reasonable to acknowledge that the expansion of the FLRW background metric will eventually incorporate components capturing the intricate distribution of matter and energy in the observed Universe, characterized by the presence of clusters and superclusters of galaxies and stars across various scales. To address this issue, it is important to consider the spatial inhomogeneity and anisotropy. Following that reasoning, the method of perturbations must be employed which will have as a starting point the spatially homogeneous and isotropic FLRW model with straightforward characteristics [19], [100].

The concept of cosmological perturbations has emerged as one of the fundamental components of quantitative cosmology. It provides the theoretical basis for establishing the connection between theories of the early Universe, such as the inflation paradigm which profiles the causal structure for the emergence of fluctuations, and the extensive array of up-to-date observational data about the complexity of cosmic structure. In the perturbation analysis, the variables are defined by a homogeneous background component which depends solely on the cosmic time and a perturbative component which is reliant on spacetime [103], [25]. The analysis of linear perturbation on a spatially flat FLRW background concerning the classical Horndeski theory was conducted in [88].

In the current chapter, the objective is to determine the appropriate configuration of the tetrad matrix before proceeding to the calculation of the action for tensor, vector and scalar perturbations. Additionally, it aims to establish the full perturbative approach in the context of metric inherited perturbations. The analysis of the perturbations is conducted by implementing the unitary gauge where the scalar field perturbations vanish, $\delta\phi = 0$. Furthermore, the investigation extends up to the second-order perturbative level, which is essential in verifying the non-existence of ghosts or gradient instabilities according to the theoretical conditions.

The expansion of the metric, up to first order, is represented by

$$g_{\mu\nu} = \bar{g}_{\mu\nu} + \delta g_{\mu\nu} \tag{5.21}$$

In Eq.(5.21), $\bar{g}_{\mu\nu}$ represents the selection of the flat FLRW spacetime. The term $\delta g_{\mu\nu}$ identifies the metric perturbation defined as

$$\delta g_{\mu\nu} \rightarrow \begin{pmatrix} -2\alpha & aB_i + a^2\partial_i\beta \\ aB_i + a^2\partial_i\beta & 2a^2\left[\zeta\delta_{ij} + \frac{1}{2}h_{ij} + 2\partial_{(i}h_{j)}\right] \end{pmatrix} \tag{5.22}$$

The composing vector fields in Eq.(5.22), $B_i = b_i + \beta_i$ and h_j, are defined by being divergence-free (solenoidal), meaning that $\partial_i X^i = 0$, leading to two DoF for each vector. The scalar contributions α, β and ζ have one DoF each. The α component represents the perturbation of the lapse function, the β component describes the shift vector and the ζ identifies the spatial curvature perturbation. Scalar perturbations can be formed from a scalar or its derivatives. Any 3-vector, such as $\partial_i X$, which is constructed from the scalar is curl-free (longitudinal), $X_{,[ij]} = 0$. The terminology used as scalar or vector perturbations reflects their transformation behaviour under spatial translations [19]. Finally, the tensor contribution h_{ij} is both divergence-free, $h^j_{ij,} = 0$ and traceless with $h_{ij}\delta^{ij} = 0$ resulting in two DoF. Physically the tensor mode represents the gravitational radiation. The two DoF correspond to the two polarizations present in a GW. It must be noted that the terms "divergence-free" or "curl-free" are defined with respect to the flat spacetime metric since perturbations are specified with respect to the FLRW background.

The perturbation of the tetrad is summarized in the subsequent form :

$$e^A{}_\mu = \bar{e}^A{}_\mu + \delta e^A{}_\mu \tag{5.23}$$

Here, the tetrad denoted as $\bar{e}^A{}_\mu = \mathrm{diag}(N, a, a, a)$ corresponds to the spatially flat FLRW background, while the perturbed component of the tetrad, $\delta e^A{}_\mu$, is defined as

$$\delta e^A{}_\mu \to \begin{pmatrix} \alpha & -a\beta_i \\ \delta^I_i(\partial^i\beta + b^i) & a\delta^{Ii}\left[\zeta\delta_{ij} + \frac{1}{2}h_{ij} + \frac{1}{8}h_{ik}h_{kj} + 2\partial_{(i}h_{j)}\right] \end{pmatrix} \tag{5.24}$$

The uppercase Latin indices correspond to the Lorentz spacetime components while the lowercase Latin indices pertain to the three-dimensional spatial part of the spacetime.

5.2.1 | Tensor Perturbations

A critical characteristic regarding the three types of perturbations is their ability to decouple. This means that each type of perturbation progresses separately and independently from the others [117 [103], [128]. Consequently, to study the tensor perturbations described in Eq.(5.24), it is necessary to assign zero values to both the scalar and vector components. Tensor perturbations are described by $h_+(t,x,y,z)$ and $h_\times(t,x,y,z)$, two functions that are assumed to have small values [137]. These independent of each other functions obey the same equations of motion and are the components of the symmetric tensor $\mathcal{H}_{ij}$ which is both traceless and divergence-free.

One effective method to streamline the following analysis is to limit the tensor perturbations only to the $x-y$ plane. This involves aligning the $z-$axis with the direction of the wavevector $\vec{k}$ resulting in $\hat{k}=z$.

By setting the vector and scalar perturbative components all to zero, the tetrad of Eq.(5.23) takes the following form :

$$e^A{}_\mu \rightarrow \begin{pmatrix} 1 & 0 & 0 & 0 \\ 0 & -a-\frac{1}{2}ah_+-\frac{1}{8}a\left(h_+^2+h_\times^2\right) & -\frac{1}{2}ah_\times & 0 \\ 0 & -\frac{1}{2}ah_\times & -a+\frac{1}{2}ah_+-\frac{1}{8}a\left(h_+^2+h_\times^2\right), & 0 \\ 0 & 0 & 0 & a \end{pmatrix} \tag{5.25}$$

In this configuration, the metric takes on a specific form as outlined below :

$$g_{\mu\nu} = -N^2 dt^2 + a^2(\delta_{ij} + h_{ij})dx^i dx^j \,, \tag{5.26}$$

where the background value of the lapse function is considered to be unity.

The next phase for the investigation of tensor perturbations within the BDLS theory, is the calculation of the scalar invariants associated with the decomposition of the torsion tensor as well as the quadratic contractions of the torsion tensor with the scalar field which are both outlined in Chapter 2.

According to Eqs.(2.13)-(2.15), the related scalars are

$$T_{\rm ax} = \quad 0 \,, \tag{5.27}$$

$$T_{\rm vec} = -\frac{9\dot{a}^2}{a^2} \,, \tag{5.28}$$

$$T_{\rm ten} = \frac{3}{4a^2}\left[\,(\boldsymbol{\nabla} h_+)^2 + (\boldsymbol{\nabla} h_\times)^2 - a^2\dot{h}_+^2 - a^2\dot{h}_\times^2\,\right] . \tag{5.29}$$

In the case of tensor perturbations, the complete set of the quadratic contractions involving the torsion tensor and the scalar field, as described in Eqs.(2.31)-(2.40), results in the following list of scalars :

$$I_2 = \frac{3\dot{a}\dot{\phi}}{a}, \tag{5.30}$$

$$J_5 = \frac{\dot{\phi}^2}{8}(\,\dot{h}_+^2 + \dot{h}_\times^2\,), \tag{5.31}$$

$$J_8 = \frac{\dot{\phi}^2}{2}(\,\dot{h}_+^2 + \dot{h}_\times^2\,), \tag{5.32}$$

$$J_1 = J_3 = J_6 = J_{10} = 0. \tag{5.33}$$

The quadratic action of Eq.(2.46) in the case of tensor perturbations takes under consideration all the scalar contributions as well as the selection of the tetrad matrix and results in the following form :

$$S_{\mathrm{T}}^{(2)} = \int d^4x \, \frac{a^3}{4} \left[\mathcal{G}_T \, \dot{h}_{ij}^2 - \frac{\mathcal{F}_T}{a^2} \, (\nabla h_{ij})^2 \right] . \tag{5.34}$$

The quadratic action of Eq.(5.34) showcases the propagation of tensor perturbations in a flat FLRW background. Moreover, the entities $\mathcal{G}_T$ and $\mathcal{F}_T$ are explicitly defined as

$$\mathcal{G}_T = 2 \left(G_4 - 2XG_{4,X} + XG_{5,\phi} - HX\dot{\phi}G_{5,X} + 2XG_{tele,J_8} + \frac{X}{2}G_{tele,J_5} - G_{tele,T} \right) \tag{5.35}$$

$$\mathcal{F}_T = 2 \left(G_4 - XG_{5,\phi} - X\ddot{\phi}G_{5,X} - G_{tele,T} \right) . \tag{5.36}$$

The expressions in the Eqs.(5.35), (5.36) involve $G_{i,A}$ terms which represent the derivative of G_i with respect to the quantity A. At this point, it is interesting to note that in the case of $G_{tele} = 0$ then the results of classical Horndeski theory are obtained, which are in agreement with the results of [88].

After varying the action of Eq.(5.34), the propagation equation of GW can be derived, [14], [15]. More precisely, the squared sound speed of GW is given by

$$c_T^2 = \frac{\mathcal{F}_T}{\mathcal{G}_T} \tag{5.37}$$

From Eq.(5.34) describing the quadratic action, it is obvious that the ghost and gradient instabilities in tensor perturbations could be prevented as long as,

$$\mathcal{F}_T > 0 \quad \text{and} \quad \mathcal{G}_T > 0 \, . \tag{5.38}$$

It is important to mention that the value of c_T^2 does not equal unity when considering a random selection of the G_i terms.

5.2.2 | Vector Perturbations

The divergence-free vector perturbations represent a significant component of the DoF in cosmological perturbation theory. In the absence of any anisotropic stress, these perturbations typically experience a rapid decay in an expanding universe. The upcoming paragraphs encompass a comprehensive examination of vector perturbations within the BDLS framework. Their behaviour is anticipated to not deviate from their typical evolutionary pattern as time progresses.

To investigate the vector perturbations the scalar contributions α, β, ζ along with the tensor contributions h_{ij} must be all adjusted to zero. The corresponding tetrad matrix is expressed as

$$e^A{}_\mu \to \begin{pmatrix} 1 & -a\beta_i \\ \delta^I_i b^i & a\delta^{Ii}\left[\delta_{ij} + 2\partial_{(i}h_{j)}\right] \end{pmatrix} \tag{5.39}$$

Considering the decomposition of the torsion tensor, the scalar invariants for the case of vector perturbations are formulated below :

$$T_{\rm ax} = \frac{1}{9a^2}\left[\boldsymbol{\nabla} \times (\boldsymbol{\beta} - \boldsymbol{b})\right]^2, \tag{5.40}$$

$$T_{\rm vec} = -\frac{9\dot{a}^2}{a^2} + \frac{1}{a^2}\Big\{ 9\dot{a}^2\left(2\boldsymbol{b}\boldsymbol{\beta} + \boldsymbol{\beta}^2\right) - 6\dot{a}a\left[\boldsymbol{b}\dot{\boldsymbol{\beta}} - 2(\boldsymbol{\nabla}\times\boldsymbol{h})(\boldsymbol{\nabla}\times\dot{\boldsymbol{h}})\right] - \tag{5.41}$$

$$- 6\dot{a}(\boldsymbol{\nabla}\times\boldsymbol{b})(\boldsymbol{\nabla}\times\boldsymbol{h}) - 6\dot{a}(\boldsymbol{b}+\boldsymbol{\beta})\left(\boldsymbol{\nabla}^2\boldsymbol{h} - a\dot{\boldsymbol{\beta}}\right) + \left(\boldsymbol{\nabla}^2\boldsymbol{h} - a\dot{\boldsymbol{\beta}}\right)^2\Big\},$$

$$T_{\rm ten} = -\frac{1}{a^2}\left[a^2\dot{\boldsymbol{\beta}}^2 - (\boldsymbol{\nabla}\times\boldsymbol{b})^2 - (\boldsymbol{\nabla}\times\boldsymbol{b})(\boldsymbol{\nabla}\times\boldsymbol{\beta}) - (\boldsymbol{\nabla}\times\boldsymbol{\beta})^2\right] \tag{5.42}$$

$$-\frac{1}{a^2}\left[3a(\boldsymbol{\nabla}\times\dot{\boldsymbol{h}})(\boldsymbol{b}-a\boldsymbol{h}) + a\dot{\boldsymbol{\beta}}\boldsymbol{\nabla}^2\boldsymbol{h} + (\nabla^2\boldsymbol{h})^2\right]\ .$$

The following step is the calculation of the contractions of the torsion tensor with the scalar field of the theory. This process involves using Eqs.(2.31)-(2.40) to identify and evaluate these contractions. The contractions that need to be taken into account include the following :

$$I_2 = \frac{3\dot{a}\dot{\phi}}{a} + \frac{1}{a}\Big\{\dot{\phi}\left[-3\dot{a}\left(2\boldsymbol{b}\boldsymbol{\beta}+\boldsymbol{\beta}^2\right) + a\big(\boldsymbol{b}\dot{\boldsymbol{\beta}} - 2(\boldsymbol{\nabla}\times\boldsymbol{h})(\boldsymbol{\nabla}\times\dot{\boldsymbol{h}})\big)\right] + \tag{5.43}$$

$$+\frac{1}{a}\left[(\dot{\phi}\boldsymbol{\nabla}\times\boldsymbol{b})(\boldsymbol{\nabla}\times\boldsymbol{h})\right] + \frac{1}{a}\Big\{\dot{\phi}(\boldsymbol{b}+\boldsymbol{\beta})\left(\boldsymbol{\nabla}^2\boldsymbol{h} - a\dot{\boldsymbol{\beta}}\right)\Big\},$$

$$J_3 = \frac{1}{6a^2}\Big\{\dot{\phi}^2\left[2a^2\dot{\boldsymbol{\beta}}^2 - (\boldsymbol{\nabla}^2\boldsymbol{h})^2 - a\dot{\boldsymbol{\beta}}\boldsymbol{\nabla}^2\boldsymbol{h}\right]\Big\}, \tag{5.44}$$

$$J_5 = \frac{1}{4a^2}\left\{\dot{\phi}^2\left[\boldsymbol{\nabla}^2\times(-a\dot{\boldsymbol{h}}+\boldsymbol{b}+\boldsymbol{\beta})\right]^2 + \dot{\phi}^2\left(a\boldsymbol{\nabla}\times\dot{\boldsymbol{h}} + \boldsymbol{\nabla}\times\boldsymbol{\beta}\right)^2\right\} - \tag{5.45}$$

$$-\frac{1}{4a^2}\frac{5\dot{\phi}^2\left(2a\dot{\boldsymbol{\beta}}+\Delta\boldsymbol{h}\right)^2}{9},$$

$$J_6 = \frac{1}{36a^2}\left[\dot{\phi}^4\left(2a\dot{\boldsymbol{\beta}}+\boldsymbol{\nabla}^2\boldsymbol{h}\right)^2\right], \tag{5.46}$$

$$J_8 = \frac{1}{2a^2}\left[\dot{\phi}^2\left(2a\boldsymbol{\nabla}\times\dot{\boldsymbol{h}} - \boldsymbol{\nabla}\times\boldsymbol{b}\right)^2 - \frac{\dot{\phi}^2\left(2a\dot{\boldsymbol{\beta}}+\Delta\boldsymbol{h}\right)^2}{9}\right], \tag{5.47}$$

$$J_{10} = \frac{\dot{\phi}^2}{6a^2}\Big[(\nabla \times \boldsymbol{b})(\nabla \times \boldsymbol{\beta}) + (\nabla \times \boldsymbol{b})^2 - 2(\nabla \times \boldsymbol{\beta})^2\Big], \tag{5.48}$$

$$J_1 = 0. \tag{5.49}$$

The expansion of the action to incorporate terms up to quadratic order when concerning the vector perturbations is outlined below :

$$S_V^{(2)} = \int dtd^3xa^3\Bigg[\frac{A_1}{a^2}(\nabla^2\boldsymbol{h})^2 + A_2\dot{\boldsymbol{\beta}}^2 + A_3(\nabla\times\dot{\boldsymbol{h}})^2 - \frac{A_3}{a}(\nabla\times\dot{\boldsymbol{h}})(\nabla\times\boldsymbol{b}) + \tag{5.50}$$

$$+\frac{A_4}{a^2}(\nabla\times\boldsymbol{b})^2 + \frac{A_5}{a^2}(\nabla\times\boldsymbol{\beta})^2 + \frac{A_6}{a}(\nabla\times\boldsymbol{h})(\nabla\times\boldsymbol{\beta}) + \frac{A_7}{a}(\nabla\times\boldsymbol{h})(\nabla\times\dot{\boldsymbol{\beta}}) +$$

$$+\frac{A_8}{a^2}(\nabla\times\boldsymbol{\beta})(\nabla\times\boldsymbol{b})\Bigg]$$

Each of the A_i entities present in Eq.(5.50) corresponds to a specific aspect of the action, and contributes to the overall result. Their analytical expressions are

$$A_1 := \frac{X}{18}\left(2XG_{tele,J_6} - 6G_{tele,J_3} - 5G_{\text{tele},J_5} - 2G_{tele}, J_8\right) + G_{tele,T_{vec}} \tag{5.51}$$

$$A_2 := \frac{2X}{9}\left(2XG_{tele,J_6} + 3G_{tele,J_3} - 5G_{tele,J_5} - 2G_{tele,J_8}\right) + G_{tele,T_{vec}} \tag{5.52}$$

$$A_3 := X\left(-4G_{4,X} - 2G_{5,X}H\dot{\phi} + 2G_{5,\phi} + G_{tele,J_5} + 4G_{tele,J_8}\right) + 2\left(G_4 - G_{tele,T}\right) \tag{5.53}$$

$$A_4 := \frac{a}{18}\left[3X\left(-6G_{4X} - 3G_{5X}H\dot{\phi} + 3G_{5\phi} + 3G_{tele,J5} + 6G_{tele,J8} + 2G_{tele,J10}\right)\right] + \tag{5.54}$$

$$+\frac{a}{18}\left[9G_4 - 9G_{tele,T} + 2G_{tele,T_{ax}}\right]$$

$$A_5 := \frac{X}{2}\left(-2G_{4,X} - G_{5,X}H\dot{\phi} + G_{5,\phi} + 2G_{tele,J_5}\right) + \frac{1}{2}G_4 - \frac{1}{2}G_{tele,T} + \tag{5.55}$$

$$+\frac{1}{9}G_{tele,T_{ax}} - \frac{2X}{3}G_{tele,J_{10}}$$

$$A_6 := -2\frac{d}{dt}(2XG_{4X} - XG_{5\phi} - G_4) - 2\dot{\phi}XG_{5,X}\dot{H} - \dot{\phi}G_{tele,I_2} - 4XG_{5.X}H^2\dot{\phi} - \tag{5.56}$$

$$H\left\{2X\left[4G_{4,X} + (2XG_{5,XX} + 3G_{5,X})\,\ddot{\phi} + 2XG_{5,\phi X} - 2G_{5,\phi}\right] - 4G_4 + 4G_{tele,T} - 6G_{tele,T_{vec}}\right\}$$

$$A_7 := \frac{X}{9}\left(-36G_{4,X} - 18G_{5,X}H\dot{\phi} + 18G_{5,\phi} - 4XG_{tele,J_6} + 3G_{tele,J_3}\right) + \tag{5.57}$$

$$\frac{X}{9}\left(10G_{tele,J_5} + 4G_{tele,J_8}\right) + 2\left(G_4 - G_{tele,T} + G_{tele,T_{vec}}\right)$$

$$A_8 := X\left(-2G_{4,X} - G_{5,X}H\dot{\phi} + G_{5,\phi} + G_{tele,J_5}\right) + G_4 - G_{tele,T} - \frac{2}{9}G_{tele,T_{ax}} \tag{5.58}$$

$$+\frac{X}{3}G_{\mathrm{tele},J_{10}}$$

The expressions provided for the components of the quadratic action are obviously quite complex and detailed. Nonetheless, the coefficients associated with the quantities $\boldsymbol{\beta}^2$, $\boldsymbol{\beta b}$ and $\boldsymbol{\nabla} \times \boldsymbol{h}$ become zero as a result of employing the background equations leading to a considerable reduction of the complexity.

By integrating this result with the conditions of $A_1 = 0$ and $A_3 = 0$, we can determine a single dynamical variable $\boldsymbol{\beta}$ along with two auxiliary fields $\boldsymbol{h}$ and $\boldsymbol{b}$.

When varying the second-order action of Eq.(5.50) with respect to these two auxiliary fields $\boldsymbol{h}$ and $\boldsymbol{b}$, we can establish the following set of constraint equations :

$$2\frac{A_4}{a^2}\left(\boldsymbol{\nabla}\times\boldsymbol{b}\right)+\frac{A_8}{a^2}\left(\boldsymbol{\nabla}\times\boldsymbol{\beta}\right)=0 \tag{5.59}$$

$$\frac{A_6}{a}\left(\boldsymbol{\nabla}\times\boldsymbol{\beta}\right)+\frac{A_7}{a}\left(\boldsymbol{\nabla}\times\dot{\boldsymbol{\beta}}\right)=0 \tag{5.60}$$

Employing the results of Eqs.(5.59)-(5.60) in Eq.(5.50), the final form of the quadratic action for vector perturbations can be expressed as

$$S_{\mathrm{V}}^{(2)}=\int dtd^3xa^3\left[\mathcal{G}_V\dot{\boldsymbol{\beta}}^2-\frac{\mathcal{F}_V}{a^2}\left(\boldsymbol{\nabla}\times\boldsymbol{\beta}\right)^2\right]. \tag{5.61}$$

The coefficients present in Eq.(5.61) are explicitly defined below :

$$\mathcal{G}_V=A_2 \quad \text{and} \quad \mathcal{F}_V=\frac{A_8^2}{4A_4}-A_5. \tag{5.62}$$

It is evident from Eq.(5.61) that the ghost and gradient instabilities in the case of vector perturbations can be avoided if the following conditions hold :

$$\mathcal{F}_V>0, \quad \text{and} \quad \mathcal{G}_V>0. \tag{5.63}$$

As in the classical Horndeski theory, vector perturbations in BDLS context seem to have minimal influence on the various eras during the evolution of the Universe, and in general, do not significantly affect cosmological phenomena following the period of inflation [98], [101].

5.2.3 | Scalar Perturbations

Unlike vector and tensor perturbations which do not produce density perturbations and therefore do not contribute to the formation of structure, scalar perturbations are coupled to the matter perturbations. This characteristic coupling between the scalar modes and matter has a crucial role in the evolution and development of the large-scale structure in the Universe.

To proceed with the analysis of scalar perturbations, it is necessary to assign zero values to the quantities b_i, β_i, h_i vectors and to the h_{ij} tensor. The tetrad that characterizes this type of perturbation has the following form :

$$e^{A}{}_{\mu} \rightarrow \begin{pmatrix} 1+\alpha & 0 \\ a\delta^I_i \partial^i \beta & a\delta^I_i (1+\zeta) \end{pmatrix} \tag{5.64}$$

In the case of scalar perturbations, the expressions of the axial, vectorial and tensorial components of the torsion tensor are :

$$T_{\text{ax}} = 0 \tag{5.65}$$

$$T_{\text{vec}} = -\frac{9\dot{a}^2}{a^2} + \frac{6\dot{a}}{a^2}\left[3\dot{a}\alpha + a(\nabla^2\beta - 3\dot{\zeta})\right] + \frac{1}{a^2}\Big\{ -27\alpha^2\dot{a}^2 + 6\,a\dot{a}\,(3\nabla\beta\,\nabla\zeta) - \tag{5.66}$$

$$6\,a\dot{a}\left(2\alpha(\nabla^2\beta - 3\,\dot{\zeta})\right) + \left[(2\nabla\zeta + \nabla\alpha)^2 - a^2(\nabla^2\beta - 3\dot{\zeta})^2 \right] \Big\}$$

$$T_{\text{ten}} = \left[\frac{(\boldsymbol{\nabla}\zeta - \boldsymbol{\nabla}\alpha)^2}{a^2} - (\boldsymbol{\nabla}^2\beta)^2 \right] \tag{5.67}$$

The following step in the procedure is to employ Eq.(2.31)-Eq.(2.40) in order to calculate the contractions of the torsion tensor with the scalar field. These contractions, in the case of scalar perturbations, include the following :

$$I_2 = \frac{3\dot{a}\dot{\phi}}{a} - \frac{\dot{\phi}}{a} \left[6\alpha\dot{a} + a(\boldsymbol{\nabla}^2\beta - 3\dot{\zeta}) - 9\alpha^2\dot{a} - 2a\alpha(\boldsymbol{\nabla}^2\beta - 3\dot{\zeta}) + 3a\boldsymbol{\nabla}\beta\boldsymbol{\nabla}\zeta \right] \tag{5.68}$$

$$J_3 = \frac{\dot{\phi}^2}{3a^2} \left[(\boldsymbol{\nabla}\alpha)^2 + \boldsymbol{\nabla}\zeta\, \boldsymbol{\nabla}\alpha - 2\,(\boldsymbol{\nabla}\zeta)^2 \right] \tag{5.69}$$

$$J_5 = \frac{\dot{\phi}^2}{18a^2} \left[3a^2\,(\boldsymbol{\nabla}^2\beta)^2 - 10\,(\boldsymbol{\nabla}\zeta - \boldsymbol{\nabla}\alpha)^2 \right] \tag{5.70}$$

$$J_6 = \frac{\dot{\phi}^4}{9a^2}\,(\boldsymbol{\nabla}\alpha - \boldsymbol{\nabla}\zeta\,)^2 \tag{5.71}$$

$$J_8 = \frac{2\dot{\phi}^2}{9a^2} \left[3a^2\,(\boldsymbol{\nabla}^2\beta)^2 - (\boldsymbol{\nabla}\zeta - \boldsymbol{\nabla}\alpha)^2 \right] \tag{5.72}$$

$$J_1 = J_8 = J_{10} = 0. \tag{5.73}$$

The calculation of the action for the case of scalar perturbations involves inserting the perturbed tetrad of Eq. (5.64) into the action of Eq.(2.46). After being expanded up to the second order, the coefficients of ζ^2 and $\alpha\zeta$ could be set equal to zero according to the background equations of Sec.(5.1).

Considering all that, the quadratic action for the case of scalar perturbations acquires the particular form :

$$S_{\mathrm{S}}^{(2)} = \int dtd^3xa^3\Bigg[-3\mathcal{A}\dot{\zeta}^2 + \frac{\mathcal{B}}{a^2}(\boldsymbol{\nabla}\zeta)^2 + \Sigma\alpha^2 - 2\Theta\alpha\boldsymbol{\nabla}^2\beta + 2\mathcal{A}\dot{\zeta}\boldsymbol{\nabla}^2\beta + \tag{5.74}$$

$$+ 6\Theta\alpha\dot{\zeta} - 2\mathcal{C}\alpha\frac{\boldsymbol{\nabla}^2}{a^2}\zeta\Bigg]$$

The coefficients that are present in Eq.(5.74) represent distinct components of the action each playing a crucial role in determining the final result. The specific mathematical formulae of these coefficients are provided below :

$$\mathcal{A} := 2\Big[G_4 - 2XG_{4,X} + XG_{5,\phi} - G_{tele,T} + \frac{3}{2}(G_{tele,T_{vec}} - XG_{tele,I_2I_2}) - \tag{5.75}$$

$$3H^2(4G_{tele,TT} - 12G_{tele,TT_{vec}} + 9G_{tele,T_{vec}T_{vec}}) - H(XG_{5,X} + 6G_{tele,TI_2} - 9G_{tele,T_{vec}I_2})\dot{\phi}\Big]$$

$$\mathcal{B} := \frac{2}{9}\Big(9G_4 - 9XG_{5,\phi} - 6XG_{tele,J_3} - 5XG_{tele,J_5} + 2X^2G_{tele,J_6} - 2XG_{tele,J_8} - \tag{5.76}$$

$$9G_{tele,T} + 18G_{tele,T_{vec}} - 9XG_{5,X}\ddot{\phi}\Big)$$

$$\Sigma := X\left(G_{tele,X} + 2XG_{tele,XX} + 2XG_{2,XX} + G_{2,X} - 2XG_{3,\phi X} - 2G_{3,\phi}\right) + \tag{5.77}$$

$$3H\dot{\phi}\big(4XG_{tele,XI_2} + G_{tele,I_2} + 2X^2G_{3,XX} + 4XG_{3,X} - 4X^2G_{4,\phi XX} - 10XG_{4,\phi X} - 2G_{4,\phi}\big) +$$

$$3H^2\big(12XG_{tele,I_2I_2} + 8XG_{tele,XT} + 2G_{tele,T} - 2G_4 - 3G_{tele,T_{vec}} + 8X^3G_{4,XXX} +$$

$$32X^2G_{4,XX} + 14XG_{4,X} - 12XG_{tele,XT_{vec}} - 4X^3G_{5,\phi XX} - 18X^2G_{5,\phi X} - 12XG_{5,\phi}\big) +$$

$$2H^3\dot{\phi}\left(36G_{tele,TI_2} - 54G_{tele,T_{vec}I_2} + 2X^3G_{5,XXX} + 13X^2G_{5,XX} + 15XG_{5,X}\right) +$$

$$18H^4\left(-12G_{tele,TT_{vec}} + 4G_{tele,TT} + 9G_{tele,T_{vec}T_{vec}}\right)$$

$$\Theta := -6H^3(4G_{tele,TT} - 12G_{tele,TT_{vec}} + 9G_{tele,T_{vec}T_{vec}}) + H(2G_4 - 8XG_{4,X} - \tag{5.78}$$

$$8X^2G_{4,XX}+6XG_{5,\phi}+4X^2G_{5,\phi X}-2G_{\text{tele},T}+3G_{tele,T_{vec}}-6XG_{tele,I_2I_2}-$$

$$4XG_{tele,XT}+6XG_{tele,XT_{vec}})-H^2(5XG_{5,X}+2X^2G_{5,XX}+18G_{tele,TI_2}-27G_{tele,T_{vec}I_2})\dot{\phi}-$$

$$(XG_{3,X}-G_{4,\phi}-2XG_{4,\phi X}+\frac{1}{2}G_{tele,I_2}+XG_{tele,XI_2})\dot{\phi}$$

$$\mathcal{C}:=2\big(G_4-2XG_{4,X}+XG_{5,\phi}-HXG_{5,X}\dot{\phi}-G_{tele,T}+G_{tele,T_{vec}}\big)+$$

$$\frac{X}{9}(3G_{tele,J_3}+10G_{tele,J_5}-4XG_{tele,J_6}+4G_{tele,J_8}) \tag{5.79}$$

As in the tensor perturbations case, by eliminating the term of G_{tele} in the above equations, the results of classical Horndeski theory can be obtained which are in agreement with the perturbation results of [88].

By varying the action of Eq.(5.74) with respect to α and β, the following constraint equations can be derived, which are

$$\Sigma\alpha-\Theta\boldsymbol{\nabla}^2\beta+3\Theta\dot{\zeta}-\mathcal{C}\frac{\boldsymbol{\nabla}^2}{a^2}\zeta=0 \tag{5.80}$$

$$\Theta\alpha-\mathcal{A}\dot{\zeta}=0 \tag{5.81}$$

Inserting the constraints of Eqs.(5.80), (5.81) into the action, Eq.(5.74), the final form of the quadratic action for scalar perturbations is

$$S_{\mathrm{S}}^{(2)}=\int dtd^3xa^3\left[\mathcal{G}_{\mathcal{S}}\dot{\zeta}^2-\frac{\mathcal{F}_{\mathcal{S}}}{a^2}(\boldsymbol{\nabla}\zeta)^2\right]. \tag{5.82}$$

The new variables introduced in the action described by Eq.(5.82) are defined as

$$\mathcal{G}_{\mathcal{S}}=3\mathcal{A}+\frac{\Sigma\mathcal{A}^2}{\Theta^2}, \tag{5.83}$$

$$\mathcal{F}_{\mathcal{S}}=\frac{1}{a}\frac{d}{dt}\left(\frac{a\mathcal{A}\mathcal{C}}{\Theta}\right)-\mathcal{B} \tag{5.84}$$

The square sound speed is given by $c_s^2 = \mathcal{F}_\mathcal{S}/\mathcal{G}_\mathcal{S}$ while the ghost and gradient instabilities are avoided if the following conditions are satisfied :

$$\mathcal{F}_\mathcal{S} > 0, \qquad \mathcal{G}_\mathcal{S} > 0. \tag{5.85}$$

The above considerations are vital for comprehending the speed at which scalar perturbations propagate from the early Universe, which probably affects the observed magnitude of BAO.

5.3 | Applications of BDLS Cosmological Perturbations

The results of the perturbations analysis discussed in Sec.(5.2) have various implications in cosmology, particularly in the investigation of the early stages of the Universe. It is crucial to fully comprehend the nature of perturbations to elucidate the development and progression of large-scale structures. The current section aims to examine the power spectrum of cosmological perturbations in the BDLS context and to present the formulas of the alpha parameters. By utilizing the most recent CMB data, it is possible to constrain the values of the alpha parameters without the need to define any specific model or initial conditions. This approach enables the detection of any deviations between the standard cosmological model and alternative theories.

5.3.1 | Primordial Power Spectrum

One of the primary concerns of cosmology involves elucidating the origins of the primordial inhomogeneities which act as the precursors of the formation of structure. As per the cosmic inflation theory, these primordial perturbations stem from quantum fluctuations. While these fluctuations exhibit substantial amplitudes only on scales near the Planck length, they stretched to galactic scales during the inflationary era and established the initial conditions for the development of large-scale structures.

Quantum fluctuations suggest that different regions in space could inflate by different amounts resulting in local differences in the expansion history related to differences in the post-inflation local densities [103], [25]. In this section, the discussion will be on the power spectrum of these fluctuations. The power spectrum encompasses both scalar and tensor modes.

- Tensor Perturbations. To begin the analysis of the power spectrum in the case of tensor perturbations, we use the canonical variables

$$\mathrm{d}y_T := \frac{\mathcal{F}_T^{1/2}}{a\mathcal{G}_T}\mathrm{d}t\,, \quad z_T := \frac{a}{2}(\mathcal{F}_T\mathcal{G}_T)^{1/4}\,, \quad v_{ij}(y_T, \boldsymbol{x}) := z_T h_{ij}\,, \tag{5.86}$$

The quadratic action of Eq. (5.34) can now be written as

$$\mathcal{S}_T^{(2)} = \int \mathrm{d}y_T \mathrm{d}^3x \left[(v'_{ij})^2 - (\boldsymbol{\nabla} v_{ij})^2 + \frac{z''_T}{z_T} v_{ij}^2\right] \tag{5.87}$$

The prime indicates derivative with respect to y_T. Upon varying the action with respect to v_{ij} and solving its equation, the result at superhorizon scales is

$$v_{ij} \propto z_T\,, \quad v_{ij} \propto z_T \int \frac{\mathrm{d}y_T}{z_T^2}\,, \tag{5.88}$$

Using the non-canonical variables, Eq.(5.88) can be rewritten as

$$h_{ij} = const\,, \quad h_{ij} = \int^t \frac{\mathrm{d}t'}{a^3\mathcal{G}_T}\,. \tag{5.89}$$

To assess the power spectral density, it is assumed that

$$\epsilon := -\frac{\dot{H}}{H^2} \simeq const\,, \; f_T := \frac{\dot{\mathcal{F}}_T}{H\mathcal{F}_T} \simeq const\,, \; g_T := \frac{\dot{\mathcal{G}}_T}{H\mathcal{G}_T} \simeq const\,. \tag{5.90}$$

To ensure that the canonical time coordinate ranges from $-\infty$ to 0 during the expansion of the Universe, it is necessary to apply the following condition :

$$\epsilon + \frac{f_T - g_T}{2} < 1 \tag{5.91}$$

In order for the decay of the second solution in Eqs. (5.88)-(5.89) to occur, it is necessary to assume that

$$\epsilon - g_T < 3\,. \tag{5.92}$$

Expressing the tensor modes using the eigenfunctions $e^{ik\cdot x}$ of the Laplacian and the polarization tensor e_{ij} in the Fourier space, the equation for the mode function has the following solution :

$$v_{ij} = \frac{\sqrt{\pi}}{2}\sqrt{-y_T}H^{(1)}_{\nu_T}(-ky_T)\mathrm{e}_{ij}\,, \tag{5.93}$$

where $H^{(1)}_{\nu_T}$ is the Hankel function of the first kind (plus sign).

The entity ν_T is a positive scalar and it is defined as

$$\nu_T := \frac{3-\epsilon+g_T}{2-2\epsilon-f_T+g_T}\,. \tag{5.94}$$

Finally, the power spectrum of the primordial tensor perturbations has the form :

$$\mathcal{P}_T = 8\gamma_T \frac{\mathcal{G}_T^{1/2}}{\mathcal{F}_T^{3/2}}\frac{H^2}{4\pi^2}\Big|_{-ky_T=1} \tag{5.95}$$

with

$$\gamma_T = 2^{2\nu_T-3}\left|\frac{\Gamma(\nu_T)}{\Gamma(3/2)}\right|^2(1-\epsilon-\frac{f_T}{2}+\frac{g_T}{2})\,.$$

The power spectrum is calculated at the sound horizon exit, $-ky_T = 1$, since c_T does not necessarily equal c in all the cases. The spectral index in tensor perturbation is given by

$$n_T = 3 - 2\nu_T \tag{5.96}$$

The scale-invariant limit for tensor perturbations would be for $\nu_T = 3/2$. It can be observed From Eq. (5.96) that, the GW spectrum exhibit a blue tilt when

$$n_T > 0 \Rightarrow 4\epsilon + 3f_T - g_T < 0\,. \tag{5.97}$$

The criteria outlined in Eqs.(5.91) and (5.92) remain unchanged by this result and even with the detection of B-mode polarization in the CMB, the theory could remain a viable option.

- Scalar Perturbations: To achieve canonical normalization of the quadratic action, Eq.(5.74), the following variables are introduced :

$$\mathrm{d}y_S := \frac{\mathcal{F}_S^{1/2}}{a\mathcal{G}_S^{1/2}}\mathrm{d}t\,, \;\; z_S := \sqrt{2}a(\mathcal{F}_S\mathcal{G}_S)^{1/4}\,, \;\; u(y_S, \boldsymbol{x}) := z_S\zeta\,. \tag{5.98}$$

Substituting the new variables into the quadratic action of scalar perturbations, the result is

$$\mathcal{S}_S^{(2)} = \frac{1}{2}\int \mathrm{d}y_S \mathrm{d}^3x \left[(u')^2 - (\boldsymbol{\nabla} u)^2 + \frac{z_S''}{z_S}u^2\right] \tag{5.99}$$

and prime denotes differentiation with respect to the canonical time variable, y_S.

Using a similar method as the one employed in tensor perturbations, the following assumption is made for the derivation of the power spectrum :

$$\epsilon := -\frac{\dot{H}}{H^2} \simeq const\,, \;\; f_S := \frac{\dot{\mathcal{F}}_S}{H\mathcal{F}_S} \simeq const\,, \;\; g_S := \frac{\dot{\mathcal{G}}_S}{H\mathcal{G}_S} \simeq const\,. \tag{5.100}$$

The power spectrum has the form

$$\mathcal{P}_S = \frac{\gamma_S}{2}\frac{\mathcal{G}_S^{1/2}}{\mathcal{F}_S^{3/2}}\frac{H^2}{4\pi^2}\Big|_{-ky_S=1}\,, \tag{5.101}$$

where

$$\nu_S := \frac{3-\epsilon+g_S}{2-2\epsilon-f_S+g_S}$$

and

$$\gamma_S = 2^{2\nu_S-3}\left|\frac{\Gamma(\nu_S)}{\Gamma(3/2)}\right|^2(1-\epsilon-\frac{f_S}{2}+\frac{g_S}{2})\,.$$

The spectral index in this case is

$$n_S = 4 - 2\nu_S \tag{5.102}$$

To obtain equal amplitudes at horizon crossing, the following must hold :

$$\epsilon + \frac{3f_S}{4} - \frac{g_S}{4} = 0\,. \tag{5.103}$$

Considering the limit $\epsilon, f_T, g_T, f_S, g_S \ll 1$, then $\nu_T, \nu_S \to 3/2$ thus $\gamma_T, \gamma_S \to 1$. Finally, the ratio of tensor-to-scalar is

$$r = 16\frac{\mathcal{F}_S}{\mathcal{F}_T}\frac{c_S}{c_T}\,. \tag{5.104}$$

In light of this, it is possible to explore various inflation models as part of the BDLS theory and derive the value of r in relation to the slow-roll parameters.

5.3.2 | Alpha Parametrization

The results of the perturbation analysis presented in Sec.(5.2) can be further revised by considering five time-dependent functions, one of which is the Hubble parameter, $H(t)$, describing the expansion history of the Universe. The remaining four functions, denoted as $\alpha_i(t)$, are dimensionless and appear only within the perturbative framework. The $\alpha_i(t)$ functions offer the benefit of representing any deviations from GR at the perturbative level [26] , [71], [90]. These four functions are independent of the background, the matter composition of the model being studied, and each independent of the other. They could be accounted for as the set of functional parameters required to explain cosmological perturbations, yet their scope is broader. Taking into account a fixed background, then any pair of trajectories associated with distinct models but with the same $\alpha_i(t)$ exhibit no differences in their behaviour.

Utilizing the $\alpha_i(t)$ functions offers numerous benefits. This method allows for a comprehensive overview of the theoretical models in cosmology, as they can now be translated into the same language. As a result, facilitating the comparison between different models is now achievable by identifying possible similarities. Furthermore, having a precise mapping of models through these functional parameters enables research to discover unexplored domains beyond that already known.

On the other hand, a unified approach to the cosmological models streamlines the process of comparing them to observational data. Rather than individually constraining each theoretical model, the research can concentrate on constraining the parametrized functions which are derived from general formalism. Then, one can analyze the implications of this procedure for each respective model.

For a cosmological model with explicit initial conditions of the background variables, the context of each $\alpha_i(t)$ is defined as follows :

- α_K, *kineticity*. This term signifies the kinetic energy of scalar perturbations arising from the action. The possible large values of α_K can reduce the sound speed of scalar perturbations. Since α_K represents the kinetic energy, it is not constrained by observations as it does not affect any of the observational quantities [26], [71], [126]. The contributions of α_K come from G_2, G_3, G_4, G_5 and G_{tele}.

- α_B, *braiding*. Whenever $\alpha_B \neq 0$, a part of the kinetic term of scalar perturbations is derived from the kinetic mixing, referred to as braiding that occurs between gravitational and scalar degrees of freedom. The function α_B indicates any possible deviation from the standard form of $a = \dot{\zeta}/H$ as specified in the notation of Eq.(5.74) [26], [71] and it receives contributions from G_3, G_4, G_5 and G_{tele}.

- α_M, *Planck mass run rate*. The third functional parameter denotes the evolution rate of the effective Planck mass. The case of $\alpha_M \neq 0$ indicates that the theory under study involves non-minimal coupling. This particular function induces anisotropic stress in curvature perturbations and modifies the development of GW [26], [71], [122]. It receives contributions from G_4, G_5 and G_{tele}.

- α_T, *tensor speed excess*. It outlines the propagation speed of tensor perturbations and measures any deviations from the typical null geodesics [26], [71]. As a result, α_M and a_T have an impact on the propagation speed with their values to be potentially constrained by cosmological observations. The contributions on a_T stem from G_4, G_5 and G_{tele}.

According to the definitions of α_i, the effective Planck mass can be formally defined

$$HM_*^2\alpha_M = \frac{dM_*^2}{dt} \tag{5.105}$$

Following that, the definition of the effective Planck mass can be further used in expressing the quantities of tensor modes. In that case, the results outlined in Eqs.(5.35)-(5.36), can now be expressed as

$$\mathcal{G}_T = M_*^2/2 \quad \text{and} \quad c_T^2 = \frac{\mathcal{F}_T}{\mathcal{G}_T} \Rightarrow \mathcal{F}_T = (1+\alpha_T)\frac{M_*^2}{2} \tag{5.106}$$

The speed excess tensor is defined as

$$M_*^2\alpha_T = 4XG_{4,X} - 4XG_{5,\phi} - 2X\ddot{\phi}G_{5,X} + 2XH\dot{\phi}G_{5,X} - 4XG_{tele,J_8} - XG_{tele,J_5} \tag{5.107}$$

The kineticity and braiding terms are formulated in the following manner :

$$\mathcal{A}H\alpha_B = 2\dot{\phi}(XG_{3X} - G_{4\phi} - 2XG_{4\phi X}) + 2XH(4G_{4X} + 8XG_{4XX} - 4G_{5\phi} - \tag{5.108}$$

$$4XG_{5\phi X} + +3G_{tele,I_2I_2} + 4G_{tele,XT} - 6G_{Tele,XT_{vec}}) + 2\dot{\phi}XH^2(3G_{5X} + 2XG_{5XX}) +$$

$$\dot{\phi}(G_{tele,I_2} + 12H^2 G_{tele,TI_2} - 18H^2 G_{tele,T_{vec}I_2} + 2XG_{tele,XI_2}),$$

$$\mathcal{A}H^2\alpha_K = 2X(G_{2X} + 2XG_{2XX} - 2G_{3\phi} - 2XG_{3\phi X}) + 12\dot{\phi}XH(G_{3X} + XG_{3XX} - \tag{5.109}$$

$$3G_{4\phi X} - 2XG_{4\phi XX}) + +12XH^2(G_{4X} + 8XG_{4XX} + 4X^2 G_{4XXX} - G_{5\phi} -$$

$$5XG_{5\phi X} - 2X^2 G_{5\phi XX}) + 4\dot{\phi}XH^3(3G_{5X} + 7XG_{5XX} + 2X^2 G_{5XXX}) +$$

$$2X(9H^2 G_{tele,I_2 I_2} + 2XG_{tele,XX} + 6\dot{\phi}HG_{tele,XI_2} + G_{tele,X}).$$

Additionally, the Planck mass run rate is determined as

$$HM_*^2\alpha_M = \frac{dM_*^2}{dt} \tag{5.110}$$

Given the functional parameters, it is possible to redefine the quantities involved in the action of scalar perturbations and the squared sound speed as

$$\Theta = \frac{\mathcal{A}H}{2}(2 - \alpha_B) \text{ and } \Sigma = -\frac{\mathcal{A}H^2}{2}(6 - \alpha_K - 6\alpha_B), \tag{5.111}$$

$$\mathcal{G}_{\mathcal{S}} = \frac{2\mathcal{A}D}{(2-\alpha_B)^2}, \text{ where } D = \alpha_K + \frac{3}{2}\alpha_B^2.$$

$$c_s^2 = \frac{\mathcal{C}}{\mathcal{A}} \frac{(2-\alpha_B)(H^2(1+\alpha_X) - \dot{H}) + \dot{\alpha_B}H}{DH^2} - \frac{\mathcal{B}}{\mathcal{A}} \frac{(2-\alpha_B)^2}{2D}. \tag{5.112}$$

To streamline the expression of squared sound speed, the parameter, $\mathcal{C}H\alpha_X = d\mathcal{C}/dt$ has been introduced. This was achieved by adopting a method similar to the approach used for deriving a_M in the Horndeski gravity. When the teleparallel term G_{tele} equals zero, the classical Horndeski formula for the squared sound speed can be derived.

5.4 | Conclusion

The comprehensive study of the expanding Universe can be conducted by considering that it can be described by a FLRW metric with perturbations about that model being adequate to explain the formation of large-scale structure. This approach enables a thorough exploration of the origins of cosmic formation and the principles governing the development of the Universe. After all, it is evident that the validity of isotropic and homogeneous FLRW metric leads to the assumption that, on a specific scale, the galaxies are distributed homogeneously in space. However, observational data reveal deviations from a uniform Hubble flow on increasing large scales. This fact prompts the question about the validity of the FLRW metric and, most importantly, about the requisite averaging scale for interpreting it as a suitable model to describe the Universe.

The current chapter utilizes the teleparallel analogue of Horndeski gravity which involves the exchanging of curvature with torsion and results in equations of motion with at most second-order derivatives. The main objective is the investigation of the cosmological perturbations in the BDLS context, propagating through a homogeneous and isotropic FLRW Universe as the background. The investigation of perturbations is conducted while assuming the choice of a zero spin connection at all perturbative levels. The reason for choosing this option regarding the spin connection is to streamline the procedure since covariantization could result in the introduction of additional variables, yet, without altering the physical predictions.

The initial stage of the perturbation analysis is to identify and establish the equations of motion that align with the chosen background settings. Through the incorporation of the background equations, the complexity of the perturbation formulas is effectively reduced making the analysis more efficient. The investigation progressed into deriving the decomposition of the torsion tensor and calculating its contractions with the scalar field for three distinct perturbation types, namely tensor, vector and scalar modes. This extensive array of scalars is then integrated into the G_{tele} term and followed by their inclusion in the expansion of the action up to the second order. By studying the second-order action, each type of perturbation could be analyzed and characterized in detail. This thorough analysis contributes to achieving a more profound understanding of the ways in which different types of perturbation influence the overall dynamics of the BDLS theory.

Scalar perturbations demonstrate a wide range of characteristics that are important in enhancing our understanding of the formation of structures in the Universe. Tensor perturbations, on the other hand, are connected with the generation of gravitational waves and thus provide valuable insights into the mechanisms of cosmic evolution. However, it is necessary to incorporate the decaying vector modes in the analysis to thoroughly assess the validity of BDLS theory. As anticipated, it was confirmed in Sec.(5.2) that vector perturbations have a negligible impact on cosmological phenomena. Moving forward with the analysis, the next objective is to guarantee that the investigation of perturbations prevents the emergence of instabilities. In order to achieve this objective, we derive the constraint equations through the variation of the relevant action with respect to the non-dynamical fields in each perturbation case. Following that, we establish the final form of the quadratic action for scalar, tensor and vector modes which enables the derivation of the stability criteria that ensure the non-existence of ghost and gradient instabilities for each type of perturbation.

Bearing in mind the wide range of implications that perturbations can have in the field of cosmology, particularly when the focus is on investigating the early phases of the Universe, Sec.(5.3) commences with a detailed discussion of the power spectrum associated with both scalar and tensor modes. This method facilitates a thorough investigation of inflationary models within the framework of the BDLS theory. In addition, the analysis of the power spectrum facilitates the evaluation of the ratio of tensor-to-scalar in relation to the slow-roll parameters.

The second part of Sec.(5.3) presents a comprehensive overview of the cosmological perturbations by utilizing a concise set of four time-dependent functions, denoted as $\alpha_i(t)$ functions. Through the use of these functions, it becomes possible to present the derived results of perturbations in a straightforward format that can be easily understood and communicated further in the scientific community. The important feature of the α-parametrization is that the $\alpha_i(t)$ functions could effectively be constrained based on cosmological observations. Along with the Hubble parameter, these functions play a critical role in providing a comprehensive description of both the overall background and the perturbations within the system. Analyzing the potential deviations between observations and a current or newly introduced model by deriving these four functions directly from the Lagrangian, presents an intriguing research opportunity.

Cosmological perturbations are widely acknowledged to have a profound impact on shaping our understanding of the Universe. Owing to this, the present-day advancement of high-precision cosmology has brought the scientific community closer to distinguishing the most suitable theory of gravity. However, despite this progress, the ongoing task of reconciling theoretical models with actual observations continues to pose a significant challenge for researchers in the field of cosmology [67], [27].

By directing attention towards this objective, the investigation of cosmological perturbations in the BDLS context could be further expanded to encompass the entire range of the tetrad perturbations. Integrating this comprehensive approach into the investigation could uncover new insights and implications. Ultimately, this could lead to a more thorough evaluation of the validity of BDLS cosmology.

The results presented in the current chapter stem from analyzing the perturbations originating from the metric combined with the implementation of the unitary gauge choice. Yet, this analysis represents a preliminary step towards a more thorough methodology which would include the gauge invariant quadratic action of perturbations as well as the full spectrum of the tetrad perturbations in the realm of BDLS theory. The quadratic action for all the perturbation modes in the gauge invariant form would lead to the identification of the propagating DoF and also to the necessary stability conditions in order to avoid any pathologies of the theory.

In the context of this method, and working in Fourier space, the non-dynamical modes will be determined and then nullified through variations of the quadratic action with respect to them. The gauge invariant action including only the dynamical modes would be expressed by evaluating its variations with respect to the spatial and temporal components of a vector field transformation and then ensuring that the result is zero. Following that, a diagonalized kinetic matrix can be generated with each element being associated with a specific constraint. According to this procedure, the concept of Laplacian instability can be removed by imposing the requirement that the propagation speed of the dynamical modes remains positive.

Furthermore, it is important to emphasize the significance of considering the dependencies on the wave number k in this methodology. By recognizing that ghosts tend to manifest themselves in high-energy domains, it is crucial to impose a high k limit consistently during the entire procedure. As a result, both ghosts and Laplacian instabilities can be avoided within this analysis.

The criteria for identifying and preventing ghost and gradient instabilities enhances the overall quality of the scientific research leading to more robust and trustworthy conclusions. According to that perspective, it would be intriguing to investigate the possibility of a non-singular solution within the BDLS framework, with a specific focus on the spatially flat sector. This line of investigation could open up the opportunity to uncover solutions that may not have been previously considered.

Additionally, exploring the generalization of the no-go argument in a non-singular BDLS model without considering a spatially flat sector could yield valuable insights in the field of theoretical physics.

6

Stable bouncing solutions in Teleparallel Horndeski gravity: violations of the no-go theorem

The Null Energy Condition (NEC), $T_{\mu\nu} k^{\mu} k^{\nu} \geq 0$, can be violated in the case of classical Horndeski theory which could potentially lead to the development of a healthy non-singular cosmological model. However, it has been demonstrated in [86] that in the classical Horndeski case non-singular cosmological models characterized by a flat spatial sector exhibit gradient instabilities and pathologies related to the tensor mode. This is known as the no-go theorem and highlights the challenges involved in creating a consistent and stable cosmological model in classical Horndeski gravity. The present chapter begins by presenting the no-go theorem in classical Horndeski theory. Subsequently, motivated by the extensive framework of the Teleparallel analogue of the Horndeski theory, this chapter discusses possible methods that can be utilized for developing stable bouncing solutions within the context of BDLS. Following the analysis of the perturbations in Chapter 5, it is crucial to consider how those results contribute to understanding the topic at hand. As a result, the following study focuses on investigating the properties and characteristics of three BDLS toy models that could evade the no-go theorem in a healthy manner.

6.1 | The no-go theorem in classical Horndeski theory

However successful, the ΛCDM concordance model faces numerous challenges when extrapolated backwards in time. One of those challenges is that it fails to provide a valid justification for the fact that baryons have been developed in an asymmetric way with respect to antibaryons [42]. In addition, it does not provide the reason for the absence of exotic relic particles, such as the monopole [130], which are expected by Grand Unified Theories (GUT) to have a high abundance at the early stages of the Universe. Finally, the ΛCDM model does not explain the origin of density perturbations that led to the formation of large-scale structures and, furthermore, the initial singularity that results in a minute horizon without any explanation for the extremely low spatial curvature.

The introduction of the inflationary phase to the ΛCDM model, [73, 83], has the potential to effectively address a number of these challenging issues. The inflation paradigm, defined as a period of accelerated expansion during the early stages of the Universe, has evolved into a quite popular theory of contemporary cosmology. The most straightforward models of inflation not only resolve the flatness and horizon issues in the Universe, but they also forecast the characteristics and properties of the temperature fluctuations in the CMB radiation. These predictions are found to be in agreement with the most recent observations in the field of cosmology.

Nevertheless, the question regarding the initial singularity remains without a definitive resolution and continues to perplex scientific research despite the notable advancement made in the context of inflationary cosmology [34]. It has been demonstrated in [32] and in [33] that generic models of inflation may indeed contain initial singularities. This fact indicates that the inflationary framework remains geodesically incomplete. The ongoing research regarding the initial singularity issue underscores the need for further investigation into the dynamics of the early Universe and highlights the limitations of our current theoretical frameworks.

The fact that the initial singularity persists in the inflationary paradigm has led scientific research towards the investigation of alternative scenarios involving non-singular stages of the early Universe. These non-singular approaches serve as an effective way of completing the inflation phase in the initial stages of the Universe, thereby eliminating the existence of a singularity. One such potential alternative proposes a non-singular bouncing cosmological model, [35], [109], where there is a primary phase of contraction that is connected to the currently expanding one by a minimal scalar factor resulting in a vanishing Hubble rate.

In the context of GR, an advantageous bouncing cosmological model which is free of singularities involves the violation of the NEC, $\rho + P \geq 0$, in the vicinity of the bounce [133]. To verify this fact, it is necessary to follow the Einstein equations which state that the Hubble rate is defined by

$$\dot{H} = \frac{k}{a(t)^2} - \frac{1}{2}(\rho + P), \tag{6.1}$$

where k characterizes the spacetime curvature, $a(t)$ is the scale factor, while ρ and P are the energy density and pressure of the matter components.

In order to achieve the bounce in a flat FLRW cosmological background the negative value of the Hubble rate during the contraction phase must increase since it reaches the positive value related to the currently expanding Universe. It follows that according to Eq.(6.1), the condition $\dot{H} > 0$ necessitates that $\rho + P < 0$ and hence, the violation of the NEC which could lead to a singularity-free cosmological model.

However, the violation of the NEC in the context of a cosmological model results in the emergence of fields possessing negative kinetic energy commonly referred to as ghosts as well as the development of general instabilities, which are frequently observed in such a model. The presence of these phenomena introduces an element of uncertainty into the model making it more difficult to interpret as they complicate the analysis. Thus, additional considerations are required to account for their effects.

Therefore, violating the NEC in a healthy manner and at the same time avoiding the emergence of pathologies proves to be a challenging task that presents difficulties and obstacles which must be navigated carefully.

The NEC is inherently satisfied considering the inclusion of a canonical scalar field ϕ in the theory. This condition is defined as $T_{\mu\nu} k^\mu k^\nu = \dot{\phi}^2 \geq 0$, where $T_{\mu\nu}$ is the energy-momentum tensor and k^μ represents the null vector. In the case of a non-canonical scalar field where the Lagrangian of the model depends upon the scalar field ϕ and its first derivatives, the NEC can be successfully violated, nevertheless, this violation could lead to potential instabilities in the cosmological model.

The complete array of cosmological models incorporating a scalar field and whose Lagrangian involves second-order derivatives of the scalar field ϕ leading to second-order field equations are classified within the classical Horndeski theory [77]. Research has demonstrated that this class of models can effectively be employed in the development of bouncing cosmological solutions that do not exhibit any pathologies at the moment of the bounce [64], [119]. Nonetheless, the challenge of avoiding the instabilities becomes increasingly complex when attempting to prolong the bouncing solutions over extended periods of time. In such cases, the encounter with gradient instabilities or even ghosts is inevitable within the Horndeski class of theories [118], [86].

This situation is referred to as the *No-go* theorem within the classical Horndeski theory. The *No-go* theorem demonstrates the inherent impossibility of developing a stable cosmological model corresponding to the course of cosmic history, $t = (-\infty, +\infty)$, without encountering issues such as gradient instabilities and ghosts. By exploring the limitations imposed by this theorem it is possible to develop more robust models that accurately capture the complexities of cosmic evolution. In addition, the *No-go* theorem challenges scientific research to go beyond the conventional paradigms and explore innovative ways of studying the dynamics of the Universe.

6.2 | The No-go theorem in BDLS Theory

In Chapter 2 it was demonstrated that the development of the BDLS theory has the potential to revive the most interesting components of the classical Horndeski gravity which had been previously constrained due to GW propagation speed. In addition, the presentation of the analysis of cosmological perturbations in Sec.5.2 allows for a more thorough examination of the intricate dynamics and mechanisms driving the evolution of the Universe according to the principles of the BDLS theory. At this point, it is important to mention that the analysis conducted in Sec.5.2 does not provide the full spectrum that can be derived from the tetrad perturbations. Nevertheless, it includes a comprehensive and accurate set of the results of perturbations as they are inherited from the metric itself when the unitary gauge is employed.

According to Eq.(2.46) which expresses the Lagrangian of the BDLS theory, the corresponding action including the presence of matter is defined as

$$\mathcal{S}_{\text{BDLS}} \sim \int d^4x\, e\mathcal{L}_{tele} + \sum_{i=2}^{5} \int d^4x\, e\mathcal{L}_i + \int d^4x\, e\mathcal{L}_{\text{m}}\,, \tag{6.2}$$

where e is the determinant of the tetrad matrix and $\mathcal{L}_m$ is the Lagrangian for the matter fields. The analytical expressions of the $\mathcal{L}_i$ components are

$$\mathcal{L}_2 = G_2(\phi, X) \tag{6.3}$$

$$\mathcal{L}_3 = -G_3\,(\phi, X)\,\mathring{\Box}\,\phi \tag{6.4}$$

$$\mathcal{L}_4 = G_4(\phi, X)\mathring{R} + G_{4X}(\phi, X)\,[\,(\mathring{\Box}\phi)^2 - \mathring{\nabla}_\mu\mathring{\nabla}_\nu\phi\,\mathring{\nabla}^\mu\mathring{\nabla}^\nu\phi\,] \tag{6.5}$$

$$\begin{aligned}\mathcal{L}_5 = G_5(\phi, X)\,\mathring{G}_{\mu\nu}\mathring{\nabla}^\mu\mathring{\nabla}^\nu\phi - \frac{1}{6}G_{5X}(\phi, X)\,[\,(\mathring{\Box}\phi)^3 + 2\,\mathring{\nabla}_\nu\mathring{\nabla}_\mu\phi\,\mathring{\nabla}^\nu\mathring{\nabla}^\lambda\phi\,\mathring{\nabla}_\lambda\mathring{\nabla}^\mu\phi \\ - 3\,\mathring{\Box}\phi\,\mathring{\nabla}_\mu\mathring{\nabla}_\nu\phi\,\mathring{\nabla}^\mu\mathring{\nabla}^\nu\phi\,]\,,\end{aligned} \tag{6.6}$$

which coincide with the expressions of Eq.(2.23)-Eq.(2.26).

Finally, the expression of the $\mathcal{L}_{tele}$ component is

$$\mathcal{L}_{tele} = G_{tele}\left(\phi, X, T, T_{\text{ax}}, T_{\text{vec}}, I_2, J_1, J_3, J_5, J_6, J_8, J_{10}\right) . \tag{6.7}$$

The arguments of the $\mathcal{L}_{tele}$ are

$$T_{\text{ax}} = a_\mu\, a^\mu = -\frac{1}{18}\left(T_{\lambda\mu\nu}T^{\lambda\mu\nu} - 2\, T_{\lambda\mu\nu}T^{\mu\lambda\nu}\right),\ T_{\text{vec}} = v_\mu\, v^\mu = T^\lambda{}_{\lambda\mu}\ T_\rho{}^{\rho\mu} \tag{6.8}$$

$$T_{\text{ten}} = t_{\lambda\mu\nu}\, t^{\lambda\mu\nu} = \frac{1}{2}\left(T_{\lambda\mu\nu}T^{\lambda\mu\nu} + T_{\lambda\mu\nu}T^{\mu\lambda\nu}\right) - \frac{1}{2}T^\lambda{}_{\lambda\mu}T_\rho{}^{\rho\mu}\,, \tag{6.9}$$

$$T = \frac{3}{2}T_{\text{ax}} + \frac{2}{3}T_{\text{vec}} - \frac{2}{3}T_{\text{ten}},\ \ I_2 = v^\mu \phi_{;\mu}, \tag{6.10}$$

$$J_1 = a^\mu\, a^\nu\, \phi_{;\mu}\, \phi_{;\nu}\,, \tag{6.11}$$

$$J_3 = v_\sigma\, t^{\sigma\mu\nu}\, \phi_{;\mu}\, \phi_{;\nu}\,, \tag{6.12}$$

$$J_5 = t^{\sigma\mu\nu}\, t_\sigma{}^\alpha{}_\nu\, \phi_{;\mu}\, \phi_{;\alpha}\,, \tag{6.13}$$

$$J_6 = t^{\sigma\mu\nu}\, t_\sigma{}^{\alpha\beta}\, \phi_{;\mu}\, \phi_{;\nu}\, \phi_{;\alpha}\, \phi_{;\beta}\,, \tag{6.14}$$

$$J_8 = t^{\sigma\mu\nu}\, t_{\sigma\mu}{}^\alpha\, \phi_{;\nu}\, \phi_{;\alpha}\,, \tag{6.15}$$

$$J_{10} = \epsilon^\mu{}_{\nu\sigma\rho}\, a^\nu\, t^{\alpha\rho\sigma}\, \phi_{;\mu}\, \phi_{;\alpha}\,. \tag{6.16}$$

For the evaluation that follows, the choice of the background is that of a flat FLRW spacetime. The corresponding tetrad, taking into account a zero-spin spin connection, is specified by Eq.(5.2), which is

$$e^a{}_\mu = \text{diag}(N(t), a(t), a(t), a(t)), \tag{6.17}$$

where $N(t)$ is the lapse function and $a(t)$ is the scale factor. As it was discussed in Sec.5.1, when varying the action obtained from Eq.(2.46) with respect to the lapse function, $N(t)$, the first equation of motion is derived, Eq.(5.3). Once the equations of motion are determined, the lapse function can be set to unity.

Based on the results obtained through the perturbation analysis while employing the unitary gauge, $\delta\phi = 0$, as they are discussed in Chapter 5, the final form of the quadratic action in the case of tensor modes, Eq.(5.34), is described by

$$S_{\mathrm{T}}^{(2)} = \int d^4x \, \frac{a^3}{4} \left[\mathcal{G}_T \, \dot{h}_{ij}^2 - \frac{\mathcal{F}_T}{a^2} \left(\boldsymbol{\nabla} h_{ij}\right)^2 \right] . \tag{6.18}$$

In addition, the quadratic action for the scalar perturbations, Eq.(5.82), is

$$S_{\mathrm{S}}^{(2)} = \int dt d^3x a^3 \left[\mathcal{G}_S \dot{\zeta}^2 - \frac{\mathcal{F}_S}{a^2} (\boldsymbol{\nabla}\zeta)^2 \right] . \tag{6.19}$$

The components of the quadratic actions are given by

$$\mathcal{G}_T = 2\left(G_4 - 2XG_{4,X} + XG_{5,\phi} - HX\dot{\phi}G_{5,X} + 2XG_{tele,J_8} + \frac{X}{2}G_{tele,J_5} - G_{tele,T} \right) , \tag{6.20}$$

$$\mathcal{F}_T = 2\left(G_4 - XG_{5,\phi} - X\ddot{\phi}G_{5,X} - G_{tele,T} \right) , \tag{6.21}$$

$$\mathcal{G}_S = 3\mathcal{A} + \frac{\Sigma\mathcal{A}^2}{\Theta^2} , \tag{6.22}$$

$$\mathcal{F}_S = \frac{1}{a}\frac{\mathrm{d}}{\mathrm{d}t}\left(\frac{a\mathcal{A}\mathcal{C}}{\Theta} \right) - \mathcal{B} . \tag{6.23}$$

The analytical expressions of the quantities $\Sigma, \Theta, \mathcal{A}, \mathcal{B}$ and $\mathcal{C}$ are in Eq.(5.75)-(5.79). In particular, the formulas for the quantities $\mathcal{A}, \mathcal{B}$ and $\mathcal{C}$ can be rewritten as

$$\mathcal{A} = \mathcal{G}_T + f_1 \left(G_{tele}\right) , \tag{6.24}$$

$$\mathcal{B} = \mathcal{F}_T + f_2 \left(G_{tele}\right) , \tag{6.25}$$

$$\mathcal{C} = \mathcal{G}_T + f_3 \left(G_{tele}\right) . \tag{6.26}$$

Considering the functions $f_i(G_{tele})$ that appear in Eqs (6.24)-(6.26), their detailed expressions are listed below

$$f_1\left(G_{tele}\right) = 3G_{tele,T_{vec}} - X\left(G_{tele,J_5} + 4G_{tele,J_8} + 3G_{tele,I_2 I_2}\right) + \tag{6.27}$$
$$+ 6H\dot{\phi}\left(3G_{tele,T_{vec}I_2} - 2G_{tele,TI_2}\right) +$$
$$+ 6H^2\left(12G_{tele,TT_{vec}} - 4G_{tele,TT} - 9G_{tele,T_{vec}T_{vec}}\right),$$

$$f_2\left(G_{tele}\right) = \frac{2}{9}\left(18G_{tele,T_{vec}} - 6XG_{tele,J_3} - 5XG_{tele,J_5} - 2XG_{tele,J_8} + 2X^2 G_{tele,J_6}\right), \tag{6.28}$$

$$f_3\left(G_{tele}\right) = \frac{1}{9}\left(18G_{tele,T_{vec}} + 3XG_{tele,J_3} + XG_{tele,J_5} - 32XG_{tele,J_8} - 4X^2 G_{tele,J_6}\right). \tag{6.29}$$

It is evident from Eqs (6.20)-(6.23), that to avoid the occurrence of ghost and gradient instabilities, the following conditions must hold :

$$\mathcal{F}_T > 0, \quad \mathcal{G}_T > 0, \tag{6.30}$$
$$\mathcal{F}_S > 0, \quad \mathcal{G}_S > 0. \tag{6.31}$$

It should be mentioned that the speed of GW is equal to the ratio $c_T^2 = \mathcal{F}_T/\mathcal{G}_T$. In the same trend, the propagation speed of scalar perturbations is $c_S^2 = \mathcal{F}_S/\mathcal{G}_S$.

Incorporating the Eqs(6.23), (6.25) and (6.26), the coefficient $\mathcal{F}_S$ could be restated as

$$\mathcal{F}_S = \frac{1}{a}\frac{\mathrm{d}}{\mathrm{d}t}\left(\frac{a\mathcal{A}\mathcal{G}_T}{\Theta}\right) - \mathcal{F}_T + \frac{1}{a}\frac{\mathrm{d}}{\mathrm{d}t}\left(\frac{a\mathcal{A}f_3(G_{tele})}{\Theta}\right) - f_2(G_{tele}) = \tag{6.32}$$
$$= \frac{1}{a}\frac{\mathrm{d}\xi}{\mathrm{d}t} - \mathcal{F}_T + \mathcal{F}_0\,.$$

The additional components introduced in Eq.(6.32) are ξ and $\mathcal{F}_0$. These new elements have a crucial role in determining the overall outcome of the *No-go* theorem in the BDLS context.

They have the following definitions :

$$\xi = \frac{a\,\mathcal{A}\,\mathcal{G}_T}{\Theta} \qquad \text{and} \qquad \mathcal{F}_0 = \frac{1}{a}\frac{\mathrm{d}}{\mathrm{d}t}\left(\frac{a\,\mathcal{A}\,f_3(G_{tele})}{\Theta}\right) - f_2(G_{tele})\,. \tag{6.33}$$

Emphasis should be placed on the definition of the quantity ξ. According to Eq.(6.33), ξ could only disappear in the case of scale factor $a = 0$, which clearly represents the singularity. This fact results from the behaviour of the quantity Θ which depends on the G_i's and G_{tele} and, similar to ϕ and the Hubble parameter H, it is expected to be a continuous function of time. Consequently, Θ is finite in all regions.

By incorporating Eq.(6.22) and Eq.(6.32), then the required conditions for preventing gradient instabilities are outlined as

$$\mathcal{G}_S > 0 \Rightarrow \mathcal{A}\left(3 + \frac{\Sigma\,\mathcal{A}}{\Theta^2}\right) > 0 \Rightarrow \mathcal{A} \neq 0\,, \tag{6.34}$$

$$\mathcal{F}_S > 0 \Rightarrow \frac{\mathrm{d}\xi}{\mathrm{d}t} > a\left(\mathcal{F}_T - \mathcal{F}_0\right) > 0\,. \tag{6.35}$$

Upon integrating Eq.(6.35) over the time interval represented by t_i and t_f, it can be inferred that

$$\xi_f - \xi_i > \int_{t_i}^{t_f} a\left(\mathcal{F}_T - \mathcal{F}_0\right)\mathrm{d}t \tag{6.36}$$

As was thoroughly demonstrated in [86], the utilization of Eq.(6.36) with the condition $\mathcal{F}_0 = 0$ served as the basis upon which the *No-go* theorem was proven in the classical Horndeski case. In particular, taking into account a non-singular and expanding Universe with $a >$ constant(> 0) for $t \to -\infty$, then the convergence or not of the integral in Eq.(6.36) is contingent upon the asymptotic properties of $\mathcal{F}_T$ as $t_i \to -\infty$ and $t_f \to +\infty$. In the case that $\mathcal{F}_T$ decreases rapidly towards zero, the integral converges as $t \to \pm\infty$. However, this behaviour could lead to strong coupling issues in the tensor sector and for that reason, this case is typically circumvented.

When the integral does not converge and $\xi_i < 0$, the Eq.(6.36) for $\mathcal{F}_0 = 0$ is

$$-\xi_f < |\xi_i| - \int_{t_i}^{t_f} a\mathcal{F}_T \, \mathrm{d}t \,. \tag{6.37}$$

In that case, we have that $a > 0$ as well as $\mathcal{F}_T > 0$ for $t \to +\infty$ and the integral becomes positive while the right-hand side is negative. This leads to the conclusion that $\xi_f > 0$, meaning that ξ crosses zero which is not possible for any value of t within a non-singular Universe. The aforementioned rationale remains valid even when considering that $\xi > 0$, leading to the result that non-singular cosmological models contain pathologies, thereby confirming the *No-go* theorem in the classical Horndeski theory.

Within the framework of the BDLS, the presence of a non-zero value for $\mathcal{F}_0$ in Eq.(6.36), implies the possibility of stable and non-singular solutions. Furthermore, when $\xi_i < 0$, then Eq.(6.36) can be expressed as follows :

$$-\xi_f \; < \; |\xi_i| - \int_{t_i}^{t_f} a \left(\mathcal{F}_T - \mathcal{F}_0 \right) \mathrm{d}t. \tag{6.38}$$

Assuming that the integral in Eq.(6.38) is an increasing function, then the right-hand side becomes negative as t grows leading to $\xi_f > 0$. This scenario means that ξ crosses zero in the BDLS case as well. Nevertheless, due to the presence of $\mathcal{F}_0$ in the BDLS context, the integral may not always be an increasing function of t_f. The upcoming analysis will showcase particular models that are free of singularities and exhibit stability, thereby providing a fresh perspective on the validity and the limitations imposed by the *No-go* theorem.

6.3 | Evade the No-go theorem in BDLS theory

This section introduces three toy models which belong to the teleparallel Horndeski framework and they satisfy the background equations Eq.(5.3), Eq.(5.10) and Eq.(5.16). Each model was carefully chosen because it can support healthy non-singular bouncing solutions. This means they can avoid pathological issues, such as ghosts and gradient instabilities which can lead to unphysical behaviour. The analysis to follow will investigate how these selected models manage to avoid these problematic issues effectively, allowing for stable cosmological behaviour. Each model's characteristics will be examined in detail, showcasing how they contribute to a framework that supports these non-singular solutions.

To achieve the bounce in the background level, we need to carefully select appropriate options for the scale factor. As different choices of the bouncing scale factor can affect the outcome of the analysis, it is essential to explore various forms to understand their implications fully. For the realization of the bounce in the current study, we consider the following choices for the scale factor [79], [115] :

$$a(t) = a_0\,(1 + b\,t^2)^{1/3} \quad \text{and} \quad a(t) = a_0 \exp\left(\frac{b\,t^2}{1+b\,t^2}\right) \tag{6.39}$$

where a_0 is the value of the scale factor at the moment of the bounce, $t = 0$, and b is a positive parameter. The expressions of the Hubble parameter for the above choices of the scale factor are respectively

$$H(t) = \frac{2\,bt}{3\,(1+b\,t^2)} \quad \text{and} \quad H(t) = \frac{2\,bt}{(1+b\,t^2)^2} \tag{6.40}$$

In each of these two cases and as $t \in (-\infty, +\infty)$, we deduce that at the time of the bounce, i.e. $t = 0$, $H(t) = 0$. Furthermore, during the expansion phase of the Universe $H(t) > 0$ whereas for the period of contraction $H(t) < 0$.

The exact formulas for the G_i terms and G_{tele} are derived through reconstruction [18]. According to that procedure, each of the bouncing scale factors indicated in Eq.(6.39) is assumed to be a valid solution within the framework of these theoretical toy models. This method involves inserting generic configurations of the functions G_i and G_{tele} into the background equations specified in Eq.(5.3), Eq.(5.10) and Eq.(5.16). This method leads directly to finding the exact solutions for these functions.

6.3.1 | Model A

According to the analysis provided in Sec.2.4, the contributions of G_4 and G_5 within the framework of the classical Horndeski theory are significantly limited due to the propagation speed of GW. On the other hand, within the context of BDLS theory, the condition $c_T = 1$ is satisfied without having the need to eliminate the coupling functions $G_4(\phi, X), G_5(\phi, X)$. This distinction between the two theories highlights the intricate balance between theoretical frameworks and the impact they have on the behaviour of gravity and its associated properties.

Motivated by the form of $G_4(\phi, X)$ and $G_5(\phi, X)$ functions in BDLS theory, our investigation begins by assuming straightforward expressions for these two contributions. Specifically, for the G_5 function, we adopt the approach of treating it as a constant. This simplifies our calculations and allows us to understand its impact more clearly. On the other hand, we define the contribution of G_4 as a linear function of the kinetic term X. In addition, the choice for the G_{tele} contribution presents a coupling between the torsion scalar and the kinetic term together with a linear term of the scalar J_5. By incorporating these choices into the background equations, Eq.(5.3), Eq.(5.10) and Eq.(5.16), along with $\phi(t) = t$, we determine the remaining functions in order to obtain the power-law bouncing solution of Eq.(6.39).

Following that procedure, the Horndeski functions $G_i(\phi, X)$ are given by

$$G_2(\phi, X) = X^2 \left(\frac{16\,b}{3(1+b\,\phi^2)} \right) + \frac{b\,\phi}{1+b\,\phi^2}\,, \tag{6.41}$$

$$G_3(\phi, X) = X + \frac{1}{2}\log\left(1+b\,\phi^2\right) + \frac{4b\phi}{3(1+b\,\phi^2)} + \frac{8\sqrt{b}}{3}\tan^{-1}(\sqrt{b}\phi)\,, \tag{6.42}$$

$$G_4(\phi, X) = 1 + mX\,, \tag{6.43}$$

$$G_5(\phi, X) = \text{const.}\,, \tag{6.44}$$

The teleparallel Lagrangian term for this BDLS model is described by

$$G_{tele} = -mTX + 4mJ_5\,, \tag{6.45}$$

where m is an arbitrary positive constant.

To effectively utilize this particular ansatz of G_i functions, is essential for the arbitrary positive constant m to be $m \geq 10$. This specific range for m is a critical factor in ensuring that the stability criteria, as they are outlined in Eqs (6.30)-(6.31), are successfully met and thus contributing to the robustness and validity of the calculations.

According to Eqs (6.20)-(6.21), the coefficients of the tensor perturbations are

$$\mathcal{G}_T = 2(1+m) \;\text{ and }\; \mathcal{F}_T = 2(1+m) \;\Rightarrow c_T^2 \;=\; 1 \tag{6.46}$$

It is evident from Eq.(6.46) that the propagation speed of GW is consistent with observations since it is independent of m and always equal to unity. In addition, for every value of the parameter m with $m \geq 10$, the stability criteria are satisfied, i.e. $\mathcal{G}_T > 0$ and $\mathcal{F}_T > 0$.

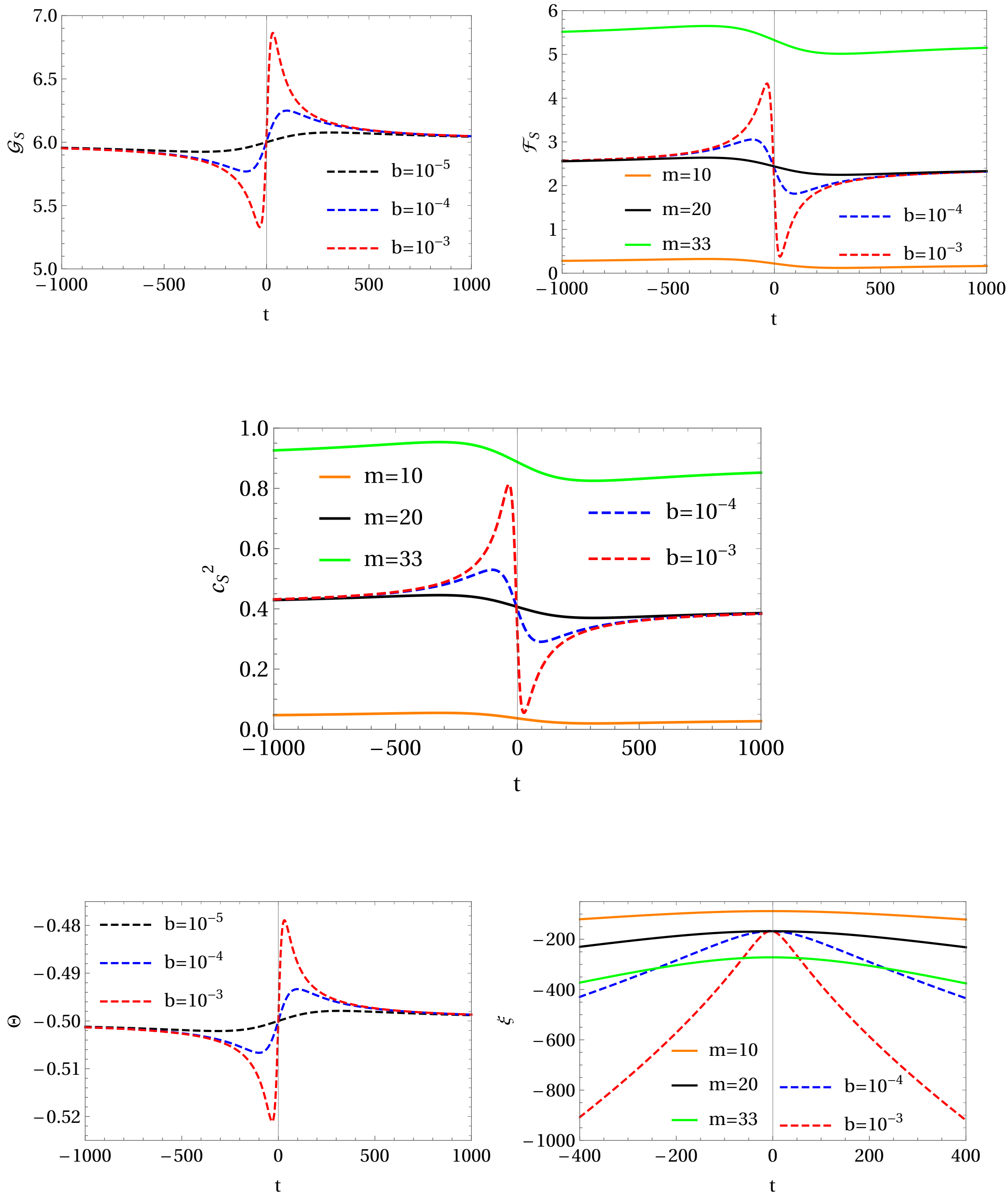

Fig. 6.1. Model A: The coefficients of the scalar perturbations versus time. The plots are presented for different values of m, i.e. $m = 10, 20, 33$ and $b = 10^{-i}$, where $i = 3, 4, 5$. All the plots are considered for $a_0 = 1$.

The coefficients of scalar perturbations can be determined by referring to Eqs (6.22)-(6.23)-(5.75)-(5.76)-(5.77)-(5.78)-(5.79). For this particular model, they are

$$\Theta = 2H - \frac{1}{2}\,,\;\; \mathcal{A} = 2\,,\;\; \mathcal{B} = \frac{2}{9}\left(9 - m\right)\,,\;\; \mathcal{C} = 2 + \frac{20m}{9}\,, \tag{6.47}$$

$$\Sigma = 18H^2 + 6\dot{H} + \frac{9}{2}H\,, \tag{6.48}$$

$$\mathcal{G}_S = 6\left(1 + 4\frac{12H^2 + 4\dot{H} + 3H}{(4H-1)^2}\right) \tag{6.49}$$

$$\mathcal{F}_S = 8\frac{4H^2 - H + 4\dot{H}}{(4H-1)^2}(1 + \frac{10\,m}{9}) - 2\,(1 - \frac{m}{9}). \tag{6.50}$$

In Figure 6.1 the plots of the scalar perturbation coefficients for the first model are displayed with respect to the cosmic time t. It can be easily observed that, for $a_0 = 1$, the value of the parameter b can alter the shape of the plot. In addition, the change in the value of the parameter m significantly impacts the vertical extent of the plot indicating a correlation between them. This fact could lead to the possibility of superluminal sound speed in certain circumstances. Nevertheless, for all the chosen values of the parameter m employed in this scenario, i.e. $m = 10, 20, 33$ and for $b = 10^{-3}, 10^{-4}, 10^{-5}$, the coefficient Θ is negative and finite and, most importantly, does not intersect zero. This behaviour of the coefficient Θ leads to the conclusion that the variable ξ remains negative for $t \in (-\infty, +\infty)$, without crossing zero which is consistent with the behaviour of the bouncing scale factor and Eq.(6.33) describing the relation between ξ and $a(t)$. Furthermore, Figure 6.1 illustrates the behaviour of $\mathcal{G}_S$ and $\mathcal{F}_S$ to be always positive and finite and the propagation speed of scalar perturbation is less than unity. Therefore, the stability conditions resulting from scalar perturbations are also satisfied, i.e. $\mathcal{G}_S > 0$ and $\mathcal{F}_S > 0$.

Consequently, this non-singular BDLS model is free of any ghost and gradient instabilities over the entire time interval $t \in (-\infty, +\infty)$.

6.3.2 | Model B

In alignment with the same underlying motivation as the first model, we assume that G_5 is currently a linear function of the scalar field ϕ, while G_4 is a linear function of the kinetic term resembling Model A. The expression of the G_{tele} contribution consists of two linear terms of the torsion scalar and J_3 respectively. According to the reconstruction method, by implementing the above choices into the background equations together with $\phi(t) = t$ we can calculate the remaining G_i functions in order to obtain the power-law bouncing solution of Eq.(6.39).

The $G_i(\phi, X)$ functions for Model B are listed below

$$G_2 = X^2 \left(\frac{16b}{3(1 + b\,\phi^2)} \right) + \frac{b\,\phi}{1 + b\,\phi^2}, \tag{6.51}$$

$$G_3 = X + \frac{1}{2} \log\left(1 + b\,\phi^2\right) + \frac{4b\,\phi}{3(1 + b\,\phi^2)} + \frac{8\sqrt{b}}{3} \tan^{-1}(\sqrt{b}\,\phi)\,, \tag{6.52}$$

$$G_4 = \frac{1}{2} + X\,, \tag{6.53}$$

$$G_5 = \phi\,. \tag{6.54}$$

Furthermore, the teleparallel Lagrangian term reads

$$G_{tele} = -\frac{T}{2} + \alpha\, J_3\,, \tag{6.55}$$

where α is a positive parameter and must be $\alpha > 3$ for the stability criteria to hold. It is evident that the Horndeski functions in this case bear a resemblance to the first model except for the G_5 contribution which is now a function of ϕ.

The coefficients for the tensor modes in this case are

$$\mathcal{G}_T = \mathcal{F}_T = 2 \Rightarrow c_T^2 = 1. \tag{6.56}$$

It is evident that the requirement for the propagation speed of GW is always satisfied for this model and $\mathcal{G}_T > 0, \mathcal{F}_T > 0$.

The coefficients of the scalar perturbations are listed below

$$\mathcal{A} = 2\,, \;\; \mathcal{B} = 2 - \frac{2\alpha}{3}\,, \;\; \mathcal{C} = 2 + \frac{\alpha}{6}, \tag{6.57}$$

$$\Sigma = 18\,H^2 + 6\,H + 6\dot{H}\,, \;\; \Theta = 2\,H - \frac{1}{2}\,, \tag{6.58}$$

$$\mathcal{G}_S = 6\left(1 + 4\frac{3H^2 + \dot{H} + H}{(4H-1)^2}\right)\,, \;\; \mathcal{F}_S = 8\frac{4H^2 - H + 4\dot{H}}{(4H-1)^2}(1 + \frac{\alpha}{12}) - 2\,(1 - \frac{\alpha}{3})\,. \tag{6.59}$$

Figure 6.2 illustrates the plots of the coefficients of scalar perturbations with respect to the cosmic time t and with $a_0 = 1$. It is evident that any change of b impacts the overall shape of the plots. In addition, by utilizing different values for the α parameter we can alter their vertical position. For the selected values of b, namely, $b = 10^{-3}, 10^{-4}, 10^{-5}$, the representation of the coefficient Θ indicates that it is always negative and finite whereas it does not cross zero. Once again, the behaviour of Θ guarantees that the coefficient ξ, which maintains a negative value, does not intersect zero, therefore aligning perfectly with the bouncing scale factor described in Eq.(6.39). This meticulous examination of the plots for Θ and ξ enhances the reliability of the model. Considering the behaviour of the $\mathcal{G}_S$, Figure 6.2 demonstrates that for the $b = 10^{-3}, 10^{-4}, 10^{-5}$, $\mathcal{G}_S$ is always positive and finite. Furthermore, for the values of $\alpha = 7, 8, 9, 10$, $\mathcal{F}_S$ remains positive for $t \in (-\infty, +\infty)$. Consequently, all the stability criteria are met for this model and the speed of scalar perturbations is less than unity.

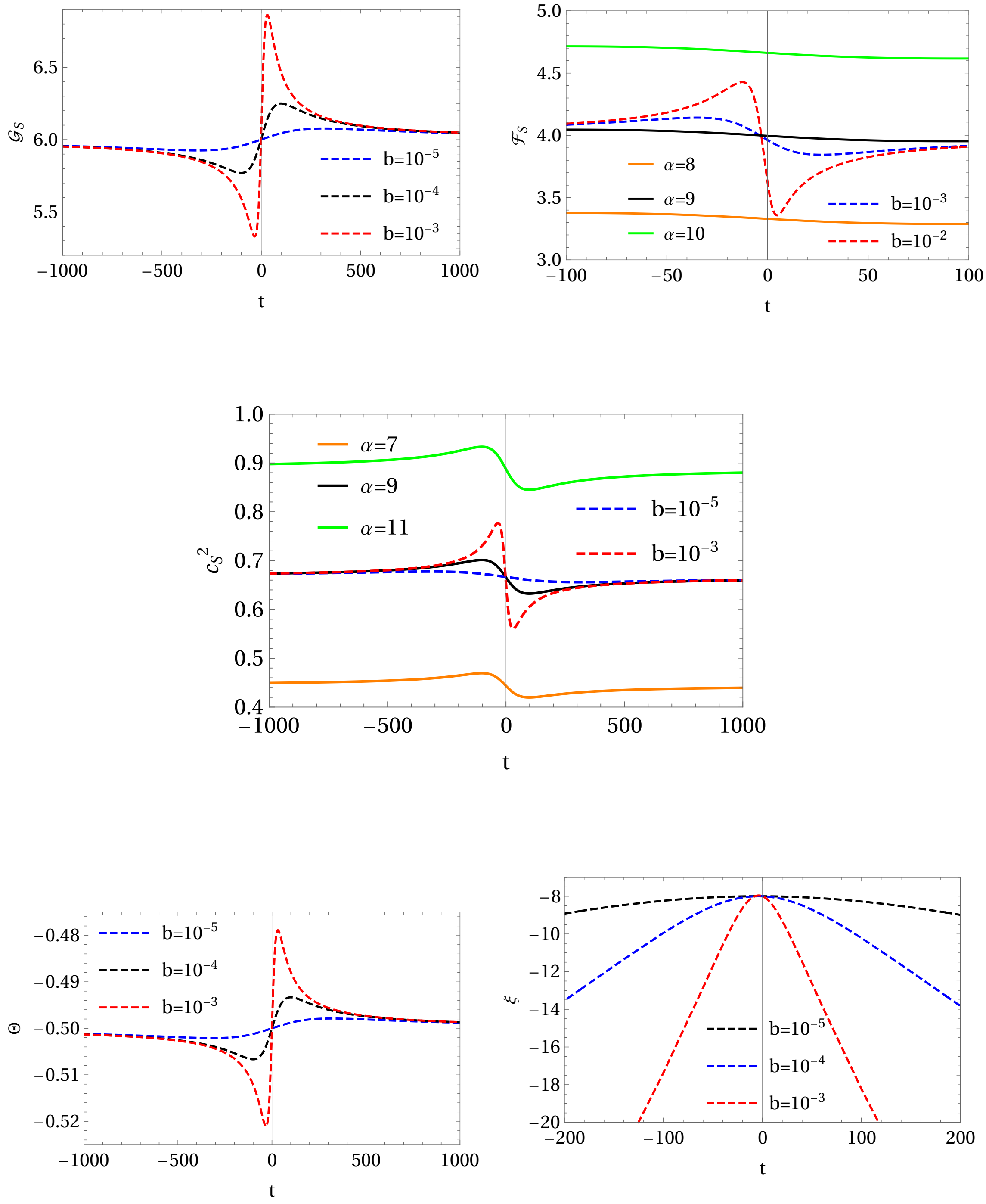

Fig. 6.2. Model B: The coefficients of the scalar perturbations versus time. For $a_0 = 1$ and different values of the α parameter, Θ is negative and never crosses zero while $\mathcal{G}_S > 0, \mathcal{F}_S > 0$.

6.3.3 | Model C

In this model, the expressions of G_4 and G_5 are the same as in Model B, while the G_{tele} contribution includes two linear terms of I_2 and J_3 respectively. Following the reconstruction procedure as before and integrating these choices into the background equations, namely Eq.(5.3), Eq.(5.10) and Eq.(5.16) alongside $\phi(t) = t$, we can determine the remaining G_i functions required to achieve the exponential form of the bouncing solution described in Eq.(6.39).

The $G_i(\phi, X)$ functions in this case are

$$G_2 = -X^2 \left[\frac{4b\left(-2 + 3\alpha\phi - 8b\phi^2 + 6b\alpha\phi^3 + 6b^2\phi^4 + 3b^2\alpha\phi^5\right)}{(1 + b\,\phi^2)^4} \right], \tag{6.60}$$

$$G_3 = \frac{b\phi\left(9 + 20b\phi^2 + 3b^2\phi^4\right)}{2(1 + b\,\phi^2)^3} + \frac{3\,\alpha}{2(1 + b\,\phi^2)} + \frac{3\sqrt{b}}{2}\tan^{-1}\left(\sqrt{b}\phi\right), \tag{6.61}$$

$$G_4 = \frac{1}{2} + X, \tag{6.62}$$

$$G_5 = \phi. \tag{6.63}$$

The teleparallel Lagrangian term is described by

$$G_{tele} = \alpha I_2 + \beta J_3, \tag{6.64}$$

where α and β are the parameters of the model.

In this case, the coefficients for the tensor perturbations are the following :

$$\mathcal{G}_T = \mathcal{F}_T = 1 \;\Rightarrow\; c_T^2 = 1, \tag{6.65}$$

therefore, the propagation speed of GW is always constant and equals unity.

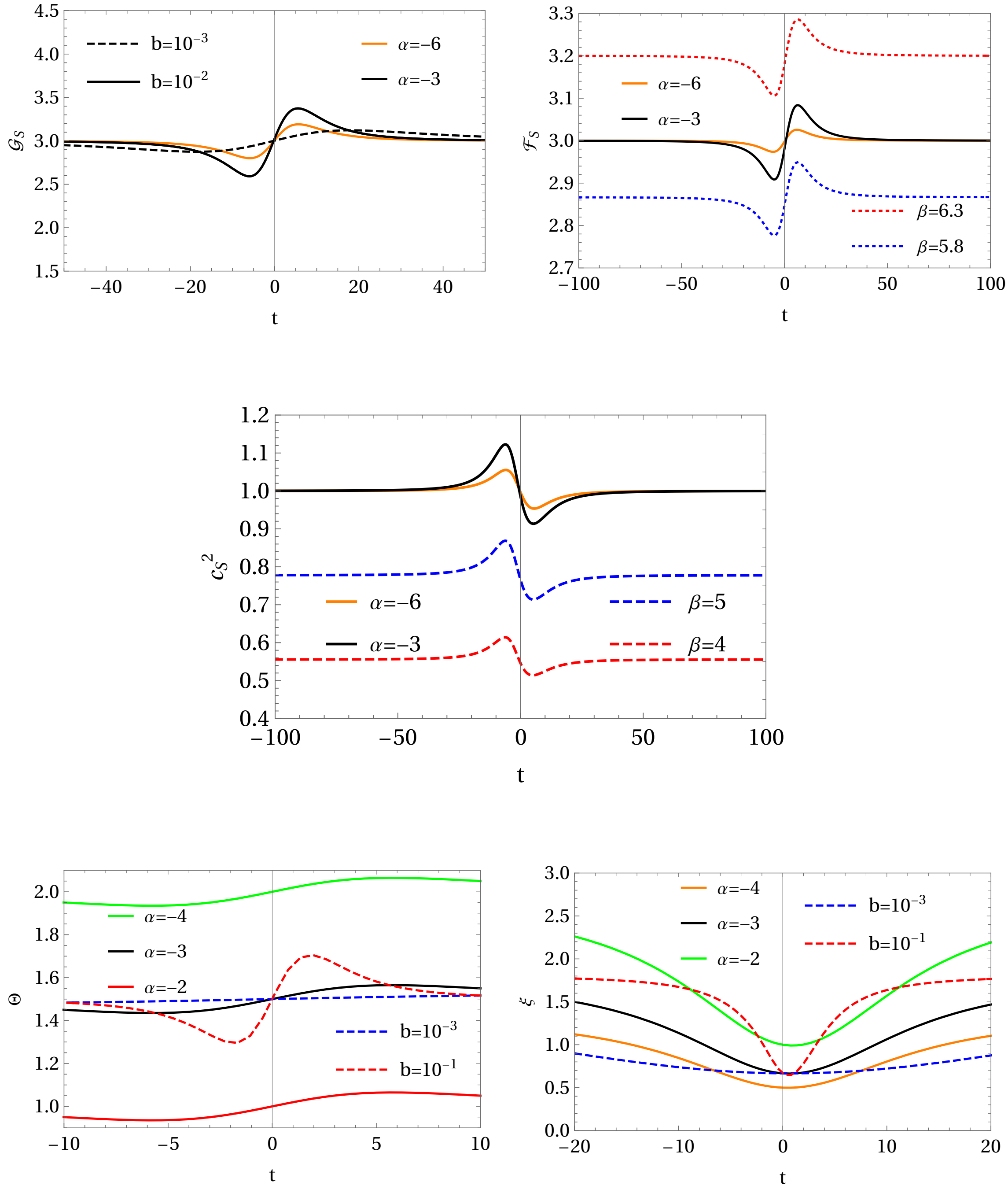

Fig. 6.3. Model C: The coefficients of the scalar perturbations versus the cosmic time with $a_0 = 1$. For the different values of the negative parameter α, namely $\alpha = -2, -3, -4, -6$ along with the values of the positive parameter β, Θ is positive and never crosses zero while $\mathcal{G}_S > 0, \mathcal{F}_S > 0$.

Incorporating the Eqs (6.22)-(6.23)-(5.75)-(5.76)-(5.77)-(5.78)-(5.79), the coefficients of the scalar perturbations in this model have the following forms :

$$\mathcal{A} = 1\,, \;\; \mathcal{B} = 1 - \frac{2\beta}{3}\,, \;\; \mathcal{C} = 1 + \frac{\beta}{6}$$

$$\Sigma = 9\,H^2 - \frac{9\alpha}{2}\,H + 3\dot{H}\,, \;\; \Theta = H - \frac{\alpha}{2}\,, \tag{6.66}$$

$$\mathcal{G}_S = 3\left(1 + 2\frac{6H^2 + 2\dot{H} - 3\alpha H}{(2H-\alpha)^2}\right), \tag{6.67}$$

$$\mathcal{F}_S = 2\frac{2H^2 - \alpha H - 2\dot{H}}{(2H-\alpha)^2}\,(\,1 + \frac{\beta}{6}\,) - \frac{1}{(2H-\alpha)^2}\,(\,1 - \frac{2\beta}{3}\,)\,. \tag{6.68}$$

According to the plots displayed in Figure 6.3, it is evident that varying the values of the positive parameter β could lead to changes in the height of the plots representing the coefficient $\mathcal{F}_S$ and the sound speed c_S^2 while the height of the plots representing Θ and ξ remain unaffected by any modification of β.

In addition, it can be observed from Figure 6.3 that different choices of the values of the negative parameter α, i.e. $\alpha = -2, -3, -4, -6$ have the ability to alter the overall shape of all the plots displayed here.

On the other hand, it must be mentioned that the values of the α parameter affect the vertical position of the Θ plot while b could change its shape. However, Θ remains positive and finite everywhere without crossing zero for all the selected values of α and b. As a result, ξ never crosses zero and the stability conditions are satisfied.

The analysis of this section reveals the possibility of developing non-singular cosmological models in the BDLS framework that are devoid of any instabilities. Even though the three toy models illustrated here, along with their graphs, constitute minimal examples, however, they provide a solid motivation and serve as a starting point to expand the research in order to incorporate several other forms of the bouncing scale factor as well as investigate more comprehensive forms for the expressions of the G_i and G_{tele} functions and thus, advancing the creation of non-singular BDLS models.

6.4 | Conclusion

In general, a *No-go* theorem is typically established when there is an inconsistency or a contradiction between the deduced outcome of a set of physical assumptions portrayed through the mathematical structure of a theoretical model, and a collection of physical assumptions of a well-established theory.

However, a unique method to interpret the same *No-go* theorem is difficult to exist as different approaches may lead to varying justifications on which elements of the *No-go* theorem must be excluded or modified.

As a result, instead of understanding a *No-go* theorem as a direct revelation of what is not possible, it should be regarded as an adequate method for developing a theoretical framework. This procedure could potentially uncover strategies for circumventing a *No-go* theorem or enhance our comprehension of how to maintain certain assumptions in order to achieve feasibility.

In the field of cosmological research, the *No-go* theorem has a pivotal role, particularly in examining the early stages of the Universe and, most of all, addressing the existence of the singularity within the ΛCDM model. Even though the concept of the inflation paradigm is widely recognized to be a significant feature of the early phases of cosmic evolution, the singularity issue cannot be disregarded even in this concept. Therefore, there is a compelling rationale for investigating the defining characteristics of non-singular cosmological models such as bouncing cosmologies. These inquiries have the potential to provide valuable insights into the dynamics and behaviour of the early Universe in scenarios where the singularity is avoided. It is important to under-line that these theoretical models of the early Universe do not serve as a replacement for inflation. Instead, their purpose is to complement the inflationary phase by removing the presence of the initial singularity.

One significant characteristic of the Horndeski theory is its ability to provide a framework for developing bouncing cosmological solutions. These solutions can be formulated within various subcategories of the Horndeski theory, encompassing both the evolution of the background as well as the advancement of perturbations. Despite the fact that the Horndeski theory has been effective in generating models with non-singular solutions, the discussion in Sec.(6.1) pointed out that these solutions with a flat spatial sector may experience challenges such as gradient instabilities or have pathological outcomes in the tensor sector [86]. This particular fact represents the core concept of the *No-go* theorem within the classical Horndeski theory.

According to the principles of the BDLS theory and in particular, because of the emergence of the new Lagrangian contribution, G_{tele}, it is possible to evade the *No-go* theorem in this context. This new possibility is explicitly stated in Eq.(6.38) and this novel aspect of constructing healthy non-singular models would greatly benefit the BDLS framework. Nevertheless, the likelihood of achieving this objective is still ambiguous. Moreover, the existence of evading solutions may only be applicable to specific scenarios due to the inequality in Eq.(6.38).

In this chapter, we discussed three toy models belonging to the framework of BDLS theory that provide the means to evade the *No-go* theorem while also ensuring compliance with the constraint related to the propagation speed of GW. In each of these three models, the cosmological perturbation results as outlined in Chapter 5 were incorporated. This integration of the perturbation results is a crucial step in refining the accuracy while also gaining new insights into the behaviour of each model under study.

Furthermore, it is important to mention that in these toy models the expressions of the Lagrangian contributions, G_4 and G_5 are not trivial ones. In addition, the first two models utilize a bouncing scale factor which is of the power law form of Eq.(6.39) while the scalar field is identified as a linear function of the cosmic time t. Regarding the third toy model, the situation is different since the bouncing scale factor is now characterized by the exponential function of the cosmic time described in Eq.(6.39).

In Model A, the expression of the G_{tele} function includes a coupling between the torsion scalar and the kinetic term while also involving a linear term of the J_5 scalar. In this case, the propagation speed of scalar perturbation displays an antisymmetric pattern around $t = 0$, while maintaining consistently positive and less than unity for a wide spectrum of the values of the parameter m. According to Figure 6.1, the vertical position and the width of the plots can alter for different values of the parameters. In addition, the coefficient Θ does not cross zero and remains negative everywhere. Therefore, Model A clearly evades the *No-go* theorem in a healthy manner.

The second model of the analysis, Model B, incorporates a form for the G_{tele} term as linear functions of the torsion scalar and also the J_3 invariant while the formula of G_4 is similar to Model A and G_5 is a function of the scalar field. By varying the parameter α of this model, it is observed that the propagation speed of scalar perturbations exhibits again an antisymmetric shape around $t = 0$. However, it remains always positive and less than unity for all the parameter values. In addition, the propagation speed of tensor modes is always unity. Similar to Model A, this case also demonstrates a healthy way to overcome the limitations imposed by the *No-go* theorem. This is evident when analyzing the plot of the component Θ in Figure 6.2 which is apparently finite leading to a healthy evasion solution.

In Model C, the bouncing scale factor is characterized by the exponential function of the cosmic time of Eq.(6.39). Furthermore, the definition of the scalar field remains the same as before, i.e. $\phi(t) = t$. The G_{tele} contribution is now a linear function for both the I_2 and the J_3 invariant and the model parameters in this case are α and β. This model also illustrates a healthy solution to circumvent the *No-go* theorem. According to the plots illustrated in Figure 6.3, the coefficient Θ always has positive values without ever reaching zero. In addition, the propagation speed of GW is unity for this model as well. Furthermore, the plots of Figure 6.3 provide a visual representation of the stability criteria being satisfied for the scalar perturbations. This fact enhances the stable behaviour of the third toy model under study.

Even though this chapter discusses the evasion of the *No-go* theorem based on the results of the perturbation analysis conducted in Chapter 5, the detailed analysis of these particular toy models provides a solid motivation and a reliable starting point for broadening the investigation even further. Potential future endeavours may encompass more than just the inherited metric perturbations, but rather the comprehensive perturbation spectrum of the tetrad itself. Moreover, the form of the bouncing scale factor could be broader and thus include several interesting formulas besides the power law and the exponential function of cosmic time.

7

Conclusions

Einstein's theory of General Relativity is recognized as one of the central principles in contemporary physics. As it is expressed within the framework of differential geometry, this theory paved the way for the subsequent gauge theories and string theories. It would not be an overstatement to say that GR marked the transformation of our understanding of the Universe challenging long-held beliefs and assumptions. However, despite the significant achievements of GR, various alternatives to this theory have been suggested. Even from its onset, there had been an effort to expand and integrate GR into a broader theoretical framework. In addition, during the last decades, observational evidence has revealed several shortcomings of Einstein's theory. This fact has prompted scientific research to reevaluate the principles of GR and led to an increasing number of theories attempting to modify it. These modifications could potentially include additional DoF such as introducing a scalar field. Another option might be to incorporate higher-order corrections in the action of each model.

Scalar-tensor theories, which are the primary focus of this thesis, represent perhaps the most straightforward form of modified gravity. Within this context, gravitation is mediated not only by the metric but also by the scalar field. Soon after the discovery of the observed accelerated expansion of the Universe, numerous researchers have turned to scalar-tensor theories aiming to extend the concept of cosmological constant and to tackle issues related to fine-tuning and the coincidence problem [21], [7], [30], [65]. The Horndeski theory [77] is recognized to be the most general scalar-tensor theory, involving a single scalar field and field equations that do not extend the second-order, regardless of the higher-order derivatives present in the Lagrangian. By selecting the appropriate mathematical forms of the $\mathcal{L}_i$ functions outlined in Eqs.(2.23)-(2.26), it is possible to formulate any second-order scalar-tensor theory.

One example of scalar-tensor theory which belongs to the Horndeski class is the Einstein Gauss-Bonnet model. This model features a non-minimally coupling of the Gauss-Bonnet term and a scalar field. The coupling of this model is described as

$$f(\phi)(R^2 - 4R_{\alpha\beta}\,R^{\alpha\beta} + R_{\alpha\beta\gamma\delta}\,R^{\alpha\beta\gamma\delta})\,, \tag{7.1}$$

where $f(\phi)$ is an arbitrary function of the dynamically evolving scalar field.
The coupling illustrated in Eq.(7.1) can indeed be obtained by selecting the following form of the functions within the standard Horndeski theory :

$$G_2 = 8f^{(4)}X^2(3 - \ln X),\ \ G_3 = 4f^{(3)}X(7 - 3\ \ln X) \tag{7.2}$$

$$G_4 = 4f^{(2)}X(2 - \ln X),\ \ \ G_5 = -4f^{(1)}\ln X \tag{7.3}$$

This model, along with its potential modifications, is recognized for its ability to offer accelerated solutions that could have significant implications for the study of large-scale structures, thereby sparking an increased interest among researchers looking to delve into this topic more thoroughly. Following these objectives, Sec.(3.2) presents a dynamical system analysis of the EGB model. A number of methods for conducting such analysis are already present in the literature [48], [7]. However, the present work focused on a different direction. The choice was to prioritize exploring the implications of the EGB model in accordance with the GW speed constraint. Based on the requirement outlined in Eq.(3.24), it was possible to identify the fraction $\dot{H}/H^2$ as a function of the dynamical variables governing the system. According to that novel approach, the autonomous feature is established right from the beginning, without relying on assumptions about the various eras of cosmic evolution. Instead, by analyzing the behaviour of the critical points, the identification of these eras was completed along with determining the corresponding value of $\dot{H}/H^2$ for each one of them.

The dynamical system analysis resulted in a total of seven critical points. These critical points present a promising and rich area for further exploration. Among these critical points, there are two that could provide valuable insights into the early phases of cosmic development as well as shed light on the inflationary process. The critical point C of the analysis, which is dominated by the potential energy of the scalar field, leads to a stable acceleration solution. This result indicates that the presence of this critical point could eventually serve as the stable attractor of the system.

It is evident that understanding the intricacies of the critical points and the general behaviour of the EGB model would prove to be highly beneficial. One of the most efficient methods to accomplish this objective is by employing numerical simulations since the emergence and development of cosmic structures involve complex nonlinear processes that can be effectively examined through the method of numerical simulations. These simulations aim to provide reliable predictions that, when compared with current and future observations, allow us to constrain the cosmological parameters. Within this method, several techniques have been developed to monitor gravitational interactions in cosmological volumes along with the impact of physical mechanisms on the baryonic component. The insights obtained from numerical simulations could provide a major understanding of the details and implications of the EGB model. This represents a significant task worth exploring in our future scientific endeavours.

Although the Horndeski Lagrangian has been able to encompass a wide range of modified gravity theories, this collection of models is now subject to severe limitations due to the GW propagation speed constraint. Recognizing this fact, the teleparallel analogue of the Horndeski theory, known as BDLS, is introduced. By considering the teleparallel framework, the objective is to overcome the constraints imposed by the propagation speed of tensor modes. This novel approach challenges the conventional perspective about the effects of these constraints by exploring the way an alternative framework can expand the range of modified gravity models.

According to that motivation, the formation of the BDLS theory has been conducted based on a specific set of principles, which requires that the theory yields second-order field equations. In addition, this theory must not be parity-violating and also it has to incorporate at most quadratic terms of the torsion tensor. Consequently, the BDLS theory involves a novel set of scalar invariants described in Sec.(2.3), thus allowing the constraint terms of the classical Horndeski to persist through the new contribution in the Lagrangian, Eq.(2.45). It is important to acknowledge the result that the classical Horndeski theory is now regarded as a subset of the BDLS theory. This serves as compelling evidence to support that this innovative scalar-tensor theory offers a more extensive platform for constructing models and introduces new perspectives on addressing the cosmological challenges and tensions. To investigate further the validity of the BDLS theory, the next reasonable course of action is to perform tensor perturbations of the tetrad and determine which models could eventually overcome the GW speed constraint. For that purpose, the flat FLRW metric is used and the corresponding tetrad with zero spin connection. Under this configuration, the presence of the correction term in Eq.(2.50) suggests that the previously ruled-out models could eventually survive the $\alpha_T = 0$ constraint and regain their viability within the BDLS theory.

At this point, it is significant to highlight the corrections in the coefficients of G_4 and G_5. These corrections, which depend on J_5 and are explicitly described in Eq.(2.56) confirm that the BDLS theory adheres to the GW speed constraint. By retaining all of the coupling functions one can conclude that the BDLS theory remains in accordance with the original principles of the classical Horndeski theory.

Considering that the BDLS theory presents a straightforward solution to overcome the limitations imposed by GW and provides a solid foundation for constructing cosmological models, the symmetries that arise from the Noether approach are a suitable mechanism for classifying those models. Since these symmetries are essential for simplifying a system of equations, this method is critical for analyzing the models in question, such as scalar-tensor theories. This method incorporates a point-like Lagrangian along with a symmetry that preserves the invariance of that Lagrangian. Given that Noether symmetries are consistently linked to conserved quantities, the initial step was to define the appropriate form of the point-like Lagrangian within a maximally symmetric FLRW spacetime, using a tetrad that aligns with the Weitzenböck gauge. As described in Sec.(4.1), through integration by parts the elimination of second-order derivatives was achieved leading to the derivation of the Lagrangian in its final form, Eq.(4.12). After that, the Rund-Trautman identity was employed resulting in a system of 62 equations for the coefficients of the Noether vector and the model functions G_i.

As anticipated, the system of equations gave rise to a vast array of cases, each of which corresponded to a distinct cosmological model. The four specific cases outlined in Sec.(4.3) serve to illustrate the advantages of utilizing this approach. Within these cases, the functions of the theory and the Noether vector coefficients have been determined in each of them to develop a complete model. Since most higher-order and curvature-based theories can be mapped into an equivalent Horndeski case, the use of Noether symmetries in BDLS theory allows for a more in-depth investigation of higher-order theories of gravity within the teleparallel context.

While there are numerous models in the realm of scalar-tensor theories, the quest for the most suitable theory of gravity remains an ongoing process. An important aspect is the correlation between the theoretical structure of these models and the high-precision observational data sets. After all, the intricate distribution of matter and energy within the observable Universe cannot be captured solely by a homogeneous model. In order to include the inhomogeneous and anisotropic distributions within the BDLS context, it is necessary to employ a perturbation method. A viable way to accomplish this is to begin with a flat FLRW spacetime as the background with straightforward characteristics upon which the study of perturbations would be performed. Additionally, the study is conducted by selecting a zero spin connection for the tetrad field. For that particular setup, the background equations have been quite advantageous in streamlining the complex mathematical calculations of perturbations. The perturbation level in the analysis, Sec.(5.2), is established by the quadratic action for tensor, vector and scalar modes. While scalar and tensor perturbations are crucial in structure formation and GW research, the comprehensive analysis of the BDLS theory should also include the vector modes. The subsequent stages of the research involve establishing the proper conditions to prevent the occurrence of ghosts and gradient instabilities. By utilizing these stability criteria, the appropriate formula for the propagation speed is derived for the three types of perturbation.

A method for gaining a concise understanding of perturbations involves the incorporation of a group of four time-dependent functions, defined in Sec.(5.3.2), which have the potential to be constrained by observations. When combined with the time evolutions of the background, the α_i functions encompass all relevant information for the background and cosmological perturbations. An interesting field for future research could involve examining deviations from observational data for an existing or novel cosmological model, by computing the α_i functions.

Knowing the conditions for avoiding ghost and gradient instabilities, a compelling area of study is examining the existence of a non-singular solution within the BDLS context and the possibilities to extend the no-go argument for non-singular BDLS models. The no-go argument asserts that, in the absence of gradient instabilities, ghosts and strong coupling in the quadratic action, it is impossible to create a singularity-free solution while allowing for complete evolution over the interval $t = (-\infty, +\infty)$ within the standard Horndeski theory. This means that in GR and provided that the energy-momentum tensor complies with the null energy condition, the expanding Universe exhibits a singularity in its past which remains unresolved by the inflation phase. One potential method to evade the no-go argument is the transition from the framework of GR to the one of TG. Consequently, the BDLS theory presents an appropriate context for investigating healthy non-singular models. Using the unitary gauge and the inherited metric perturbations as described in Chapter 5, we discussed three toy models belonging to the BDLS context. These models demonstrate the possibility of evading the no-go argument while meeting the constraint of the GW propagation speed. One of the most crucial results of these models is that Θ does not cross zero which means that ξ is not zero either in accordance with a non-singular cosmological model. Additionally, the propagation speed of tensor modes remains unity at all times. In the first two models, the choice is a power law function for the scale factor while the scalar field is a linear function of cosmic time. The G_{tele} term in the first model presents a coupling between the torsion scalar and the kinetic term while incorporating the J_5 scalar. The propagation speed of scalar perturbations remains positive and exhibits an antisymmetric pattern around the zero point of time. This indicates that the first toy model could healthily evade the no-go argument. The second model of the analysis features a G_{tele} which is a linear function of the torsion scalar and a linear term for the J_3 invariant. The classical Horndeski terms are analogous with the first model, except G_4, G_5 terms that show slight alterations. Similar to the first toy model, the scalar perturbations exhibit a consistently positive propagation speed, characterized by an antisymmetric pattern that can be prolonged depending on the values of the parameters.

The third toy model differs from the first two since it incorporates an exponential form of the scale factor. The G_{tele} term in this model has contributions from I_2 and J_3 scalars in linear order. According to the plots displayed in Figure 6.3, the outcome for this model is, once again, a healthy evasion of the no-go argument since the scalar mode propagation speed remains positive.

Motivated by the third toy model of the analysis, the investigation of alternative forms of the scale factor presents a compelling avenue for further research within the context of evasion of the no-go argument. Furthermore, prospective scientific endeavours could involve analyzing the impact that these early Universe models could have on the power spectrum of the CMB radiation.

In the field of cosmology, scalar-tensor theories present numerous promising characteristics for the development of models and alleviating the tensions between observational data and theoretical context. Consequently, the following points outline potential areas for further research in that direction.

- **Full tetrad perturbation spectrum in BDLS theory**

  The results of the analysis in Chapter 5 are based on the perturbation originating from the metric in conjunction with the application of the unitary gauge choice. Nevertheless, this analysis serves as the initial phase towards a more comprehensive approach. An area with significant potential for a forthcoming research endeavour involves examining the complete spectrum of the tetrad perturbations in the BDLS context. According to this perspective, the analysis will also include both the pseudoscalar and pseudovector modes without utilizing any gauge choice in the course of the research. Using this approach would allow for the incorporation of gauge invariant variables in the expression of the quadratic action for each type of perturbation. It is anticipated that this method will be highly beneficial in advancing our understanding of the dynamical features and behaviour of perturbations in the realm of BDLS. In particular, expanding the gauge invariant action up to the second order would enable the detection of the potential presence of ghosts and Laplacian instabilities in the BDLS context. Additionally, by employing the respective dispersion relations of the different perturbative modes it would be possible to determine the full spectrum of BDLS propagating DoF. The BDLS theory can be reduced for particular subclasses of modified gravity models that have a smaller number of DoF. By incorporating these subclasses into the gauge invariant action method, we could confirm the expected number of DoF for each type of modified gravity theory belonging to the general BDLS framework. Moreover, the results obtained from applying this approach would probably contribute to the development of further BDLS cosmological models that could evade the *No-go* theorem in addition to the three toy models discussed in Chapter 6.

- **Reconstruction methods in BDLS theory.**

A promising research area in scalar-tensor theories is to focus on utilizing observational data to enhance the development of a solid theoretical model within the TG context, meaning within the BDLS framework. In advancing towards that research field, reconstruction methods offer a direct approach to describe the behaviours consistently, thereby leading to the formation of valid cosmological models that can produce these behavioural patterns. The central idea of this research involves directly incorporating observations and selecting an appropriate set of kinematic parameters, such as the deceleration parameter in order to formulate the gravitational Lagrangian. In that way, the formulation of the Lagrangian is influenced to some extent by physical considerations. Through maximum likelihood analysis, the values of these parameters can be determined based on observational sources such BAO and Planck-CMB data. Nevertheless, the process of reconstruction is subjected to two general issues. The first is that the observational data are defined only at discrete redshift values and are usually affected by systematic and statistical errors that can impact the accuracy of the reconstructed model. The second issue is that discovering a cosmological model that includes a trajectory does not necessarily ensure that the trajectory is stable. Even if a reconstructed solution exits, a small perturbation could lead away from the solution. Therefore, it is important to conduct a thorough stability analysis of the reconstructed model. An alternative strategy involves conducting a non-parametric reconstruction, where the evolution is determined exclusively from observational data without any predefined assumptions about parameters. However, since a valid cosmological model encompassing the entire history of the Universe is still an ongoing study, utilizing a nonparametric methodology presents a compelling area for future research.

- **Stability of FLRW cosmologies**

In researching cosmological perturbations, the stability of the flat FLRW Universe as a background serves as a vital indicator of the validity of the cosmological theory under study. Within the BDLS cosmological models, the study of the stability conditions of the background evolution of the Universe has the potential to narrow down the range of parameters employed in that theory. In this analysis, the first-order perturbations of the Hubble parameter and the matter energy density of the homogeneous and isotropic FLRW metric must be determined. In addition, one should also examine possible connections between these two types of perturbations with the Lagrangian coefficients of the BDLS theory. These first-order perturbations depend only on the cosmic time and represent small deviations of the Hubble parameter and the matter energy density from their zero-order values. Following that, one should analyze the behaviour of these first-order perturbations, since their evolution indicates whether the cosmological solutions are stable or not. According to that, the next step is constructing the perturbed form of the field and the continuity equations. At this point, it is important to recognize that stability is achieved when the perturbations of the Hubble parameter and the energy density decay with cosmic time as the Universe evolves. Therefore, understanding the stability criteria of FLRW cosmologies cannot only reduce the number of parameters but it can also be used to limit the potential models based purely on theoretical considerations. Furthermore, applying the results of the stability analysis, we can create innovative models in the realm BDLS theory that explore the intricacies of the gravitational interaction and cosmic dynamics. Such advancements can deepen our understanding of the Universe and drive further research in cosmology.

References

[1] *Dynamical Systems in Cosmology*. Cambridge University Press, 1997.

[2] Abbott. Gravitational waves and gamma-rays from a binary neutron star merger: Gw170817 and grb 170817a. *The Astrophysical Journal Letters*, 848(2):L13, Oct. 2017. ISSN 2041-8213. doi: 10.3847/2041-8213/aa920c. URL http://dx.doi.org/10.3847/2041-8213/aa920c.

[3] B. P. Abbott et al. GW170817: Observation of Gravitational Waves from a Binary Neutron Star Inspiral. *Phys. Rev. Lett.*, 119(16):161101, 2017. doi: 10.1103/PhysRevLett.119.161101.

[4] R. Abraham and C. Shaw. *Dynamics: The Geometry Of Behavior*. Addison-Wesley studies in nonlinearity. Basic Books, 1992. ISBN 9780201567175. URL https://books.google.gr/books?id=OtEQAQAAIAAJ.

[5] R. Aldrovandi and J. Pereira. *Introduction To Geometrical Physics, An (Second Edition)*. World Scientific Publishing Company, 2016. ISBN 9789813146839. URL https://books.google.gr/books?id=NWhtDQAAQBAJ.

[6] R. Aldrovandi and J. G. Pereira. *Teleparallel Gravity: An Introduction*. Springer, 2013. ISBN 978-94-007-5142-2, 978-94-007-5143-9. doi: 10.1007/978-94-007-5143-9.

[7] L. Amendola. Scaling solutions in general nonminimal coupling theories. *Physical Review D*, 60 (4), jun 1999. doi: 10.1103/physrevd.60.043501. URL https://doi.org/10.1103%2Fphysrevd.60.043501.

[8] L. Amendola and S. Tsujikawa. *Dark Energy: Theory and Observations*. Cambridge University Press, 2010.

[9] S. Bahamonde and S. Capozziello. Noether symmetry approach in f(t, b) teleparallel cosmology. *The European Physical Journal C*, 77(2), Feb. 2017. ISSN 1434-6052. doi: 10.1140/epjc/s10052-017-4677-0. URL http://dx.doi.org/10.1140/epjc/s10052-017-4677-0.

[10] S. Bahamonde, C. G. Böhmer, and M. Wright. Modified teleparallel theories of gravity. *Physical Review D*, 92(10), nov 2015. doi: 10.1103/physrevd.92.104042. URL https://doi.org/10.1103%2Fphysrevd.92.104042.

[11] S. Bahamonde, C. G. Boehmer, and M. Krssak. New classes of modified teleparallel gravity models, 2017.

[12] S. Bahamonde, C. G. Böhmer, S. Carloni, E. J. Copeland, W. Fang, and N. Tamanini. Dynamical systems applied to cosmology: Dark energy and modified gravity. *Physics Reports*, 775-777:1–122, nov 2018. doi: 10.1016/j.physrep.2018.09.001. URL https://doi.org/10.1016%2Fj.physrep.2018.09.001.

[13] S. Bahamonde, K. F. Dialektopoulos, and J. L. Said. Can horndeski theory be recast using teleparallel gravity? *Physical Review D*, 100(6), sep 2019. doi: 10.1103/physrevd.100.064018. URL https://doi.org/10.1103%2Fphysrevd.100.064018.

[14] S. Bahamonde, K. F. Dialektopoulos, V. Gakis, and J. L. Said. Reviving horndeski theory using teleparallel gravity after GW170817. *Physical Review D*, 101(8), apr 2020. doi: 10.1103/physrevd.101.084060. URL https://doi.org/10.1103%2Fphysrevd.101.084060.

[15] S. Bahamonde, M. Hohmann, M. Caruana, K. F. Dialektopoulos, V. Gakis, J. Levi Said, E. N. Saridakis, and J. Sultana. Gravitational-wave propagation and polarizations in the teleparallel analog of horndeski gravity. *Physical Review D*, 104(8), Oct. 2021. ISSN 2470-0029. doi: 10.1103/physrevd.104.084082. URL http://dx.doi.org/10.1103/PhysRevD.104.084082.

[16] S. Bahamonde, M. Hohmann, M. Caruana, K. F. Dialektopoulos, V. Gakis, J. Levi Said, E. N. Saridakis, and J. Sultana. Gravitational-wave propagation and polarizations in the teleparallel analog of horndeski gravity. *Phys. Rev. D*, 104:084082, Oct 2021. doi: 10.1103/PhysRevD.104.084082. URL https://link.aps.org/doi/10.1103/PhysRevD.104.084082.

[17] S. Bahamonde, K. F. Dialektopoulos, C. Escamilla-Rivera, G. Farrugia, V. Gakis, M. Hendry, M. Hohmann, J. L. Said, J. Mifsud, and E. D. Valentino. Teleparallel gravity: from theory to cosmology. *Reports on Progress in Physics*, 86(2):026901, feb 2023. doi: 10.1088/1361-6633/ac9cef. URL https://doi.org/10.1088%2F1361-6633%2Fac9cef.

[18] S. Banerjee, Y.-F. Cai, and E. N. Saridakis. Evading the theoretical no-go theorem for nonsingular bounces in horndeski/galileon cosmology. *Classical and Quantum Gravity*, 36(13):135009, June 2019. ISSN 1361-6382. doi: 10.1088/1361-6382/ab256a. URL http://dx.doi.org/10.1088/1361-6382/ab256a.

[19] J. M. Bardeen. Gauge Invariant Cosmological Perturbations. *Phys. Rev. D*, 22:1882–1905, 1980. doi: 10.1103/PhysRevD.22.1882.

[20] J. D. Barrow and S. Cotsakis. Inflation and the Conformal Structure of Higher Order Gravity Theories. *Phys. Lett. B*, 214:515–518, 1988. doi: 10.1016/0370-2693(88)90110-4.

[21] N. Bartolo and M. Pietroni. Scalar-tensor gravity and quintessence. *Physical Review D*, 61(2), dec 1999. doi: 10.1103/physrevd.61.023518. URL https://doi.org/10.1103%2Fphysrevd.61.023518.

[22] S. Basilakos, M. Tsamparlis, and A. Paliathanasis. Using the noether symmetry approach to probe the nature of dark energy. *Physical Review D*, 83(10), May 2011. ISSN 1550-2368. doi: 10.1103/physrevd.83.103512. URL http://dx.doi.org/10.1103/PhysRevD.83.103512.

[23] S. Basilakos, M. Tsamparlis, and A. Paliathanasis. Using the noether symmetry approach to probe the nature of dark energy. *Phys. Rev. D*, 83:103512, May 2011. doi: 10.1103/PhysRevD.83.103512. URL https://link.aps.org/doi/10.1103/PhysRevD.83.103512.

[24] S. Basilakos, S. Capozziello, M. De Laurentis, A. Paliathanasis, and M. Tsamparlis. Noether symmetries and analytical solutions in $f(t)$ cosmology: A complete study. *Phys. Rev. D*, 88:103526, Nov 2013. doi: 10.1103/PhysRevD.88.103526. URL https://link.aps.org/doi/10.1103/PhysRevD.88.103526.

[25] D. Baumann. *The Physics of Inflation*. CreateSpace Independent Publishing Platform, 2015. ISBN 9781506124629. URL https://books.google.gr/books?id=7_orrgEACAAJ.

[26] E. Bellini and I. Sawicki. Maximal freedom at minimum cost: linear large-scale structure in general modifications of gravity. *Journal of Cosmology and Astroparticle Physics*, 2014(07):050–050, jul 2014. doi: 10.1088/1475-7516/2014/07/050. URL https://doi.org/10.1088%2F1475-7516%2F2014%2F07%2F050.

[27] E. Bellini, A. J. Cuesta, R. Jimenez, and L. Verde. Constraints on deviations from ΛCDM within horndeski gravity. *Journal of Cosmology and Astroparticle Physics*, 2016(02):053–053, feb 2016. doi: 10.1088/1475-7516/2016/02/053. URL https://doi.org/10.1088%2F1475-7516%2F2016%2F02%2F053.

[28] J. Beltrán Jiménez, L. Heisenberg, and T. S. Koivisto. The geometrical trinity of gravity. *Universe*, 5 (7), 2019. ISSN 2218-1997. doi: 10.3390/universe5070173. URL https://www.mdpi.com/2218-1997/5/7/173.

[29] E. Bertschinger. Cosmological perturbation theory and structure formation, 2000.

[30] B. Boisseau, G. Esposito-Farè se, D. Polarski, and A. A. Starobinsky. Reconstruction of a scalar-tensor theory of gravity in an accelerating universe. *Physical Review Letters*, 85(11):2236–2239, sep 2000. doi: 10.1103/physrevlett.85.2236. URL https://doi.org/10.1103%2Fphysrevlett.85.2236.

[31] A. Bonanno, G. Esposito, C. Rubano, and P. Scudellaro. Noether symmetry approach in pure gravity with variable g and λ. *Classical and Quantum Gravity*, 24(6):1443, mar 2007. doi: 10.1088/0264-9381/24/6/005. URL https://dx.doi.org/10.1088/0264-9381/24/6/005.

[32] A. Borde. Open and closed universes, initial singularities, and inflation. *Phys. Rev. D*, 50:3692–3702, Sep 1994. doi: 10.1103/PhysRevD.50.3692. URL https://link.aps.org/doi/10.1103/PhysRevD.50.3692.

[33] A. Borde and A. Vilenkin. Eternal inflation and the initial singularity. *Physical Review Letters*, 72(21): 3305–3308, May 1994. ISSN 0031-9007. doi: 10.1103/physrevlett.72.3305. URL http://dx.doi.org/10.1103/PhysRevLett.72.3305.

[34] A. BORDE and A. VILENKIN. Singularities in inflationary cosmology: A review. *International Journal of Modern Physics D*, 05(06):813–824, Dec. 1996. ISSN 1793-6594. doi: 10.1142/s0218271896000497. URL http://dx.doi.org/10.1142/S0218271896000497.

[35] R. Brandenberger, V. Mukhanov, and A. Sornborger. Cosmological theory without singularities. *Physical Review D*, 48(4):1629–1642, Aug. 1993. ISSN 0556-2821. doi: 10.1103/physrevd.48.1629. URL http://dx.doi.org/10.1103/PhysRevD.48.1629.

[36] C. Brans and R. H. Dicke. Mach's principle and a relativistic theory of gravitation. *Phys. Rev.*, 124: 925–935, 1961. doi: 10.1103/PhysRev.124.925.

[37] N. Bretó n, J. L. Cervantes-Cota, and M. Salgado, editors. *The Early Universe and Observational Cosmology*. Springer Berlin Heidelberg, 2004. doi: 10.1007/b97189. URL https://doi.org/10.1007%2Fb97189.

[38] H. Broer and F. Takens. *Dynamical Systems and Chaos*. Applied Mathematical Sciences. Springer New York, 2010. ISBN 9781441968708. URL https://books.google.gr/books?id=yaov2qvj5YQC.

[39] C. G. Böhmer and N. Chan. *Dynamical Systems in Cosmology*, page 121–156. WORLD SCIENTIFIC (EUROPE), Dec. 2016. doi: 10.1142/9781786341044_0004. URL http://dx.doi.org/10.1142/9781786341044_0004.

[40] R.-G. Cai and T. Yang. Estimating cosmological parameters by the simulated data of gravitational waves from the einstein telescope. *Physical Review D*, 95(4), Feb. 2017. ISSN 2470-0029. doi: 10.1103/physrevd.95.044024. URL http://dx.doi.org/10.1103/PhysRevD.95.044024.

[41] Y.-F. Cai, S. Capozziello, M. De Laurentis, and E. N. Saridakis. f(t) teleparallel gravity and cosmology. *Reports on Progress in Physics*, 79(10):106901, Sept. 2016. ISSN 1361-6633. doi: 10.1088/0034-4885/79/10/106901. URL http://dx.doi.org/10.1088/0034-4885/79/10/106901.

[42] L. Canetti, M. Drewes, and M. Shaposhnikov. Matter and antimatter in the universe. *New Journal of Physics*, 14(9):095012, Sept. 2012. ISSN 1367-2630. doi: 10.1088/1367-2630/14/9/095012. URL http://dx.doi.org/10.1088/1367-2630/14/9/095012.

[43] S. Capozziello and F. Bajardi. Minisuperspace quantum cosmology in metric and affine theories of gravity. *Universe*, 8(3):177, Mar. 2022. ISSN 2218-1997. doi: 10.3390/universe8030177. URL http://dx.doi.org/10.3390/universe8030177.

[44] S. Capozziello and A. De Felice. f(r) cosmology from noether's symmetry. *Journal of Cosmology and Astroparticle Physics*, 2008(08):016, Aug. 2008. ISSN 1475-7516. doi: 10.1088/1475-7516/2008/08/016. URL http://dx.doi.org/10.1088/1475-7516/2008/08/016.

[45] S. Capozziello, R. De Ritis, C. Rubano, and P. Scudellaro. Noether symmetries in cosmology. *Riv. Nuovo Cim.*, 19N4:1–114, 1996. doi: 10.1007/BF02742992.

[46] S. Capozziello, K. F. Dialektopoulos, and S. V. Sushkov. Classification of the horndeski cosmologies via noether symmetries. *The European Physical Journal C*, 78(6), jun 2018. doi: 10.1140/epjc/s10052-018-5939-1. URL https://doi.org/10.1140%2Fepjc%2Fs10052-018-5939-1.

[47] S. Capozziello, M. Caruana, J. L. Said, and J. Sultana. Ghost and laplacian instabilities in teleparallel horndeski gravity. *Journal of Cosmology and Astroparticle Physics*, 2023(03):060, mar 2023. doi: 10.1088/1475-7516/2023/03/060. URL https://doi.org/10.1088%2F1475-7516%2F2023%2F03%2F060.

[48] N. Chatzarakis and V. Oikonomou. Autonomous dynamical system of einstein–gauss–bonnet cosmologies. *Annals of Physics*, 419:168216, aug 2020. doi: 10.1016/j.aop.2020.168216. URL https://doi.org/10.1016%2Fj.aop.2020.168216.

[49] T. Clifton, P. G. Ferreira, A. Padilla, and C. Skordis. Modified gravity and cosmology. *Physics Reports*, 513(1-3):1–189, mar 2012. doi: 10.1016/j.physrep.2012.01.001. URL https://doi.org/10.1016%2Fj.physrep.2012.01.001.

[50] G. Cognola, E. Elizalde, S. Nojiri, S. D. Odintsov, and S. Zerbini. Dark energy in modified gauss-bonnet gravity: Late-time acceleration and the hierarchy problem. *Phys. Rev. D*, 73:084007, Apr 2006. doi: 10.1103/PhysRevD.73.084007. URL https://link.aps.org/doi/10.1103/PhysRevD.73.084007.

[51] A. A. Coley. Dynamical systems in cosmology, 1999.

[52] P. Collaboration. Planck 2013 results. XVI. cosmological parameters. *Astronomy & Astrophysics*, 571:A16, oct 2014. doi: 10.1051/0004-6361/201321591. URL https://doi.org/10.1051%2F0004-6361%2F201321591.

[53] E. J. Copeland, A. R. Liddle, and D. Wands. Exponential potentials and cosmological scaling solutions. *Physical Review D*, 57(8):4686–4690, apr 1998. doi: 10.1103/physrevd.57.4686. URL https://doi.org/10.1103%2Fphysrevd.57.4686.

[54] R. de Ritis, G. Marmo, G. Platania, C. Rubano, P. Scudellaro, and C. Stornaiolo. New approach to find exact solutions for cosmological models with a scalar field. *Phys. Rev. D*, 42:1091–1097, Aug 1990. doi: 10.1103/PhysRevD.42.1091. URL https://link.aps.org/doi/10.1103/PhysRevD.42.1091.

[55] R. de Ritis, A. A. Marino, C. Rubano, and P. Scudellaro. Tracker fields from nonminimally coupled theory. *Physical Review D*, 62(4), July 2000. ISSN 1089-4918. doi: 10.1103/physrevd.62.043506. URL http://dx.doi.org/10.1103/PhysRevD.62.043506.

[56] C. Deffayet, G. Esposito-Farè se, and A. Vikman. Covariant galileon. *Physical Review D*, 79(8), apr 2009. doi: 10.1103/physrevd.79.084003. URL https://doi.org/10.1103%2Fphysrevd.79.084003.

[57] C. Deffayet, O. Pujolàs, I. Sawicki, and A. Vikman. Imperfect dark energy from kinetic gravity braiding. *Journal of Cosmology and Astroparticle Physics*, 2010(10):026–026, oct 2010. doi: 10.1088/1475-7516/2010/10/026. URL https://doi.org/10.1088%2F1475-7516%2F2010%2F10%2F026.

[58] C. Deffayet, O. Pujolàs, I. Sawicki, and A. Vikman. Imperfect dark energy from kinetic gravity braiding. *Journal of Cosmology and Astroparticle Physics*, 2010(10):026–026, Oct. 2010. ISSN 1475-7516. doi: 10.1088/1475-7516/2010/10/026. URL http://dx.doi.org/10.1088/1475-7516/2010/10/026.

[59] J. DeRose, R. H. Wechsler, J. L. Tinker, M. R. Becker, Y.-Y. Mao, T. McClintock, S. McLaughlin, E. Rozo, and Z. Zhai. The aemulus project. i. numerical simulations for precision cosmology. *The Astrophysical Journal*, 875(1):69, apr 2019. doi: 10.3847/1538-4357/ab1085. URL https://dx.doi.org/10.3847/1538-4357/ab1085.

[60] E. Di Valentino. A combined analysis of the H_0 late time direct measurements and the impact on the Dark Energy sector. *Mon. Not. Roy. Astron. Soc.*, 502(2):2065–2073, 2021. doi: 10.1093/mnras/stab187.

[61] K. F. Dialektopoulos, T. S. Koivisto, and S. Capozziello. Noether symmetries in symmetric teleparallel cosmology. *The European Physical Journal C*, 79(7), July 2019. ISSN 1434-6052. doi: 10.1140/epjc/s10052-019-7106-8. URL http://dx.doi.org/10.1140/epjc/s10052-019-7106-8.

[62] K. F. Dialektopoulos, J. L. Said, and Z. Oikonomopoulou. Classification of teleparallel horndeski cosmology via noether symmetries, 2022.

[63] S. Dodelson. *Modern Cosmology*. Academic Press, Amsterdam, 2003. ISBN 978-0-12-219141-1.

[64] D. A. Easson, I. Sawicki, and A. Vikman. G-bounce. *Journal of Cosmology and Astroparticle Physics*, 2011(11):021–021, Nov. 2011. ISSN 1475-7516. doi: 10.1088/1475-7516/2011/11/021. URL http://dx.doi.org/10.1088/1475-7516/2011/11/021.

[65] G. Esposito-Farè se and D. Polarski. Scalar-tensor gravity in an accelerating universe. *Physical Review D*, 63(6), feb 2001. doi: 10.1103/physrevd.63.063504. URL https://doi.org/10.1103%2Fphysrevd.63.063504.

[66] A. et al. Planck2018 results: Vi. cosmological parameters. *Astronomy & Astrophysics*, 641:A6, Sept. 2020. ISSN 1432-0746. doi: 10.1051/0004-6361/201833910. URL http://dx.doi.org/10.1051/0004-6361/201833910.

[67] S. N. et al. Forecast constraints on consistency tests of the ΛCDM model. *Astronomy and Astrophysics*, 660:A67, apr 2022. doi: 10.1051/0004-6361/202142503. URL https://doi.org/10.1051%2F0004-6361%2F202142503.

[68] V. Faraoni and S. Capozziello. *Beyond Einstein Gravity: A Survey of Gravitational Theories for Cosmology and Astrophysics*. Springer, Dordrecht, 2011. ISBN 978-94-007-0164-9, 978-94-007-0165-6. doi: 10.1007/978-94-007-0165-6.

[69] P. G. S. Fernandes, P. Carrilho, T. Clifton, and D. J. Mulryne. The 4d einstein–gauss–bonnet theory of gravity: a review. *Classical and Quantum Gravity*, 39(6):063001, feb 2022. doi: 10.1088/1361-6382/ac500a. URL https://doi.org/10.1088%2F1361-6382%2Fac500a.

[70] R. García-Salcedo, T. Gonzalez, F. A. Horta-Rangel, I. Quiros, and D. Sanchez-Guzmán. Introduction to the application of dynamical systems theory in the study of the dynamics of cosmological models of dark energy. *European Journal of Physics*, 36(2):025008, Jan. 2015. ISSN 1361-6404. doi: 10.1088/0143-0807/36/2/025008. URL http://dx.doi.org/10.1088/0143-0807/36/2/025008.

[71] J. Gleyzes, D. Langlois, and F. Vernizzi. A unifying description of dark energy. *International Journal of Modern Physics D*, 23(13):1443010, nov 2014. doi: 10.1142/s021827181443010x. URL https://doi.org/10.1142%2Fs021827181443010x.

[72] A. Golovnev. The geometrical meaning of the weitzenbock connection. *International Journal of Geometric Methods in Modern Physics*, 20, 06 2023. doi: 10.1142/S0219887823502195.

[73] A. H. Guth. Inflationary universe: A possible solution to the horizon and flatness problems. *Phys. Rev. D*, 23:347–356, Jan 1981. doi: 10.1103/PhysRevD.23.347. URL https://link.aps.org/doi/10.1103/PhysRevD.23.347.

[74] A. K. Halder, A. Paliathanasis, and P. G. L. Leach. Noether's theorem and symmetry, 2018.

[75] K. Hayashi and T. Shirafuji. New general relativity. *Phys. Rev. D*, 19:3524–3553, 1979. doi: 10.1103/PhysRevD.19.3524. [Addendum: Phys.Rev.D 24, 3312–3314 (1982)].

[76] I. P. C. Heard and D. Wands. Cosmology with positive and negative exponential potentials. *Classical and Quantum Gravity*, 19(21):5435–5447, Oct. 2002. ISSN 0264-9381. doi: 10.1088/0264-9381/19/21/309. URL http://dx.doi.org/10.1088/0264-9381/19/21/309.

[77] G. W. Horndeski. Second-order scalar-tensor field equations in a four-dimensional space. *International Journal of Theoretical Physics*, 10:363–384, 1974.

[78] S. Hou, Y. Gong, and Y. Liu. Polarizations of gravitational waves in horndeski theory. *The European Physical Journal C*, 78(5), May 2018. ISSN 1434-6052. doi: 10.1140/epjc/s10052-018-5869-y. URL http://dx.doi.org/10.1140/epjc/s10052-018-5869-y.

[79] A. Ijjas and P. J. Steinhardt. Classically stable nonsingular cosmological bounces. *Physical Review Letters*, 117(12), Sept. 2016. ISSN 1079-7114. doi: 10.1103/physrevlett.117.121304. URL http://dx.doi.org/10.1103/PhysRevLett.117.121304.

[80] M. Ishak. Testing general relativity in cosmology. *Living Reviews in Relativity*, 22(1), dec 2018. doi: 10.1007/s41114-018-0017-4. URL https://doi.org/10.1007%2Fs41114-018-0017-4.

[81] A. S. W. Y. L. B. K. C. Jones;B.E.Tucker. New parallaxes of galactic cepheids from spatially scanning the hubble space telescope: Implications for the hubble constant. *The Astrophysical Journal*, 855(2): 136, mar 2018. doi: 10.3847/1538-4357/aaadb7. URL https://doi.org/10.3847%2F1538-4357%2Faaadb7.

[82] A. Katok and B. Hasselblatt. *Introduction to the Modern Theory of Dynamical Systems*. Encyclopedia of Mathematics and its Applications. Cambridge University Press, 1995. doi: 10.1017/CBO9780511809187.

[83] D. Kazanas. *Cosmological Inflation: A Personal Perspective*, page 485–496. Springer Berlin Heidelberg, 2008. ISBN 9783540758266. doi: 10.1007/978-3-540-75826-6_49. URL http://dx.doi.org/10.1007/978-3-540-75826-6_49.

[84] A. Kehagias and G. Kofinas. Cosmology with exponential potentials. *Classical and Quantum Gravity*, 21(16):3871–3885, jul 2004. doi: 10.1088/0264-9381/21/16/003. URL https://doi.org/10.1088%2F0264-9381%2F21%2F16%2F003.

[85] A. Klypin. Numerical simulations in cosmology i: Methods, 2000.

[86] T. Kobayashi. Generic instabilities of nonsingular cosmologies in horndeski theory: A no-go theorem. *Physical Review D*, 94(4), Aug. 2016. ISSN 2470-0029. doi: 10.1103/physrevd.94.043511. URL http://dx.doi.org/10.1103/PhysRevD.94.043511.

[87] T. Kobayashi. Horndeski theory and beyond: a review. *Reports on Progress in Physics*, 82(8):086901, jul 2019. doi: 10.1088/1361-6633/ab2429. URL https://doi.org/10.1088%2F1361-6633%2Fab2429.

[88] T. Kobayashi, M. Yamaguchi, and J. Yokoyama. Generalized g-inflation: –inflation with the most general second-order field equations–. *Progress of Theoretical Physics*, 126(3):511–529, sep 2011. doi: 10.1143/ptp.126.511. URL https://doi.org/10.1143%2Fptp.126.511.

[89] T. Koivisto and D. F. Mota. Gauss-bonnet quintessence: Background evolution, large scale structure, and cosmological constraints. *Physical Review D*, 75(2), jan 2007. doi: 10.1103/physrevd.75.023518. URL https://doi.org/10.1103%2Fphysrevd.75.023518.

[90] C. Kreisch and E. Komatsu. Cosmological constraints on horndeski gravity in light of GW170817. *Journal of Cosmology and Astroparticle Physics*, 2018(12):030–030, dec 2018. doi: 10.1088/1475-7516/2018/12/030. URL https://doi.org/10.1088%2F1475-7516%2F2018%2F12%2F030.

[91] M. Krš šák, R. J. van den Hoogen, J. G. Pereira, C. G. Böhmer, and A. A. Coley. Teleparallel theories of gravity: illuminating a fully invariant approach. *Classical and Quantum Gravity*, 36(18):183001, aug 2019. doi: 10.1088/1361-6382/ab2e1f. URL https://doi.org/10.1088%2F1361-6382%2Fab2e1f.

[92] M. Kuhlen, M. Vogelsberger, and R. Angulo. Numerical simulations of the dark universe: State of the art and the next decade. *Physics of the Dark Universe*, 1(1):50–93, 2012. ISSN 2212-6864. doi: https://doi.org/10.1016/j.dark.2012.10.002. URL https://www.sciencedirect.com/science/article/pii/S2212686412000064. Next Decade in Dark Matter and Dark Energy.

[93] M. Lagos, T. Baker, P. G. Ferreira, and J. Noller. A general theory of linear cosmological perturbations: scalar-tensor and vector-tensor theories. *Journal of Cosmology and Astroparticle Physics*, 2016(08):007–007, aug 2016. doi: 10.1088/1475-7516/2016/08/007. URL https://doi.org/10.1088%2F1475-7516%2F2016%2F08%2F007.

[94] G. Lemaître. The expanding universe. *mnras*, 91:490–501, Mar. 1931. doi: 10.1093/mnras/91.5.490.

[95] R. Leone and T. Gourieux. Classical noether theory with application to the linearly damped particle. *European Journal of Physics*, 36(6):065022, sep 2015. doi: 10.1088/0143-0807/36/6/065022. URL https://doi.org/10.1088%2F0143-0807%2F36%2F6%2F065022.

[96] D. Lovelock. The Einstein tensor and its generalizations. *J. Math. Phys.*, 12:498–501, 1971. doi: 10.1063/1.1665613.

[97] D. Lovelock. The four-dimensionality of space and the einstein tensor. *J. Math. Phys.*, 13:874–876, 1972. doi: 10.1063/1.1666069.

[98] T. H.-C. Lu, K. Ananda, C. Clarkson, and R. Maartens. The cosmological background of vector modes. *Journal of Cosmology and Astroparticle Physics*, 2009(02):023–023, feb 2009. doi: 10.1088/1475-7516/2009/02/023. URL https://doi.org/10.1088%2F1475-7516%2F2009%2F02%2F023.

[99] F. Lucchin and S. Matarrese. Power Law Inflation. *Phys. Rev. D*, 32:1316, 1985. doi: 10.1103/PhysRevD.32.1316.

[100] K. A. Malik and D. Wands. Cosmological perturbations. *Physics Reports*, 475(1-4):1–51, may 2009. doi: 10.1016/j.physrep.2009.03.001. URL https://doi.org/10.1016%2Fj.physrep.2009.03.001.

[101] S. Mironov and A. Shtennikova. Stable cosmological solutions in horndeski theory, 2023.

[102] C. Misner, K. Thorne, and J. Wheeler. *Gravitation*. Number pt. 3 in Gravitation. W. H. Freeman, 1973. ISBN 9780716703440. URL https://books.google.com.mt/books?id=w4Gigq3tY1kC.

[103] V. F. Mukhanov, H. A. Feldman, and R. Brandenberger. Theory of cosmological perturbations. *Physics Reports*, 215:203–333, 1992.

[104] Y. S. Murakami, A. G. Riess, B. E. Stahl, W. D. Kenworthy, D.-M. A. Pluck, A. Macoretta, D. Brout, D. O. Jones, D. M. Scolnic, and A. V. Filippenko. Leveraging sn ia spectroscopic similarity to improve the measurement of h_0, 2023.

[105] M. P. Müller, J. Oppenheim, and O. C. Dahlsten. The black hole information problem beyond quantum theory. *Journal of High Energy Physics*, 2012(9), Sept. 2012. ISSN 1029-8479. doi: 10.1007/jhep09(2012)116. URL http://dx.doi.org/10.1007/JHEP09(2012)116.

[106] I. P. Neupane. Accelerating cosmologies from exponential potentials. *Classical and Quantum Gravity*, 21(18):4383–4397, Aug. 2004. ISSN 1361-6382. doi: 10.1088/0264-9381/21/18/007. URL http://dx.doi.org/10.1088/0264-9381/21/18/007.

[107] E. Noether. Invariant variation problems. *Transport Theory and Statistical Physics*, 1(3):186–207, Jan. 1971. ISSN 1532-2424. doi: 10.1080/00411457108231446. URL http://dx.doi.org/10.1080/00411457108231446.

[108] S. Nojiri, S. D. Odintsov, and M. Sasaki. Gauss-bonnet dark energy. *Physical Review D*, 71(12), jun 2005. doi: 10.1103/physrevd.71.123509. URL https://doi.org/10.1103%2Fphysrevd.71.123509.

[109] M. NOVELLO and S. BERGLIAFFA. Bouncing cosmologies. *Physics Reports*, 463(4):127–213, July 2008. ISSN 0370-1573. doi: 10.1016/j.physrep.2008.04.006. URL http://dx.doi.org/10.1016/j.physrep.2008.04.006.

[110] S. Odintsov and V. Oikonomou. Inflationary phenomenology of einstein gauss-bonnet gravity compatible with GW170817. *Physics Letters B*, 797:134874, oct 2019. doi: 10.1016/j.physletb.2019.134874. URL https://doi.org/10.1016%2Fj.physletb.2019.134874.

[111] S. D. Odintsov, V. K. Oikonomou, and F. P. Fronimos. Rectifying einstein-gauss-bonnet inflation in view of gw170817, 2020.

[112] V. K. Oikonomou. A refined einstein–gauss–bonnet inflationary theoretical framework. *Classical and Quantum Gravity*, 38(19):195025, Sept. 2021. ISSN 1361-6382. doi: 10.1088/1361-6382/ac2168. URL http://dx.doi.org/10.1088/1361-6382/ac2168.

[113] J. Oppenheim. A postquantum theory of classical gravity? *Phys. Rev. X*, 13:041040, Dec 2023. doi: 10.1103/PhysRevX.13.041040. URL https://link.aps.org/doi/10.1103/PhysRevX.13.041040.

[114] A. Paliathanasis, N. Dimakis, and T. Christodoulakis. Minisuperspace description of f(q)-cosmology. *Physics of the Dark Universe*, 43:101410, 2024. ISSN 2212-6864. doi: https://doi.org/10.1016/j.dark.2023.101410. URL https://www.sciencedirect.com/science/article/pii/S2212686423002431.

[115] P. Pavlović and M. Sossich. Cosmological bounce and the cosmological constant problem, 2022.

[116] F. Perrotta, C. Baccigalupi, and S. Matarrese. Extended quintessence. *Physical Review D*, 61(2), Dec. 1999. ISSN 1089-4918. doi: 10.1103/physrevd.61.023507. URL http://dx.doi.org/10.1103/PhysRevD.61.023507.

[117] M. G. Phelps, A. Amarasinghe, and P. D. Mannheim. Three-dimensional and four-dimensional scalar, vector, tensor cosmological fluctuations and the cosmological decomposition theorem. *General Relativity and Gravitation*, 52(11), nov 2020. doi: 10.1007/s10714-020-02757-0. URL https://doi.org/10.1007%2Fs10714-020-02757-0.

[118] T. Qiu and Y.-T. Wang. G-bounce inflation: towards nonsingular inflation cosmology with galileon field. *Journal of High Energy Physics*, 2015(4), Apr. 2015. ISSN 1029-8479. doi: 10.1007/jhep04(2015)130. URL http://dx.doi.org/10.1007/JHEP04(2015)130.

[119] T. Qiu, J. Evslin, Y.-F. Cai, M. Li, and X. Zhang. Bouncing galileon cosmologies. *Journal of Cosmology and Astroparticle Physics*, 2011(10):036–036, Oct. 2011. ISSN 1475-7516. doi: 10.1088/1475-7516/2011/10/036. URL http://dx.doi.org/10.1088/1475-7516/2011/10/036.

[120] A. G. Riess, W. Yuan, L. M. Macri, D. Scolnic, D. Brout, S. Casertano, D. O. Jones, Y. Murakami, G. S. Anand, L. Breuval, T. G. Brink, A. V. Filippenko, S. Hoffmann, S. W. Jha, W. D. Kenworthy, J. Mackenty, B. E. Stahl, and W. Zheng. A comprehensive measurement of the local value of the hubble constant with $1km/s/mpc$ uncertainty from the hubble space telescope and the SH0es team. *The Astrophysical Journal Letters*, 934(1):L7, jul 2022. doi: 10.3847/2041-8213/ac5c5b. URL https://doi.org/10.3847%2F2041-8213%2Fac5c5b.

[121] I. D. Saltas, I. Sawicki, L. Amendola, and M. Kunz. Anisotropic Stress as a Signature of Nonstandard Propagation of Gravitational Waves. *Phys. Rev. Lett.*, 113(19):191101, 2014. doi: 10.1103/PhysRevLett.113.191101.

[122] I. D. Saltas, I. Sawicki, L. Amendola, and M. Kunz. Anisotropic stress as a signature of nonstandard propagation of gravitational waves. *Physical Review Letters*, 113(19), Nov. 2014. ISSN 1079-7114. doi: 10.1103/physrevlett.113.191101. URL http://dx.doi.org/10.1103/PhysRevLett.113.191101.

[123] A. K. Sanyal and B. Modak. Is the nöther symmetric approach consistent with the dynamical equation in non-minimal scalar-tensor theories? *Classical and Quantum Gravity*, 18(17):3767–3774, Aug. 2001. ISSN 1361-6382. doi: 10.1088/0264-9381/18/17/324. URL http://dx.doi.org/10.1088/0264-9381/18/17/324.

[124] A. K. Sanyal, B. Modak, C. Rubano, and E. Piedipalumbo. Noether symmetry in the higher order gravity theory. *General Relativity and Gravitation*, 37(2):407–417, Feb. 2005. ISSN 1572-9532. doi: 10.1007/s10714-005-0028-9. URL http://dx.doi.org/10.1007/s10714-005-0028-9.

[125] K. Sarkar, N. Sk, S. Debnath, and A. K. Sanyal. Viability of noether symmetry of f(r) theory of gravity. *International Journal of Theoretical Physics*, 52(4):1194–1213, Dec. 2012. ISSN 1572-9575. doi: 10.1007/s10773-012-1436-8. URL http://dx.doi.org/10.1007/s10773-012-1436-8.

[126] I. Sawicki and E. Bellini. Limits of quasistatic approximation in modified-gravity cosmologies. *Physical Review D*, 92(8), Oct. 2015. ISSN 1550-2368. doi: 10.1103/physrevd.92.084061. URL http://dx.doi.org/10.1103/PhysRevD.92.084061.

[127] N. Sk. Noether symmetry in f(t) teleparallel gravity. *Physics Letters B*, 775:100–104, 2017. ISSN 0370-2693. doi: https://doi.org/10.1016/j.physletb.2017.10.048. URL https://www.sciencedirect.com/science/article/pii/S0370269317308602.

[128] C. Skordis. Tensor-vector-scalar cosmology: Covariant formalism for the background evolution and linear perturbation theory. *Phys. Rev. D*, 74:103513, Nov 2006. doi: 10.1103/PhysRevD.74.103513. URL https://link.aps.org/doi/10.1103/PhysRevD.74.103513.

[129] S. Strogatz. *Nonlinear Dynamics and Chaos: With Applications to Physics, Biology, Chemistry and Engineering*. Studies in nonlinearity. Westview, 2000. URL https://books.google.gr/books?id=NZZDnQEACAAJ.

[130] R. J. Tayler. Magnetic Monopoles and Cosmology. *Monthly Notices of the Royal Astronomical Society*, 176(1):69P–71P, 07 1976.

[131] K. S. Thorne. Gravitational waves, 1995.

[132] M. J. G. Veltman. Quantum Theory of Gravitation. *Conf. Proc. C*, 7507281:265–327, 1975.

[133] M. Visser. General relativistic energy conditions: The hubble expansion in the epoch of galaxy formation. *Phys. Rev. D*, 56:7578–7587, Dec 1997. doi: 10.1103/PhysRevD.56.7578. URL https://link.aps.org/doi/10.1103/PhysRevD.56.7578.

[134] H. Wei, X.-J. Guo, and L.-F. Wang. Noether symmetry in f(t) theory. *Physics Letters B*, 707(2):298–304, Jan. 2012. ISSN 0370-2693. doi: 10.1016/j.physletb.2011.12.039. URL http://dx.doi.org/10.1016/j.physletb.2011.12.039.

[135] S. Weinberg. *Gravitation and Cosmology: Principles and Applications of the General Theory of Relativity*. John Wiley and Sons, New York, 1972. ISBN 978-0-471-92567-5, 978-0-471-92567-5.

[136] S. Weinberg. The Cosmological Constant Problem. *Rev. Mod. Phys.*, 61:1–23, 1989. doi: 10.1103/RevModPhys.61.1.

[137] S. Weinberg. Damping of tensor modes in cosmology. *Phys. Rev. D*, 69:023503, Jan 2004. doi: 10.1103/PhysRevD.69.023503. URL https://link.aps.org/doi/10.1103/PhysRevD.69.023503.

[138] R. Weitzenböck. *Invarianten-Theorie*. Noordhoff, 1923. URL https://books.google.gr/books?id=gN7zoAEACAAJ.

[139] Y. Zhang and H. Zhang. Distinguish the f(t) model from

$$\lambda$$

cdm model with gravitational wave observations. *The European Physical Journal C*, 81(8), Aug. 2021. ISSN 1434-6052. doi: 10.1140/epjc/s10052-021-09501-1. URL http://dx.doi.org/10.1140/epjc/s10052-021-09501-1.

[140] Y. Zhang, Y.-G. Gong, and Z.-H. Zhu. Noether symmetry approach in multiple scalar fields scenario. *Physics Letters B*, 688(1):13–20, 2010. ISSN 0370-2693. doi: https://doi.org/10.1016/j.physletb.2010.03.071. URL https://www.sciencedirect.com/science/article/pii/S0370269310004053.